1 **Small Molecule Sensors for the Colorimetric Detection of Copper(II): A Review of the**

2 **Literature from 2010- 2022**

3 Kimberly M. Trevino[a], Caitlyn R. Wagner[b], Eric K. Tamura[b], Joel Garcia[c]*, Angelique Y.

4 Louie[a,b,*]

5 [a] *Chemistry Graduate Group, University of California at Davis, One Shields Ave, Davis, CA 95616, USA*

6 [b] *Department of Biomedical Engineering, University of California at Davis, One Shields Ave, Davis, CA,*

7 *95616, USA*

8 [c] *Chemistry Department, De La Salle University, 2401 Taft Avenue, 1004 Manila, Philippines*

9 *Corresponding authors: joel.garcia@dlsu.edu.ph, aylouie@ucdavis.edu*

10

11 **Abstract**

12 Small molecules can display certain electronic and structural features that enable their use for

13 metal-sensing applications in different fields. Of the reported metal sensors, there has been

14 increasing interest in copper sensing in the past decade, given the biological importance of

15 copper as well as its presence as a potential contaminant in water and fuels. Molecules used for

16 copper(II) sensing generally consist of a fluorophore/chromophore and a ligand for selective

17 metal ion recognition. This review article focuses on literature contributions since the year 2010

18 concerning small molecule copper(II) sensors that provide a naked-eye color response in

19 solution. We present molecular structural features and sensing mechanisms for the colorimetric

20 and fluorometric detection of copper(II) ions in different environmental, agricultural, and

21   biological samples. In addition, the sensing performance of these chemosensors is compared and

22   discussed, which could aid in the future design of chemosensors for copper(II). Finally, we

23   outline the challenges and future prospects of fluorophore/chromophore–ligand chemistry in

24   applications of small molecules for fluorometric and colorimetric assays of copper(II).

25

26   Keywords: copper, naked-eye, detection limit, chemosensor

27   **Contents**

46

1. Introduction

Copper is a first-row transition metal and an essential trace mineral that plays key roles in physiological functions, such as serving as a cofactor for many enzymes involved in energy production and metabolism [1]. However, as with many essential minerals, excessive amounts can result in toxicity. Copper is common in the environment and contamination of soil and waterways can occur from agricultural sources, where copper is found in pesticides and fertilizers, and from industrial sources, such as mining and manufacturing operations [2]. The World Health Organization (WHO) has determined the maximum acceptable level of copper in drinking water to be 2 mg/L (31.5 µM) [3] and the Environmental Protection Agency (EPA) sets the threshold at 1.3 mg/L (20.5 µM) [4]. Due to the potential health risks of environmental copper contamination, there is great interest in methods for the analytical detection of Cu^{2+} ions, particularly for use in field applications. The use of colorimetric sensors offers quick and accurate naked-eye detection without the need for expensive instrumentation, such as inductively coupled plasma mass spectrometry and atomic absorption spectrometry. Several colorimetric and fluorescent sensors with structures ranging from small molecules, large macrocycles [5–9], and nanoparticle/quantum dots have been created [10–16]. The strong interest in copper sensors is highlighted by a recent PubMed search for "colorimetric copper sensor", which revealed a steady

64 increase in the numbers of copper sensors reported from 2007-2019 (decreasing number of

65 reports from 2020-21 were likely due to work disruption during the 2020 COVID pandemic)

66 (**Fig. 1**).
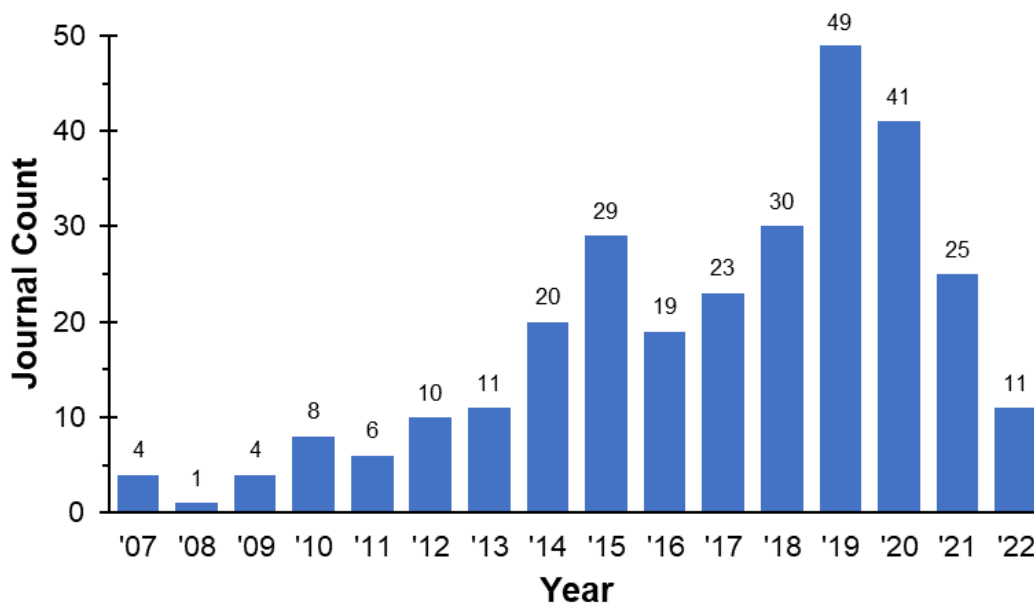
67

68 *Fig. 1: PubMed search of "colorimetric copper sensor" resulting in the depiction of published*

69 *copper sensors over the years 2007-2022.*

70   To date, most reviews on copper(II) sensors report fluorescent sensors for copper(II) [17–

71 22]. However, there have been fewer reviews addressing small molecules for the colorimetric

72 detection of copper(II). These reviews were narrowly focused on copper(II) sensors that are

73 carbohydrate-based [23], pyrene-based [24] or reviewed from the years 2013-2015 [25]. Other

74 reviews discuss colorimetric and fluorescent copper(II) sensors in a range of sizes such as small

75 molecules, enzymes, polymers and nanoparticles [26,27] or organize by the type of optical

76 emission   produced   (colorimetric,   fluorescent,   luminescent,   chemiluminescent,

77 photoluminescent, surface plasmon resonance) from these copper(II) sensors [28]. Further

78 reviews on colorimetric sensing of metals have broadly focused on a number of metals [29–32].

79   This review focuses on small molecule copper(II) sensors that offer a colorimetric

80 response in solution, with naked eye detection, published in the years 2010-2022. We felt that

81 researchers developing new copper sensors, or who are interested in using copper sensors, might

82 be most concerned about sensitivity as a starting point. 102 sensors are reviewed and are

83 organized by their reported limits of detection (LOD) by absorbance or fluorescence

84 spectroscopy. Sensors that did not report colorimetric LOD but only fluorescence LOD are

85 organized into a separate section. Sensors that possessed naked-eye detection but did not report a

86 LOD are included at the end of the review

87

88 **2. Determination of the limit of detection**

89   When evaluating the performance of a sensor for further development or potential

90 application, one of the most salient features of interest to users is the limit of detection (LOD).

91 The LOD is defined as the lowest concentration of analyte that can be consistently detected

92 within a degree of certainty, usually 95% or higher [33]. Upon evaluation of the literature, there

93 are two common methods used in detecting LOD. The first method determines the LOD from

94 standard deviations at a low concentration [33–36]. The second method determines the LOD

95 using standard deviations of the response and slope [34–37]. Although there is no consensus on

96 which method is best, the one employed most often by articles in this review was the second

97 method. Briefly, the standard deviations of the response and slope method uses the equation

98 $LOD = 3\sigma/k$, where σ = standard deviation and k = slope of the calibration curve. The standard

99   deviation can be calculated from a group of blank samples [38] or using the regression function

100   on the calibration curve [34]. The slope of the calibration curve is calculated by examining the

101   absorbance or fluorescence intensity change with varying Cu^{2+} concentration. For example, in a

102   "turn-on" sensor, an absorbance or fluorescence wavelength is initially silent and displays no

103   signal. Once Cu^{2+} is introduced at increasing concentrations, a noticeable increase in absorbance

104   or fluorescence intensity is observed. The maximum wavelength of the peak is identified, and

105   these values are plotted against the Cu^{2+} concentration used, which ultimately provides the slope.

106

107   **3. Limit of detection determined by fluorescence spectroscopy**

108   The sensors in this section calculated their respective LOD's using a fluorometer (Table 1

109   – Table 5). Even though fluorometry was used, all the sensors provided naked-eye detection for

110   copper(II). In fact, seven sensors can be found in two tables (Sensor **3** = Table 1 & 11, Sensor **4**

111   = Table 1 & 6, Sensor **7** = Table 2 & 8, Sensor **13** = Table 2 & 7, Sensor **20** = Table 3 & 8,

112   Sensor **23** = Table 4 & 7, Sensor **31** = Table 5 & 8) as they reported LODs that were calculated

113   using UV-Vis and fluorescence spectroscopy. Since a fluorometer is more sensitive than a UV-

114   Vis, it was not surprising to see that the lowest LOD determined via fluorescence spectroscopy

115   was 1 nM, while the lowest LOD determined via UV-Vis was 8.6 nM.

116   ***3.1   1.0 nM - 9.9 nM***

117   Paul et al. [39] synthesized a quinazoline functionalized benzimidazole-based fluorescent

118   "on-off" sensor **2** for Cu^{2+} detection (Table 1 Sensor #2). When one equivalent of Cu^{2+} was

119   gradually added into 5 μM of **2** in DMF:20 mM HEPES (1:1, v/v, pH = 7.4), the fluorescence

120   intensity at 425 nm was dramatically reduced by *ca.* 58-fold in *ca.* 2.5 min, which was not

121 observed in other metal ions. **2** showed a 1:1 metal–ligand stoichiometry with a binding constant

122 of 2.6×10^4 M^{-1} and a low LOD of 1.62 nM for Cu^{2+}. In the presence of 2 equivalents of S^{2-}, a

123 significant increase in fluorescence at 425 nm was observed because of S^{2-}-induced displacement

124 of Cu^{2+} from the weakly fluorescent **2**–Cu^{2+} complex. Bioimaging studies demonstrated the

125 utility of sensor **2** (5 μM) for the detection of 5 μM Cu^{2+} and 10 μM S^{2-} in DL (1 x 10^6) cancer

126 cells.

127 A Schiff-base in the form of acylhydrazine derivative was utilized for metal ion

128 coordination. Wang (2020) et al. [40] synthesized a coumarin-appended naphthohydrazide **4** "on-

129 off" sensor by condensation of 7-diethylaminocoumarine-3-aldehyde and 3-hydroxy-2-

130 naphthohydrazide (Table 1 Sensor #4). Fluorescent sensor **4** (2.5 μM) could recognize 1

131 equivalent of Cu^{2+} and Co^{2+} selectively over a wide range of biologically and environmentally

132 relevant metal ions in EtOH:10 mM phosphate buffer (7:13, v/v, pH = 7.2), with a color change

133 from green to colorless under UV light, and from yellow to orange-red under ambient light. The

134 fluorescent quenching of **4** upon addition of 2.5 μM Cu^{2+} was attributed to the binding of

135 carbonyl oxygen and imine nitrogen atoms of the acylhydrazide moiety with Cu^{2+} following a 2:1

136 ligand–metal stoichiometry. In the presence of 25 μM GSH, the fluorescence at 525 nm was

137 restored, which is likely due to the displacement of Cu^{2+} by GSH, liberating fluorescent sensor **4**.

138 This fluorescence recovery was not observed for Co^{2+} (**Fig. 2**). Adjusting pH to 4 using 0.1 M

139 HCl or HNO_3 would also allow **4** to distinguish between the two metal ions as **4**-Cu^{2+} complex is

140 nonfluorescent while **4**-Co^{2+} complex is fluorescent (**Fig. 2**). As shown in **Fig. 2**, this

141 chemosensor was successfully applied to visualize and monitor Cu^{2+}/Co^{2+} in MCF-7 breast

142 cancer cells and zebrafish larvae by incubating **4** (2.5 μM, 1 h) to demonstrate its efficacy in
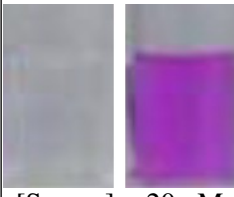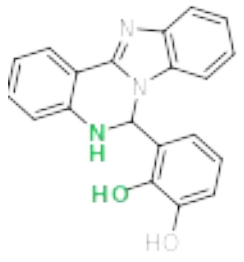
143 bioimaging
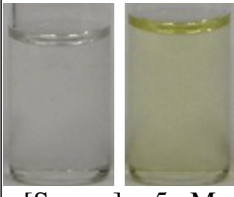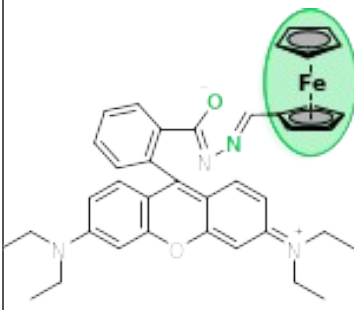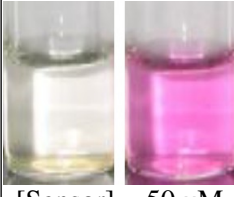

144
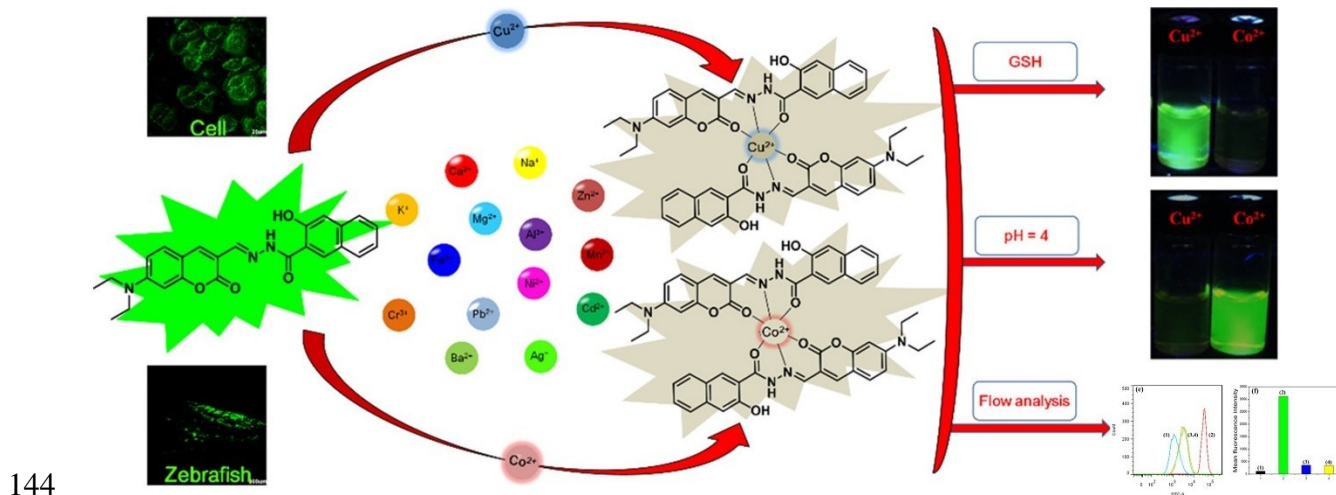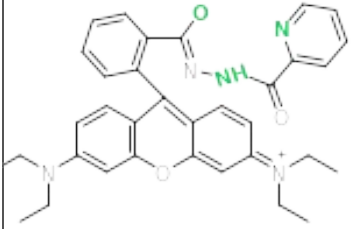
Fig. 2: *Sensor **4** produces a green fluorescent color under 365 nm UV light. Fluorescence*
145

146 *imaging of MCF-7 breast cancer cells and zebrafish larvae incubated with **4** (2.5 μM, 1hr)*

147 *demonstrates intracellular permeation. **4** displays a "turn-off" fluorescence signal upon the*

148 *addition of 2.5 μM copper(II) or cobalt(II), over competing metal ions. In a solution of **4** (2.5*

149 *μM), copper(II) (0.5 eq.) and cobalt(II) (0.5 eq.), the binding of cobalt(II) to **4** can be*

150 *distinguished by adding 10 eq. of GSH. Vice versa, under the same conditions, the binding of*

151 *copper(II) to **4** can be distinguished by adjusting the pH to 4. Flow analysis quantitatively*

152 *proved this quenching in MCF-7 cells. Reproduced from Wang(2020) et al. [40].*

153   Liu (2020) et al. [41] designed and synthesized a highly sensitive and selective Schiff

154 base "on-off" sensor **5** using naphthalimide fluorophore and thiophene moiety that was able to

155 achieve a LOD of 9.15 nM (Table 1 Sensor #5). Fluorescent data revealed a 1:1 metal–ligand

156 stoichiometry in **5**–Cu^{2+} complex, and the binding constant was calculated to be 2.23 x 10^4 M^{-1}.

157 The proposed Cu^{2+} coordination with probe **5** could be described by soft-soft metal-donor

158 interaction between Cu^{2+} and the sulfur atom of thiophene moiety and the nitrogen atom of the

8

159 amino group in **5**. Fluorescence quenching was observed upon the addition of 25 µM Cu^{2+} in a 10

160 µM probe **5** solution in MeCN: H_2O (3:1, v/v) due to Cu^{2+}-induced hydrolysis forming a

161 nonfluorescent product. Probe **5** (10 µM) was successfully applied for detecting Cu^{2+} in ultrapure

162 and tap water samples spiked with 6 µM, 12µM, and 18 µM copper(II) to display its accuracy in

163 aqueous conditions. Also, the low cytotoxicity of probe **5** (0.5 µM) made it possible to detect

164 Cu^{2+} (10 µM) ions in human hepatoma cells, HepG2.
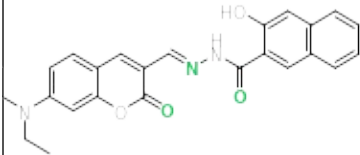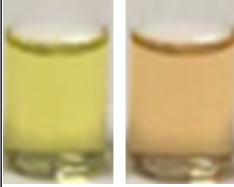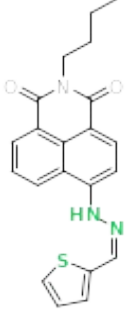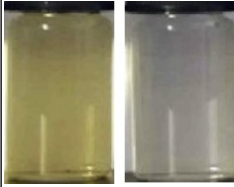
Limit of Detection Determined by Fluorescence Spectroscopy
1.0 nM – 9.9 nM

Sensor #	Cu²⁺ Sensor	Ion Sensing	Cu²⁺ LOD	K_a	Binding Stoichiometry Sensor: Cu²⁺	Naked-Eye Detection [Sensor]: [Cu²⁺]	Cu²⁺ Selectivity Assay Conditions	Solvent	Ref
1		Cu²⁺ & ClO⁻ Colorimetric & Fluorometric	1 nM	3.9×10^5 M⁻¹ UV-Vis 1.79×10^6 M⁻¹ Fluorometer	1:1	[Sensor] = 20 µM [Cu²⁺] = 160 µM	[Sensor] = 20 µM [Cu²⁺] = 160 µM [Competing Metal Ions] = 160 µM	MeCN: 10 mM Tris-HCl (9:1, v/v) pH= 7.0	[42]
2		Cu²⁺ & S²⁻ Colorimetric & Fluorometric	1.62 nM	3.8×10^4 M⁻¹ UV-Vis 2.6×10^4 M⁻¹ Fluorometer	1:1	[Sensor] = 5 µM [Cu²⁺] = 5 µM	[Sensor] = 5 µM [Cu²⁺] = 5 µM [Competing Metal Ions] = 5 µM	DMF: 20 mM HEPES (1:1, v/v) pH = 7.4	[39]
3		Cu²⁺ Colorimetric & Fluorometric	2.0 nM	4.65×10^7 M⁻¹ Fluorometer	2:1	[Sensor] = 50 µM [Cu²⁺] = 100 µM	[Sensor] = 20 µM [Cu²⁺] = 20 µM [Fe³⁺, Al³⁺ & Hg²⁺] = 20 µM [Competing Metal Ions] = 200 µM	MeCN: HEPES (1:3, v/v) pH=7.1	[43]

Limit of Detection Determined by Fluorescence Spectroscopy									
1.0 nM – 9.9 nM									
Sensor #	Cu²⁺ Sensor	Ion Sensing	Cu²⁺ LOD	K_a	Binding Stoichiometry Sensor: Cu²⁺	Naked-Eye Detection [Sensor]: [Cu²⁺]	Cu²⁺ Selectivity Assay Conditions	Solvent	Ref
4		**Cu²⁺ & Co²⁺** Colorimetric & Fluorometric	**3.84 nM**	**1.26 x 10⁶ M⁻¹** Fluorometer	**2:1**	[Sensor] = 10 µM [Cu²⁺] = 10 µM	[Sensor] = 2.5 µM [Cu²⁺] = 2.5 µM [Competing Metal Ions] = 2.5 µM	EtOH:10 mM Phosphate buffer (7:13, v/v) pH= 7.2	[40]
5		**Cu²⁺** Colorimetric & Fluorometric	**9.15 nM**	**2.23 x 10⁴ M⁻¹** Fluorometer	**1:1**	[Sensor] = 10 µM [Cu²⁺] = 50 µM	[Sensor] = 10 µM [Cu²⁺] = 50 µM [Competing Metal Ions] = 100 µM	MeCN: H₂O (3:1, v/v) pH = 7.4	[41]

Table 1: Copper(II) sensors arranged from lowest to highest limit of detection in the range of 1.0 nM – 9.9 nM determined by fluorescence spectroscopy. Information provided: Sensor number, chemical structure (green atoms indicate the proposed mechanism of Cu²⁺ coordination. Shaded green indicates the proposed sensing unit/s in Cu²⁺ coordination), additional cations and anions detected by the sensor, K_a = association constant, binding stoichiometry (sensor: Cu²⁺), concentration of sensor and Cu²⁺ for naked eye detection, the Cu²⁺ selectivity assay conditions including concentration of sensor, Cu²⁺ and competing metal ions tested and solvent.

3.2   10.0 nM – 36 nM

171   Fang et al. [44] synthesized a weakly fluorescent *p*-dimethylaminobenzamide derivative

172   as an "off-on" fluorescence sensor for Cu^{2+} detection (Table 2 Sensor #7). When Cu^{2+} was

173   gradually added to 1 μM of **7** in MeCN:Tris-HCl (3:2, v/v, pH = 7.4), the fluorescence intensity

174   at 470 nm was greatly enhanced, with the color change from colorless to yellow. **7** showed a 1:1

175   stoichiometry with a binding constant of 5.4×10^7 M^{-1} and a low LOD of 15 nM for Cu^{2+}.

176   Fluorescence intensity at 470 nm decreased upon gradual addition from 0 μM - 16 μM of S^{2-} into

177   a solution of 1 μM of **7**–Cu^{2+} complex. Complete conversion from **7**-Cu^{2+} to **7** was achieved once

178   10 μM of S^{2-} was added with a response time of 2 min. Subsequent addition of 1 μM Cu^{2+}

179   restored the fluorescence. The reversibility of **7** was tested with 5 cycles of Cu^{2+} followed by S^{2-}

180   addition and showed minimal decay, confirming the potential to be a reusable sensor.

181   Kaur et al. [45] reported a ratiometric fluorescent sensor **10** based on carbazole as the

182   fluorophore and pyrimidine as the metal coordinating unit (Table 2 Sensor #10). Titration of 1

183   μM **10** in THF:HEPES buffer (7:3, v/v, pH 7.4) with Cu^{2+} (0.01 - 2 equivalents) exhibited a

184   significant emission intensity reduction at 505 nm and an emission intensity increase at 663 nm.

185   The emission intensity ratio (I_{663}/I_{505}) changed from 0.014 to 12 upon the addition of 2

186   equivalents of Cu^{2+}. The paramagnetic nature of Cu^{2+} and the proximity of this ion to the

187   carbazole units might have contributed to the reduction in emission intensity at 505 nm. On the

188   other hand, coordination of Cu^{2+} in the pyrimidine moiety could prevent the photo-induced

189   electron transfer process from taking place from the pyrimidine unit to carbazole moiety, leading

190   to an emission intensity enhancement at 663 nm. Binding of Cu^{2+} to **10** followed 1:1

191   stoichiometry with a binding constant of 1.6×10^7 M^{-1}. While **10** is sensitive (LOD: 21 nM) to

192   Cu^{2+}, it also responds to Hg^{2+}. It is, therefore, necessary to perform pretreatment methods to mask

193   Hg^{2+} before detecting Cu^{2+} levels in samples that also contain Hg^{2+}.

194   Biao Gu et al. [46] prepared a dicyanometylene-4H-pyran-based "off-on" probe **11** where

195   a dicyanometylene-4H-pyran derivative serves as the fluorophore and the 2-picolinic ester group

196   as the Cu^{2+} recognition unit (Table 2 Sensor #11). The 2-pyridinecarbonyl group protecting the

197   hydroxyl prevents the intramolecular charge transfer process from taking place, resulting in

198   fluorescence quenching of probe **11**. Upon addition of 20 μM Cu^{2+}, **11** (10 μM) in 10 mM

199   PBS:DMSO (1:1, v/v, pH 7.4) exhibited naked-eye color change from yellow to purple with

200   significant NIR fluorescent enhancement at 676 nm. This enhancement was attributed to Cu^{2+}-

201   promoted hydrolysis of the picolinoyl ester moiety leading to the release of the fluorophore with

202   a deprotonated hydroxyl group (**Fig. 3**). This reaction-based copper(II) sensing possesses good

203   selectivity against biologically and environmentally relevant metal ions. It also exhibited a linear

204   relationship in the range of 0–8 μM with an LOD of 23 nM. The favorable sensing properties of

205   **11** such as its low cytotoxicity and good membrane permeability make this molecule a promising

206   sensor for the detection of Cu^{2+} in biological systems.
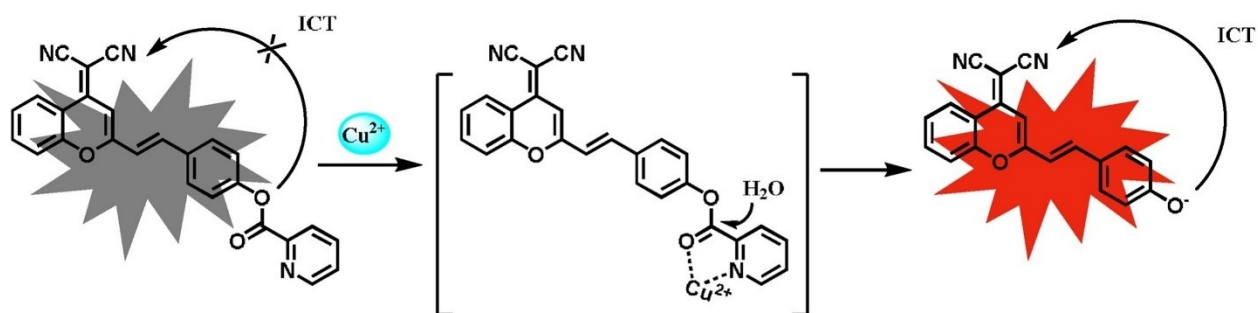
207

208   ***Fig. 3****: In the presence of Cu^{2+}, weakly fluorescent probe **11** (left structure) is hydrolyzed into a*

209   *highly fluorescent dicyanometylene-4H-pyran derivative with deprotonated hydroxyl group*

210   *(right structure), enabling intramolecular charge transfer in **11***. *Reproduced from Biao Gu et al.*
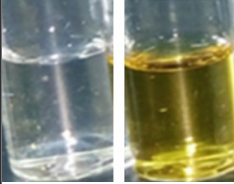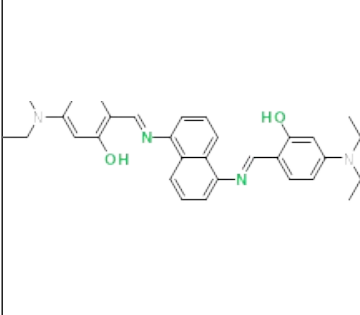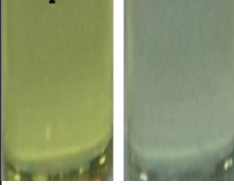
211   *[46].*

212
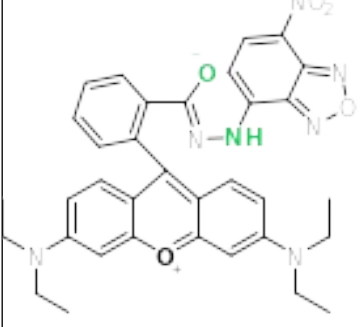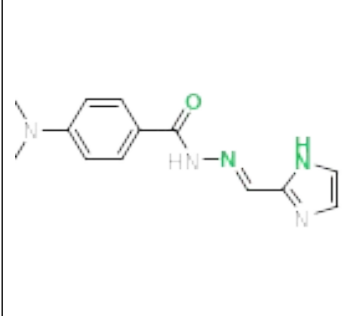
213   Xie et al. [47] reported a rhodamine derivative of spirolactam **13** "on-off" ratiometric

214   sensor, which was synthesized by a condensation reaction of 3-(benzo[*d*]thiazol-2-yl)-2-

215   hydroxy-5-methylbenzaldehyde and rhodamine 101 hydrazide (Table 2 Sensor #13). The Cu^{2+}-

216   induced spirolactam ring-opening of **13** resulted in fluorescence enhancement at 600 nm (λ_{ex} =

217   540 nm) in 10 mM PBS:40% EtOH (1:1, v/v, pH 7.4). On the other hand, excitation at 350 nm

218   led to an increase in fluorescence at 565 nm along with a decrease in fluorescence intensity at

219   460 nm giving rise to a 6.4-fold change for I_{460}/I_{565} in the presence of 0.5 equivalent Cu^{2+}. The

220   LOD obtained from ratiometric fluorometric measurements was 26 nM. A linear relationship was

221   observed between 0 and 10 μM Cu^{2+} when I_{460}/I_{565} was plotted as a function of Cu^{2+}

222   concentration. Job's plot analysis revealed a metal-ligand stoichiometry of 1:1 with a binding

223   constant of 9.94×10^4 M^{-1} for **13**–Cu^{2+} complex, where Cu^{2+} is coordinated to the carbonyl O,

224   imino N, and phenolic O atoms of **13**. The free **13** could be released from the complex upon the

225   addition of EDTA, indicating the reversibility of the sensing process. Finally, probe **13** exhibited

226   good recoveries (91.6–103.0%) in the determination of spiked Cu^{2+} in water samples and in

227   serum.

228   Guo et al. [48] designed and synthesized a fluorescent "on-off" chemosensor **14**

229   possessing an oligothiophene as the fluorophore and an appended Schiff-base as the Cu^{2+}

230   coordinating unit (Table 2 Sensor #14). In the presence of 2 equivalents of Cu^{2+} in DMF:H_2O

231   (2:3, v/v), 5 μM **14** exhibited fluorescence quenching at 580 nm, which may be attributed to the

232   paramagnetic nature of Cu^{2+}. Binding of Cu^{2+} with **14** followed 1:1 stoichiometry with a binding

233   constant of 2.52×10^4 M^{-1}. The facile preparation, excellent sensitivity (LOD: 28.1 nM Cu^{2+}) and

234   selectivity for Cu^{2+} in an aqueous system, and high recoveries in water and food samples (97.6–

235   102.3%) make **14** a promising sensor for the analysis of Cu^{2+} in different samples. Su et al. [49]

236   also used a Schiff-base as the metal ion recognition unit and an *N,N*-diethyl group as the

237   fluorophore in the design of their fluorescent "on-off" sensor **14** that was able to achieve a LOD

238   of 16.09 nM (Table 2 Sensor #63). Upon addition of 400 μM Cu^{2+} to 20 μM of **14**, the formation

239   of the **14**-Cu^{2+} complex led to a significant decrease in fluorescence and a hypsochromic shift in

240   fluorescence emission from 498 to 480 nm in DMSO:H$_2$O (9:1, v/v, pH = 7.2). The fluorescence

241   was recovered upon addition of 1 mM H$_2$PO$_4^-$ into the **14**-Cu^{2+} complex solution and was

242   quenched again after adding Cu^{2+}, indicating reversibility of the sensing process. A change in the

243   molecular planarity of **14** due to Cu^{2+} coordination was proposed as the mechanism of
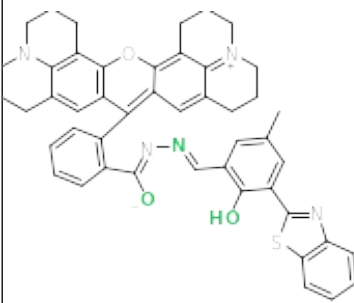
244   fluorescence quenching.
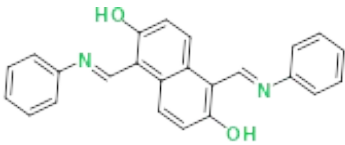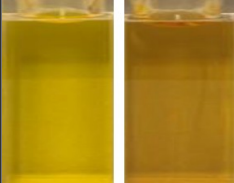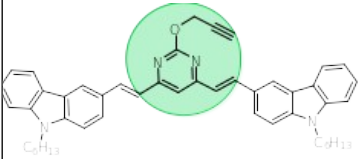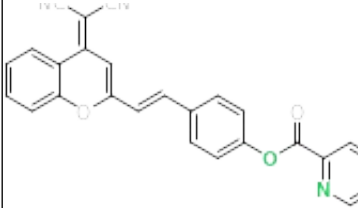
Limit of Detection Determined by Fluorescence Spectroscopy
10.0 nM – 36 nM

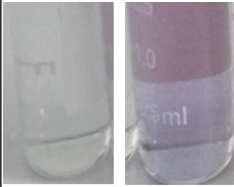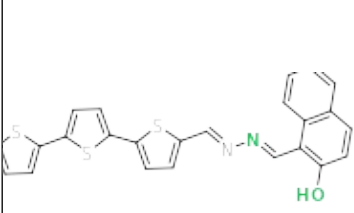| Sensor #	Cu²⁺ Sensor	Ion Sensing	Cu²⁺ LOD	K_a	Binding Stoichiometry Sensor: Cu²⁺	Naked-Eye Detection [Sensor]: [Cu²⁺]	Cu²⁺ Selectivity Assay Conditions	Solvent	Ref
6		**Cu²⁺** Colorimetric & Fluorometric **Fe³⁺** Fluorometric	**10 nM**	**4.22 x 10⁵ M⁻¹** Fluorometer	**1:1**	[Sensor] = 1 μM [Cu²⁺] = 10 μM	[Sensor] = 1 μM [Cu²⁺] = 10 μM [Competing Metal Ions] = 10 μM	H₂O: MeCN (1:1, v/v)	[50]
7		**Cu²⁺ & S²⁻** Colorimetric & Fluorometric	**15 nM**	**4.3 x 10⁷ M⁻¹** UV-Vis **5.4 x 10⁷ M⁻¹** Fluorimeter	**1:1**	[Sensor] = 10 μM [Cu²⁺] = 500 μM	[Sensor] = 10 μM [Cu²⁺] = 500 μM [Competing Metal Ions] = 500 μM	MeCN: Tris-HCl (3:2, v/v) pH= 7.4	[44]
8		**Cu²⁺ & H₂PO₄⁻** Colorimetric & Fluorometric	**16.09 nM**	**1.19 x 10⁹ M⁻²** Fluorimeter	**1:1**	[Sensor] = 20 μM [Cu²⁺] = 184 μM	[Sensor] = 20 μM [Cu²⁺] = 1 mM [Competing Metal Ions] = 1 mM	DMSO: H₂O (9:1, v/v) pH = 7.2	[49]
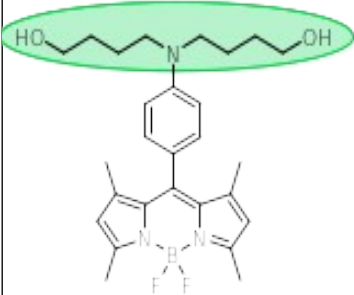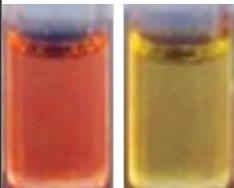
Limit of Detection Determined by Fluorescence Spectroscopy

10.0 nM – 36 nM

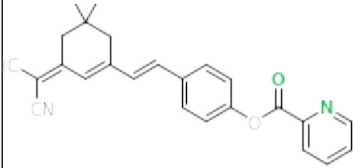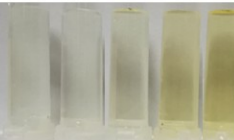| Sensor #	Cu²⁺ Sensor	Ion Sensing	Cu²⁺ LOD	K_a	Binding Stoichiometry Sensor: Cu²⁺	Naked-Eye Detection [Sensor]: [Cu²⁺]	Cu²⁺ Selectivity Assay Conditions	Solvent	Ref
9		Cu²⁺ Colorimetric & Fluorometric	16.4 nm.	1.22×10^3 M⁻² Fluorimeter	1:2	[Sensor] = 40 µM [Cu²⁺] = 200 µM	[Sensor] = 40 µM [Cu²⁺] = 200 µM [Competing Metal Ions] = 200 µM	THF: H₂O (4:1, v/v)	[51]
10		Cu²⁺ & Hg²⁺ Colorimetric & Fluorometric	21 nM	1.6×10^7 M⁻¹ Fluorimeter	1:1	[Sensor] = 3 µM [Cu²⁺] = 3 µM	[Sensor] = 1 µM [Cu²⁺] = 2 µM [Competing Metal Ions] = 10 µM	THF: HEPES (7:3, v/v) pH = 7.4	[45]
11		Cu²⁺ Colorimetric & Fluorometric	23 nM	–	1:1	[Sensor] = 10 µM [Cu²⁺] = 20 µM	[Sensor] = 10 µM [Cu²⁺] = 10 µM [Competing Metal Ions] = 100 µM	10 mM PBS: DMSO (1:1, v/v) pH = 7.4	[46]

17

Limit of Detection Determined by Fluorescence Spectroscopy
10.0 nM – 36 nM

Sensor #	Cu^{2+} Sensor	Ion Sensing	Cu^{2+} LOD	K$_a$	Binding Stoichiometry Sensor: Cu^{2+}	Naked-Eye Detection [Sensor]: [Cu^{2+}]	Cu^{2+} Selectivity Assay Conditions	Solvent	Ref
12		Cu^{2+} Colorimetric & Fluorometric	25 nM	3.7 × 10^7 M^{-1} Fluorometer	1:1	 [Sensor] = 10 µM [Cu^{2+}] = 30 µM	[Sensor] = 10 µM [Cu^{2+}] = 30 µM [Competing Metal Ions] = 500 µM	20 mM PBS buffer (10% MeCN) pH = 7.4	[52]
13		Cu^{2+}, Co^{2+} Colorimetric Cu^{2+}, Co^{2+} Ni^{2+} Fluorometric	26 nM	9.9 x 10^4 M^{-1} UV-Vis	1:1	 [Sensor] = 20 µM [Cu^{2+}] = 20 µM	[Sensor] = 20 µM [Cu^{2+}] = 20 µM [Competing Metal Ions] = 20 µM	10 mM PBS buffer: 40% EtOH (1:1, v/v) pH= 7.4	[47]
14		Cu^{2+} Colorimetric & Fluorometric	28.1 nM	2.52 x 10^4 M^{-1} Fluorometer	1:1	 [Sensor] = 5 µM [Cu^{2+}] = 10 µM	[Sensor] = 5 µM [Cu^{2+}] = 10 µM [Competing Metal Ions] = 10 µM	DMF: H$_2$O (2:3, v/v)	[48]

Limit of Detection Determined by Fluorescence Spectroscopy									
10.0 nM – 36 nM									
Sensor #	Cu²⁺ Sensor	Ion Sensing	Cu²⁺ LOD	K_a	Binding Stoichiometry Sensor: Cu²⁺	Naked-Eye Detection [Sensor]: [Cu²⁺]	Cu²⁺ Selectivity Assay Conditions	Solvent	Ref
15		Cu²⁺ Colorimetric & Fluorometric	36 nM	–	1:1	**[Cu²⁺] μM** 0 0.1 1 2 4 [Sensor] = 10 μM [Cu²⁺] = 0-4 μM	[Sensor] = 10 μM [Cu²⁺] = 10 μM [Competing Metal Ions] = 20 μM	10 mM PBS buffer (20% DMSO) pH = 7.45	[53]

Table 2: Copper(II) sensors arranged from lowest to highest limit of detection in the range of 10.0 nM – 36 nM determined by fluorescence spectroscopy. Information provided: Sensor number, chemical structure (green atoms indicate the proposed mechanism of Cu²⁺ coordination. Shaded green indicates the proposed sensing unit/s in Cu²⁺ coordination), additional cations and anions detected by the sensor, K_a = association constant, binding stoichiometry (sensor: Cu²⁺), concentration of sensor and Cu²⁺ for naked eye detection, the Cu²⁺ selectivity assay conditions including concentration of sensor, Cu²⁺ and competing metal ions tested and solvent.

3.3   40.0 nM - 190 nM

251   Mani et al. [54] synthesized a coumarin-based hydrazone "on-off" sensor **16** by

252 combining *N,N'*-diethylamino-3-acetyl coumarin and 2-hydrazino benzothiazole (Table 3 Sensor

253 #16). **16** (5 μM) showed high selectivity towards Cu^{2+} (5 μM) over other biologically and

254 environmentally relevant metal ions via the intramolecular charge transfer (ICT) mechanism.

255 The fluorescence quenching upon the addition of Cu^{2+} in the DMF solvent system of **16** was

256 attributed to the chelation of Cu^{2+} through coumarin carbonyl O, benzothiazole N, and hydrazine

257 N of **16**, following a 1:1 metal–ligand stoichiometry. Fluorescence microscopic experiment

258 results showed that **16** could be used for monitoring Cu^{2+} in HeLa cells (cervical cancer cells)

259 due to its low toxicity, good cell permeability, and low LOD of 40 nM.

260   Hanmeng et al. [55] employed an "on-off" fluorescent sensor **17** (LOD = 47 nM) that is

261 based on heptamethine cyanine dyes for Cu^{2+} (Table 3 Sensor #17). These dyes are known to

262 exhibit absorption and emission bands reaching the near-infrared (NIR) range, where absorption

263 and autofluorescence of a biological matrix are said to be minimum. In the presence of 12 μM

264 Cu^{2+}, the naked-eye color of 10 μM **17** in HEPES:MeCN (3:7, v/v, pH 7.2) changed from blue to

265 colorless. In the fluorescence emission spectrum, the addition of 8 μM Cu^{2+} resulted in a dramatic

266 fluorescence quenching of 5 μM **17** following an intramolecular charge transfer (ICT) upon

267 binding of soft Cu^{2+} with the soft sulfur atoms in **17**. The resulting **17**-Cu^{2+} complex followed a

268 1:1 stoichiometry and had a binding constant of 1.24×10^6 M^{-1}. The sensing utility of **17** was

269 tested in hydroponic fertilizers and HepG2, human hepatoma cells. The cell experiments

270 demonstrated that Cu^{2+} was able to be intracellularly recognized by **17** in living cancer cells.

271   Rhodamine-based fluorophores have been widely used in designing "off-on" fluorescence

272   chemosensors because of their favorable molar extinction coefficient, high fluorescence quantum

273   yields, and good photostability. Nair et al. [56] synthesized a highly sensitive (LOD: ~3 ppb)

274   rhodamine 6G hydrazide "off-on" fluoroprobe **18** as a Cu^{2+}-specific chemosensor (Table 3 Sensor

275   #18). **18** (10 μM) exhibited an approximately 25-fold fluorescent enhancement at 553 nm upon

276   addition of 1 equivalent of Cu^{2+} in MeCN:50 mM HEPES buffer (1:1 v/v, pH = 7.4). Binding of

277   Cu^{2+} was proposed to occur at the ONN donor sites of probe **18** following a 1:1 metal–ligand

278   stoichiometry. Incubation of Brine shrimp *Artemia* with different concentrations of Cu^{2+} (84, 64,

279   42, and 9 ppb) followed by exposure to probe **18** (2 equivalents) highlighted the intrinsic

280   bioaccumulation nature of *Artemia* as **18** can detect Cu^{2+} even at a very low concentration of 10

281   ppb, indicating the potential applications of **18** in bioimaging and monitoring Cu^{2+}-induced

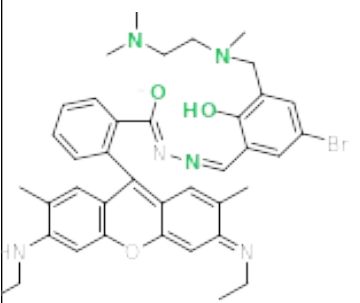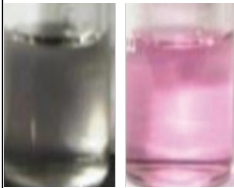282   pollution.
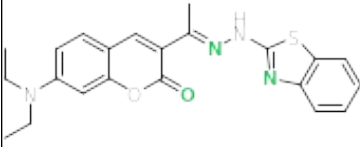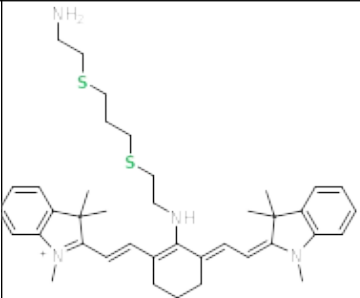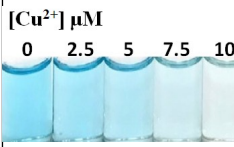
283   Deepa et al. [57] reported a rhodamine 6G derivative **19** as an "off-on" sensor for Cu^{2+}

284   detection that attained a LOD of 74 nM (Table 3 Sensor #19). Free **19** in DMSO:H_2O (1:9, v/v)

285   is weakly fluorescent. However, fluorescent enhancement was observed upon the addition of

286   Cu^{2+}, which could be attributed to the photoinduced electron transfer (PET) mechanism. Cu^{2+}

287   binds to **19** in 1:1 stoichiometry with a binding constant of 5.2×10^6 M^{-1}. The addition of EDTA

288   to the **19**-Cu^{2+} complex resulted in fluorescence quenching, suggesting the reversibility of the

289   Cu^{2+} sensing process.

290   Chen et al. [58] synthesized a fluorescent "on-off" sensor **20** using a bis(2-

291   pyridylmethyl)amine as the metal recognition and electron-donating unit and 2-(3-cyano-4,5,5-

292   trimethylfuran-2(5*H*)-ylidene)malononitrile) as the electron-accepting moiety (Table 3 Sensor #20).

293   **20** (10 μM) exhibited pronounced fluorescent quenching in the presence of Cu^{2+} (50 μM) in

294   EtOH:HEPES (1:4, v/v, pH = 7.2), which remained unaffected in the presence of other metal

295   ions (50 μM). The significant fluorescence quenching is likely due to the paramagnetic nature of

296   Cu^{2+}. Also, the electron-donating ability of bis(2-pyridylmethyl)amine is expected to decrease as

297   a result of Cu^{2+} coordination, leading to a reduced intramolecular charge transfer. Probe **20** was

298   successfully affixed to a paper strip for sensing Cu^{2+} and reached a detection limit of 1 μM,

299   where the fluorescence signal was generated upon excitation using a UV lamp.
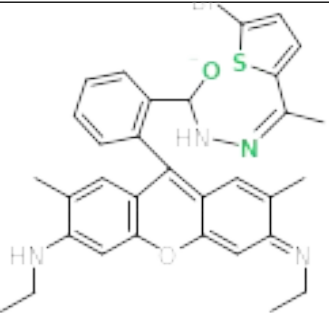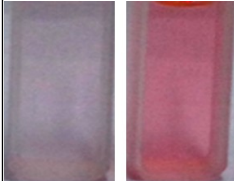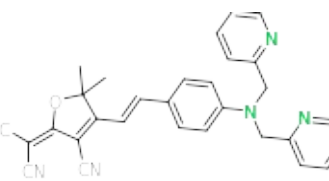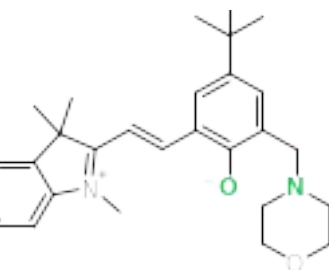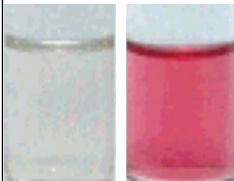
Limit of Detection Determined by Fluorescence Spectroscopy
40.0 nM – 190 nM

Sensor #	Cu²⁺ Sensor	Ion Sensing	Cu²⁺ LOD	K_a	Binding Stoichiometry Sensor: Cu²⁺	Naked-Eye Detection [Sensor]: [Cu²⁺]	Cu²⁺ Selectivity Assay Conditions	Solvent	Ref
16		Cu²⁺ Colorimetric & Fluorometric	40 nM	$4.89 \times 10^5 \, M^{-1}$ Fluorometer	1:1	 [Sensor] = 5 µM [Cu²⁺] = 5 µM	None	DMF	[54]
17		Cu²⁺ Colorimetric & Fluorometric	47 nM	$1.24 \times 10^6 \, M^{-1}$ Fluorometer	1:1	[Cu²⁺] µM 0 2.5 5 7.5 10 [Sensor] = 5 µM [Cu²⁺] = 10 µM	[Sensor] = 5 µM [Cu²⁺] = 0.5 µM [Competing Metal Ions] = 5 µM	HEPES: MeCN (3:7, v/v) pH = 7.2	[55]
18		Cu²⁺ Colorimetric & Fluorometric	~3 ppb ~47.2 nM	$0.44 \times 10^5 \, M^{-1}$ UV-Vis $0.3 \times 10^5 \, M^{-1}$ Fluorometer	1:1	 [Sensor] = 10 µM [Cu²⁺] = 30 ppb = 0.47 µM	[Sensor] = 10 µM [Cu²⁺] = 50 µM [Competing Metal Ions] = 50 µM	MeCN: 50 mM HEPES (1:1, v/v) pH = 7.4	[56]

Limit of Detection Determined by Fluorescence Spectroscopy
40.0 nM – 190 nM

Sensor #	Cu²⁺ Sensor	Ion Sensing	Cu²⁺ LOD	K_a	Binding Stoichiometry Sensor: Cu²⁺	Naked-Eye Detection [Sensor]: [Cu²⁺]	Cu²⁺ Selectivity Assay Conditions	Solvent	Ref
19		**Cu²⁺** Colorimetric & Fluorometric	**74 nM**	**5.2 x 10⁶ M⁻¹** Fluorometer	**1:1**	 [Sensor] = 10 μM [Cu²⁺] = 100 μM	[Sensor] = 10 μM [Cu²⁺] = 100 μM [Competing Metal Ions] = 100 μM	DMSO: H_2O (1:9, v/v)	[57]
20		**Cu²⁺** Colorimetric & Fluorometric	**102 nM**	**3.6 x 10⁴ M⁻¹** Fluorometer	**1:1**	 [Sensor] = 10 μM [Cu²⁺] = 50 μM	[Sensor] = 10 μM [Cu²⁺] = 50 μM [Competing Metal Ions] = 50 μM	EtOH: HEPES (1:4, v/v) pH= 7.2	[58]
21		**Cu²⁺** Colorimetric & Fluorometric	**106 nM**	**1.21 x 10⁴ M⁻²** Fluorometer	**2:1**	 [Sensor] = 100 μM [Cu²⁺] = 50 μM	[Sensor] = 200 μM [Cu²⁺] = 2, 20 & 200 μM Competing Mixture [Li⁺, K⁺, Ca²⁺, Mg²⁺] = 0.1 M [Hg²⁺, Zn²⁺, Cd²⁺, Ni²⁺, Fe³⁺, Pb²⁺] = 50 μM [Gly, His, Cys, Glu, Asp] = 50 μM [BSA] = 0.1 mg/mL	50% EtOH: H_2O (1:1, v/v)	[59]

300 **Table 3**: Copper(II) sensors arranged from lowest to highest limit of detection in the range of 40.0 nM – 190 nM determined by fluorescence
301 spectroscopy. Information provided: Sensor number, chemical structure (green atoms indicate the proposed mechanism of Cu^{2+} coordination. Shaded
302 green indicates the proposed sensing unit/s in Cu^{2+} coordination), additional cations and anions detected by the sensor, K_a = association constant,
303 binding stoichiometry (sensor: Cu^{2+}), concentration of sensor and Cu^{2+} for naked eye detection, the Cu^{2+} selectivity assay conditions including
304 concentration of sensor, Cu^{2+} and competing metal ions tested and solvent.

3.4   0.20 μM - 0.30 μM

306   An et al. [60] synthesized a dicyanoisophorone-based derivative "off-on" sensor **22** as a

307   selective sensor for Cu^{2+} (LOD = 0.2 μM) in MeCN:10 mM HEPES buffer (1:4, v/v, pH 7.4)

308   (Table 4 Sensor #22). Weakly fluorescent **22** (quantum yield, Φ = 0.0039) used 2-picolinate as

309   the recognition unit for Cu^{2+}, which catalyzed the hydrolysis of **22** to form a fluorescent product

310   (Φ = 0.04). The formation of this fluorescent product led to a bathochromic shift from 545 nm to

311   590 nm and a fluorescent enhancement at 590 nm. Fluorescence imaging for the detection of 40

312   μM Cu^{2+} using **22** (20 μM) incubated in HeLa, cervical cancer, cells demonstrated low

313   cytotoxicity and good cell membrane permeability of the sensor.

314   Mohammadi and Ghasemi [61] developed an "on-off" fluorescent pyrimidine-based Cu^{2+}

315   sensor **23** (Table 4 Sensor #23). Upon excitation at 350 nm of **23** (10 μM) in the presence of 100

316   μM Cu^{2+} in DMSO:H_2O (8:2, v/v), there was a significant reduction in fluorescence emission at

317   507 nm, which could be attributed to the paramagnetic nature of this metal ion. The binding

318   mode of probe **23** towards Cu^{2+} follows 1:1 stoichiometry and has a binding constant of 1.55 ×

319   10^5 M^{-1}. While Cu^{2+} sensing using **23** was found to be reversible as the fluorescence profile of the

320   probe can be recovered using EDTA, detecting Cu^{2+} in Fe^{2+}-containing samples might pose some

321   problems because of Fe^{2+} fluorometric interference. Nevertheless, the colorimetric utility of

322   probe **23** has been demonstrated for detecting Cu^{2+} in well and seawater samples. To further

323   expand the application, **23** was fixed to paper to perform as **23**-based test strips in Cu^{2+} detection.

324   The test strips were exposed to a range of 0.1 μM to 50 μM Cu^{2+} concentrations, and naked-eye

325   detection of 1 μM copper(II) was observed. This makes **23** a promising in-field sensor, but since

326   Cu^{2+} was the only metal tested, it would be interesting to analyze other metal ions in this range to
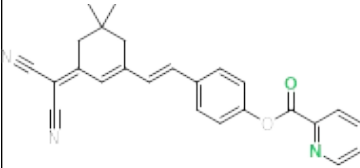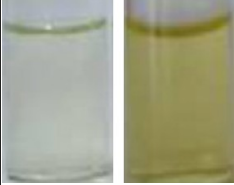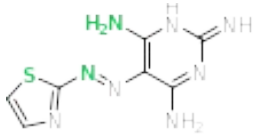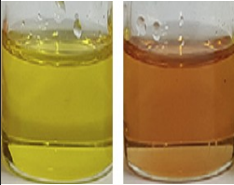
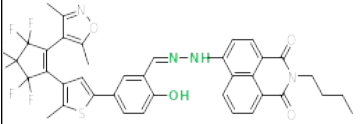327   investigate potential interference.

328   Fu et al. [62] reported an "on-off" fluorescent diarylethene-based probe **24** using 1,8-

329   naphthalimide Schiff base as Cu^{2+} recognition unit (Table 4 Sensor #24). Diarylethene-based

330   molecules are known for their excellent thermal stability and fatigue resistance, while 1,8-

331   naphthalimide is characterized by having good photostability and a large Stoke's shift. **24** in

332   MeCN exhibited reversible photoswitching when irradiated with 297 nm light followed by

333   irradiation with visible light. The fluorescence of **24** (20 μM) was selectively quenched by the

334   addition of 200 μM of Cu^{2+}, with a color change from greenish-yellow to colorless and a

335   detection limit of 2.4 μM. Fluorescence recovery was not attained upon the addition of EDTA,

336   indicating the irreversibility of the sensing process. As this sensor was used and applied in

337   organic solvents such as acetonitrile and DMSO-d_6, this might limit its application in the

338   detection of Cu^{2+} in aqueous media.

339   Zhengye Gu et al. [63] conjugated a BODIPY derivative to dipyridylamino as a metal ion

340   recognition unit to yield an "off-on" chemosensor **26** with an LOD of 0.2 μM (Table 4 Sensor

341   #26). **26** (2 μM) exhibited fluorescent enhancement in the presence of 50 μM Cu^{2+} in MeCN, with

342   a color change from dark red to green. This enhancement could be due to a relative decrease in

343   the degree of π conjugation between the BODIPY moiety and the dipyridylamino unit, resulting

344   in the inhibition of the ICT process. The binding interaction between **26** and Cu^{2+} follows 1:1

345   stoichiometry with a binding constant of 8.86×10^5 M^{-1}. The addition of EDTA into **26**-Cu^{2+}

346   solution did not restore the fluorescence profile of the solution back to that of free **26**, indicating

347   irreversibility. The use of organic solvents such as acetonitrile and the fact that it acts as a dual

348   colorimetric and fluorometric sensor for Hg^{2+} and Pb^{2+} may limit the practical applications of this
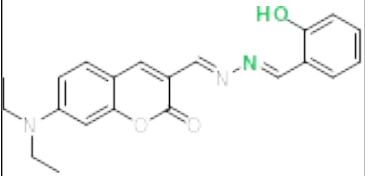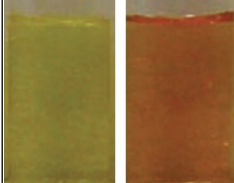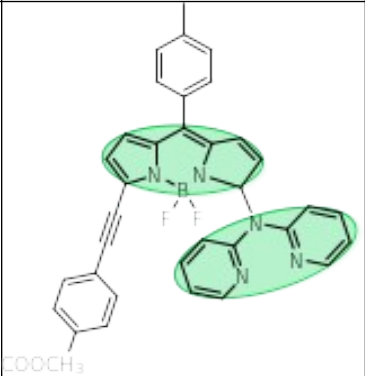
349   sensor.

Limit of Detection Determined by Fluorescence Spectroscopy

0.20 μM – 0.30 μM

Sensor #	Cu²⁺ Sensor	Ion Sensing	Cu²⁺ LOD	K_a	Binding Stoichiometry Sensor: Cu²⁺	Naked-Eye Detection [Sensor]: [Cu²⁺]	Cu²⁺ Selectivity Assay Conditions	Solvent	Ref
22		**Cu²⁺** Colorimetric & Fluorometric	**0.2 μM**	–	**reaction based**	[Sensor] = 10 μM [Cu²⁺] = 10 μM	[Sensor] = 10 μM [Cu²⁺] = 10 μM [Competing Metal Ions] = 10 μM	MeCN: 10 mM HEPES (1:4, v/v) pH = 7.4	[60]
23		**Cu²⁺ & CN⁻** Colorimetric & Fluorometric	**0.240 μM**	**$1.55 \times 10^5 \, M^{-1}$** UV-Vis	**1:1**	[Sensor] = 10 μM [Cu²⁺] = 100 μM	[Sensor] = 10 μM [Cu²⁺] = 100 μM [Competing Metal Ions] = 100 μM	DMSO: H₂O (8:2, v/v)	[61]
24		**Cu²⁺ & F⁻** Colorimetric & Fluorometric	**2.4 μM**	**$3.13 \times 10^4 \, M^{-1}$** Fluorometer	**1:1**	[Sensor] = 20 μM [Cu²⁺] = 20 μM	[Sensor] = 20 μM [Cu²⁺] = 200 μM [Competing Metal Ions] = 200 μM	MeCN	[62]

## Limit of Detection Determined by Fluorescence Spectroscopy

0.20 μM – 0.30 μM

Sensor #	Cu²⁺ Sensor	Ion Sensing	Cu²⁺ LOD	K_a	Binding Stoichiometry Sensor: Cu²⁺	Naked-Eye Detection [Sensor]: [Cu²⁺]	Cu²⁺ Selectivity Assay Conditions	Solvent	Ref
25		**Cu²⁺** Colorimetric & Fluorometric	0.27 μM	9.56×10^9 M⁻² Fluorometer	2:1	 [Sensor] = 10 μM [Cu²⁺] = 20 μM	[Sensor] = 10 μM [Cu²⁺] = 20 μM [Competing Metal Ions] = 20 μM	MeOH: 10 mM HEPES (1:1, v/v) pH = 7.0	[64]
26		**Cu²⁺, Hg⁺, Pb²⁺** Colorimetric & Fluorometric	0.27 μM	8.86×10^5 M⁻¹ Fluorometer	1:1	 [Sensor] = 2 μM [Cu²⁺] = 50 μM	[Sensor] = 2 μM [Cu²⁺] = 15 μM [Competing Metal Ions] = 50 μM	MeCN	[63]

350 **Table 4**: Copper(II) sensors arranged from lowest to highest limit of detection in the range of 0.20 μM – 0.30 μM determined by fluorescence
351 spectroscopy. Information provided: Sensor number, chemical structure (green atoms indicate the proposed mechanism of Cu²⁺ coordination. Shaded
352 green indicates the proposed sensing unit/s in Cu²⁺ coordination), additional cations and anions detected by the sensor, K_a = association constant,
353 binding stoichiometry (sensor: Cu²⁺), concentration of sensor and Cu²⁺ for naked eye detection, the Cu²⁺ selectivity assay conditions including
354 concentration of sensor, Cu²⁺ and competing metal ions tested and solvent

3.5   0.35 μM – 15 μM

356   Long et al. [65] designed and synthesized a rhodamine B hydrazone derivative **27** as a

357   highly selective "on-off" fluorescence sensor for the identification of Cu^{2+} (Table 5 Sensor #27).

358   The addition of 200 μM Cu^{2+} induced the ring-opening of the spirolactam of 20 μM of **27** in

359   DMSO:H_2O (1:9, v/v), resulting in a decrease of the emission peak at 492 nm. The addition of

360   200 μM EDTA to the **27**-Cu^{2+} complex (**Fig. 4**) could release **27** from the complex and recover

361   the fluorescence intensity of free **27** at 492 nm, indicating the reversibility of the sensor.

362   However, this reversibility was not tested for more than one cycle, therefore it is unknown how

363   practical the reversibility is.
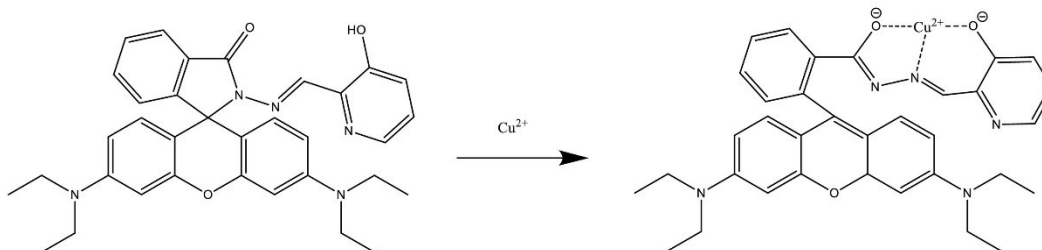
364

365   ***Fig. 4****: The proposed mechanism of Cu^{2+} coordination involving C=O, −OH, and C=N groups in*

366   ***27*** *is supported by the Cu^{2+}-induced changes in the stretching vibration absorption peaks*

367   *corresponding to these bonds. Reproduced from Long et al. [65].*

368

369   Hu et al. [66] synthesized 3-hydroxyflavone derivative **28** as an "on-off" sensor for Cu^{2+}

370   detection (Table 5 Sensor #28). Free **28**, 20 μM in EtOH: PBS buffer (3:7, v/v, pH 7.0) exhibited

371   a red fluorescence with a maximum emission at 617 nm. The fluorescence of **28** could be

372   selectively quenched in the presence of 20 μM of Cu^{2+} (**Fig. 5**) as excited-state intramolecular

373   proton-transfer (ESIPT) is inhibited. The fluorescence could be partially restored by the addition

374   of 20 μM EDTA. The fluorescent probe **28** (10 μM) was applied to the detection and fluorescent

375   imaging of 20 μM Cu^{2+} in biological systems, such as the human hepatoma cells, HepG2, using

376   the "on-off" approach.

377
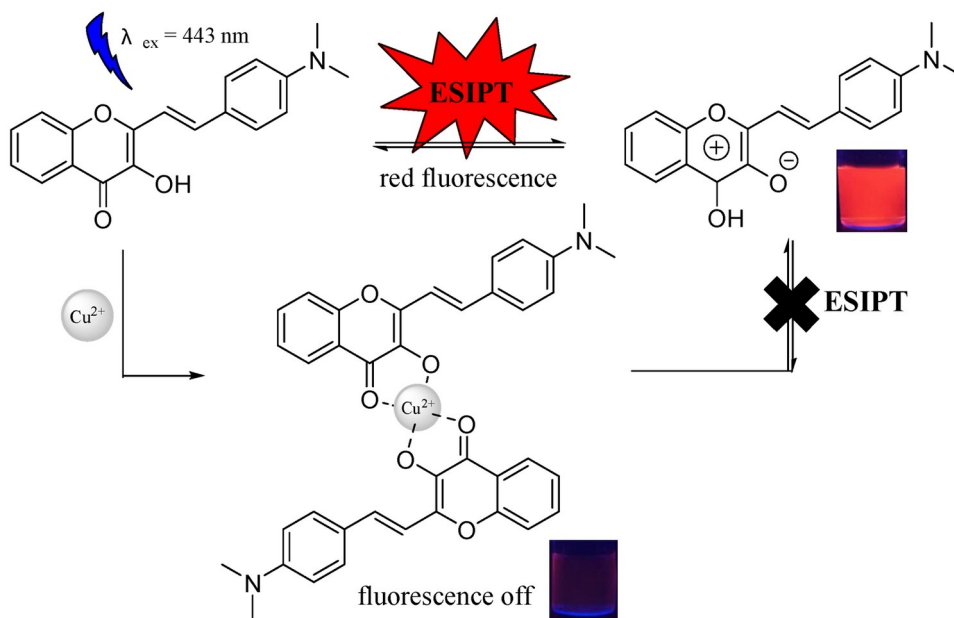
Fig. 5: *The proposed interaction mechanism of **28** with Cu^{2+} shows the inhibition of the excited-state intramolecular proton transfer (ESIPT) upon Cu^{2+} coordination. Modified from Hu et al. [66].*

381

382   He et al. [67] reported the sensing and photophysical properties of an "on-off" fluorescent

383   BODIPY derivative **29** with a bis[2-(phenylseleno)ethyl]amine as the metal recognition unit for

384   both Cu^{2+} and Hg^{2+} (Table 5 Sensor #29). Upon addition of 15 μM of Cu^{2+}, **29** (2 μM) exhibited a

385   large fluorescent enhancement and red-shift of 27 nm. Visible color change under UV light from

386   orange to pink due to the formation of **29**-Cu^{2+}complex in MeCN was noticed. Sensor **29** had a

387   fluorometric response to both Cu^{2+} and Hg^{2+}, therefore as shown in **Fig. 6**, **29** may work as a two-

388   input "IMPLICATION" logic gate using Hg^{2+} (input 1) and Cu^{2+} (input 2) ions as inputs, and the

389   fluorescence intensity at 610 nm as the signal output. The fluorescence intensity at 610 nm was

390   lower than the threshold value of 100 nm when the input was (1,0), while the output was high

391   when the inputs were (0,1), (0,0), and (1,1). Employing this logic gate system that examines the

392   fluorescence intensities at 610 nm with a 100 nm threshold could be a potential way to

393   distinguish between Hg^{2+} and Cu^{2+}.

IN1	IN2	OUT
0	0	1
1	0	0
0	1	1
1	1	1
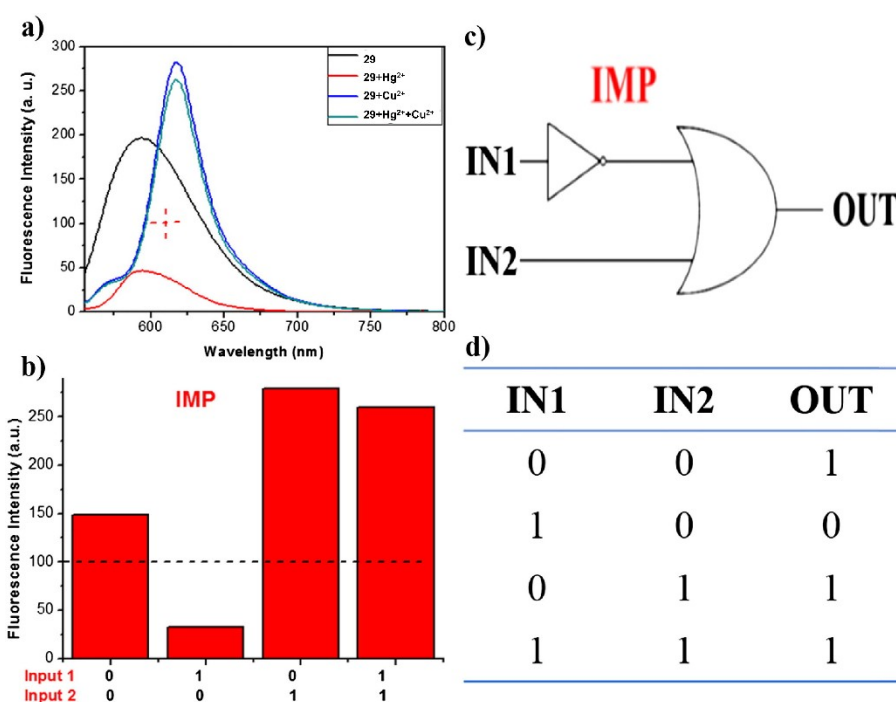
394

395   *Fig. 6: (A) Fluorescence intensity spectrum of 29 (2 μm), $\square_{ex}$ = 530 nm, in the absence*

396   *(black) and presence of 20 μm Hg^{2+}(red), 15 μm Cu^{2+}(blue) and both metal ions (green). (B)*

397   *Changes in fluorescence intensity values of 29 when exposed to 4 different input conditions and*

398   *examining the 610 nm wavelength with a threshold of 100 nm. (C) The "IMPLICATION" logic*

399   *gate for 29 with IN1= $Hg^{2+}$and IN2= Cu^{2+}. (d) The "IMPLICATION" truth table for IN1 and*

400   *IN2 inputs with corresponding outputs with 100 nm threshold examining at 610 nm. Reproduced*

401   *from He et al. [67].*

402   Manna et al. [68] prepared a benzohydrazide Schiff-base derivative "off-on" sensor **31** for

403   detecting Cu^{2+} (Table 5 Sensor #31). The formation of the **31**-Cu^{2+} complex in MeOH:H_2O (1:1,

404   v/v) showed enhancement in fluorescent intensity at 450 nm, which could be due to the inhibition

405   of PET and electron-state intramolecular proton-transfer (ESIPT) processes following the

406   coordination of Cu^{2+} to imine N and salicylaldehyde hydroxyl O moiety. The same processes

407   were inhibited, resulting in fluorescent enhancement when Ni^{2+} was added instead of Cu^{2+},

408   indicating that **31** could work as a two-input "OR" logic gate. As shown in **Fig. 7**, Cu^{2+} and Ni^{2+}

409   were used as inputs when exposed to **31** in MeOH:H_2O (1:1, v/v), while the fluorescent

410   enhancement at 450 nm was the output in this system. When the inputs were (1,0), (0,1), and

411   (1,1), (Cu^{2+}, Ni^{2+}) respectively, the emission intensity at 450 nm was high. When the inputs were

412   (0,0) the emission intensity at 450 nm was low. **31** may also work as a two-input "INHIBIT"

413   logic gate (**Fig. 7**) using Cu^{2+} and cysteine as inputs and taking emission intensity at 450 nm as

414   output.
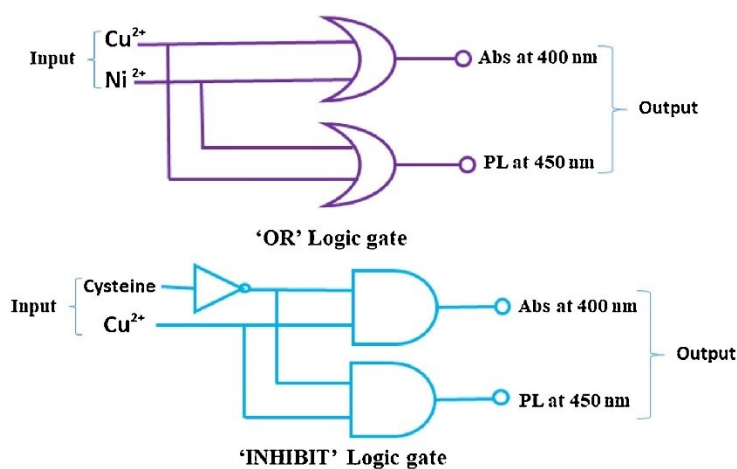
415

416   ***Fig. 7**: Logic scheme for the proposed "OR" and "INHIBIT" logic gates using probe **31**.*

417   *Reproduced from Manna et al. [68].*

418

419   Yufen Wang (2019) et al. [69] synthesized a spiropyran derivative **34** as an "off-on"

420   sensor for multi-ion detection, responding to Cu^{2+} and other ions, Hg^{2+}, Al^{3+}, Cr^{3+} & Ce^{3+} (Table 5

421   Sensor #34). Spiropyrans are small molecular switches that isomerize in response to a variety of

422   stimuli including light [70], redox-active molecules [71,72], and metal ions [73]. Sensor **34** (200

423   µM) in EtOH displayed a weak emission band at 510 nm. Upon addition of 200 µM Cu^{2+}, the

424   formation of the **34**-Cu^{2+} complex showed a strong fluorescent enhancement at 510 and 675 nm,

425   as the complexation facilitated the isomerization of the spiropyran to its ring-open and

426   fluorescent merocyanine isomer. **34** also exhibited fluorescent and colorimetric enhancement in

427   the presence of 200 µM of Hg^{2+}, Ce^{3+}, Al^{3+}, and Cr^{3+}. Even though this multi-sensor does not

428   exclusively detect Cu^{2+}, it may be useful in narrowing down the pool of potential contaminants in

429   a sample.

430   Bayindir and Toprak [74] synthesized a weakly "off-on" fluorescent bis-pyrene

431   compound **35** to recognize Cu^{2+} with a limit of detection of 14.5 µM (Table 5 Sensor #35).

432   Insight into **35-**Cu^{2+} complexation was examined using FT-IR, and a noticeable disappearance of

433   NH and C=S vibrational bands of the **35**-Cu^{2+} complex indicated tautomerization resulting in

434   Cu^{2+} being bound to a thiol moiety and imine N (**Fig. 8**). Fluorescence titration experiments of **35**

435   (10 µM) showed a gradual increase in the fluorescent intensity at 439 nm (λ_{ex} = 376 nm) upon

436   the addition of Cu^{2+} in MeCN. Full saturation in fluorescence intensity was achieved at 8

437   equivalents of Cu^{2+}. A notable increase in emission at 437 nm was also observed in the presence

438   of 10 µM Hg^{2+}, and competition experiments revealed that 50 µM of Ni^{2+} could interfere with 50

439   µM of Cu^{2+} in the presence of 10 µM **35**, as a significant reduction in emission was observed.

440   Nickel(II) interference was not found in the colorimetric studies. However, when 50 µM of Hg^{2+}

441 was incubated with 10 µM **35**, a faint yellow color was observed. Since Cu^{2+} produced a yellow

442 color under the same conditions, the optical analysis of Cu^{2+} detection could be ambiguous due to
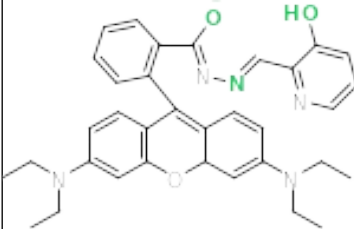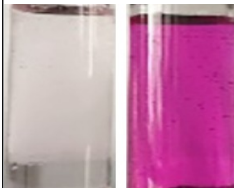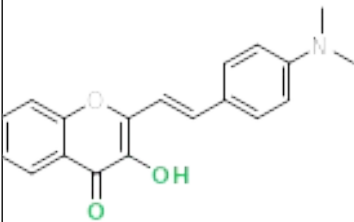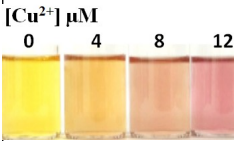
443 the possibility of a false positive.
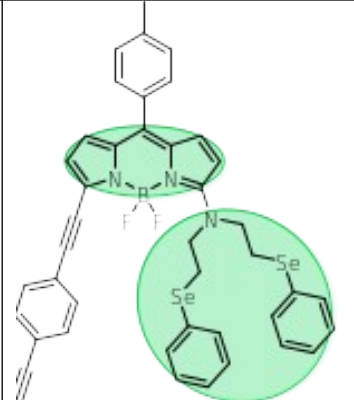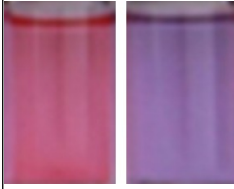
444

35

35-Cu^{2+}
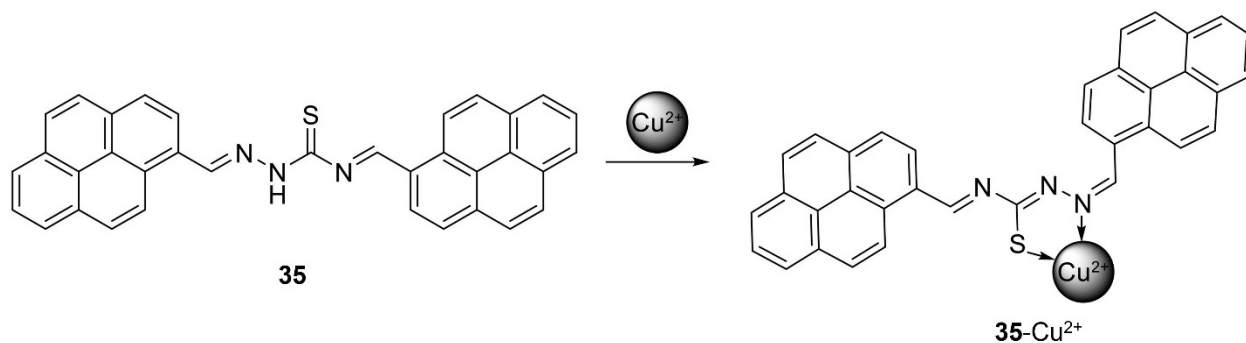
445 ***Fig. 8****: Proposed interaction mechanism of probe **35** with Cu²⁺. FT-IR data indicated Cu²⁺*

446 *binding to the thiol and imine moieties, suggesting possible tautomerization from C–NH and*

447 *C=S to C=N and C–SH. Reproduced from Bayindir et al. [74].*
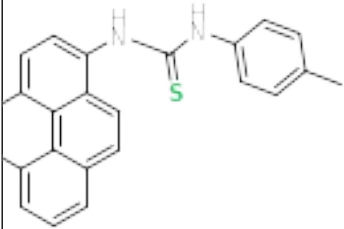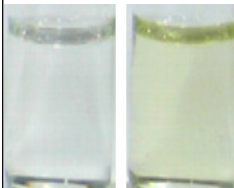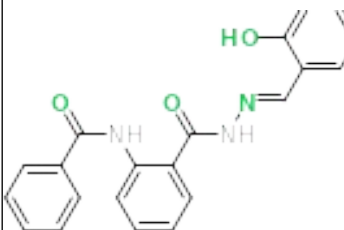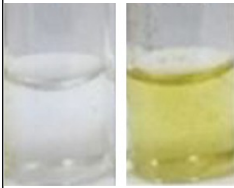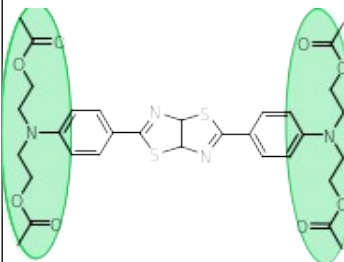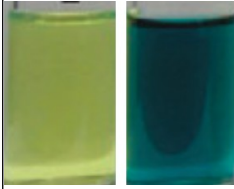
Limit of Detection Determined by Fluorescence Spectroscopy
0.35 μM – 15 μM

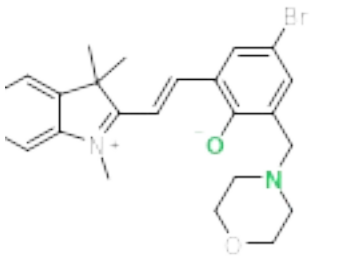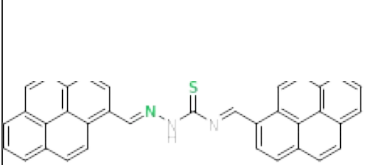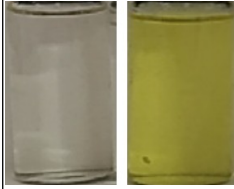| Sensor #	Cu^{2+} Sensor	Ion Sensing	Cu^{2+} LOD	K_a	Binding Stoichiometry Sensor: Cu^{2+}	Naked-Eye Detection [Sensor]: [Cu^{2+}]	Cu^{2+} Selectivity Assay Conditions	Solvent	Ref
27		Cu^{2+}, CN$^-$ Colorimetric & Fluorometric	0.363 μM	–	1:1	[Sensor] = 20 μM [Cu^{2+}] = 1 mM	[Sensor] = 20 μM [Cu^{2+}] = 1 mM [Competing Metal Ions] = 1 mM	DMSO: H$_2$O (1:9, v/v)	[65]
28		Cu^{2+} Colorimetric & Fluorometric	0.57 μM	3.2 x 10^4 M^{-1} Fluorometer	2:1	[Sensor] = 20 μM [Cu^{2+}] = 8 μM	[Sensor] = 20 μM [Cu^{2+}] = 20 μM [Competing Metal Ions] = 20 μM	EtOH: PBS (3:7, v/v) pH = 7.0	[66]
29		Cu^{2+} & Hg^{2+} Colorimetric & Fluorometric	0.92 μM	2.95 x 10^4 M^{-1} Fluorometer	1:1	[Sensor] = 2 μM [Cu^{2+}] = 50 μM	[Sensor] = 2 μM [Cu^{2+}] = 15 μM [Competing Metal Ions] = 50 μM	MeCN	[67]
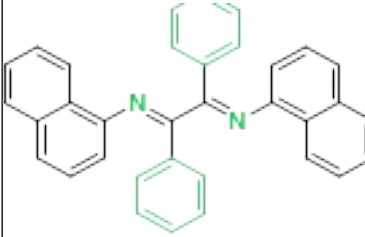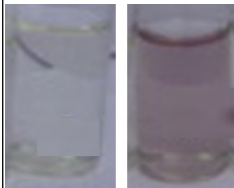
Limit of Detection Determined by Fluorescence Spectroscopy

0.35 μM – 15 μM

Sensor #	Cu²⁺ Sensor	Ion Sensing	Cu²⁺ LOD	K_a	Binding Stoichiometry Sensor: Cu²⁺	Naked-Eye Detection [Sensor]: [Cu²⁺]	Cu²⁺ Selectivity Assay Conditions	Solvent	Ref
30		Cu²⁺ & Hg²⁺ Colorimetric & Fluorometric	0.10 ppm ≈ 1.57 μM	1.09×10^4 M⁻¹ Fluorometer	1:1	[Sensor] = 30 μM [Cu²⁺] = 100 μM	[Sensor] = 30 μM [Cu²⁺] = 300 μM [Competing Metal Ions] = 300 μM	DMSO: H_2O (4:1, v/v) buffered with HEPES pH = 7.8	[75]
31		Cu²⁺, Ni²⁺ Colorimetric & Fluorometric	2.26 μM	1.13×10^6 M⁻¹ UV-Vis	1:1	[Sensor] = 10 μM [Cu²⁺] = 50 μM	[Sensor]= 10 μM [Cu²⁺] = 30 μM [Competing Metal Ions] = 30 μM	MeOH: H_2O (1:1, v/v)	[68]
32		Cu²⁺ Colorimetric & Fluorometric	6.13 μM	–	reaction based	[Sensor] = 100 μM [Cu²⁺] = 2 mM	None	MeCN: Distilled H_2O (95:5, v/v)	[76]

Limit of Detection Determined by Fluorescence Spectroscopy
0.35 μM – 15 μM

Sensor #	Cu^{2+} Sensor	Ion Sensing	Cu^{2+} LOD	K$_a$	Binding Stoichiometry Sensor: Cu^{2+}	Naked-Eye Detection [Sensor]: [Cu^{2+}]	Cu^{2+} Selectivity Assay Conditions	Solvent	Ref
33		Cu^{2+} Colorimetric & Fluorometric	10 μM	2.5 x 10^6 M^{-1} Fluorometer	1:2	 [Sensor] = 150 μM [Cu^{2+}] = 300 μM	[Sensor] = 15 μM [Cu^{2+}] = 300 μM [Competing Metal Ions] = 300 μM	MeCN: H$_2$O (1:1, v/v) pH = 7.0	[77]
34		Cu^{2+}, Hg^{2+} Al^{3+}, Cr^{3+} & Ce^{3+} Colorimetric & Fluorometric	10 μM	–	2:1	 [Sensor] = 2 mM [Cu^{2+}] = 2 mM	None	EtOH	[69]
35		Cu^{2+} Colorimetric & Fluorometric	14.5 μM	3.26 x 10^4 M^{-1} Fluorometer	1:1	 [Sensor] = 10 μM [Cu^{2+}] = 50 μM	[Sensor] = 10 μM [Cu^{2+}] = 50 μM [Competing Metal Ions] = 50 μM	MeCN	[74]

448 **Table 5**: Copper(II) sensors arranged from lowest to highest limit of detection in the range of 0.35 μM – 15 μM determined by fluorescence
449 spectroscopy. Information provided: Sensor number, chemical structure (green atoms indicate the proposed mechanism of Cu^{2+} coordination. Shaded
450 green indicates the proposed sensing unit/s in Cu^{2+} coordination), additional cations and anions detected by the sensor, K$_a$ = association constant,

451 binding stoichiometry (sensor: Cu^{2+}), concentration of sensor and Cu^{2+} for naked eye detection, the Cu^{2+} selectivity assay conditions including

452 concentration of sensor, Cu^{2+} and competing metal ions tested and solvent.

453

4. Limit of detection determined by UV-Vis spectroscopy

The sensors in this section calculated their respective LOD's for Cu^{2+} detection using a UV-Vis spectrophotometer (Table 1). Further details such as alternative ions recognized, association constant (K_a), binding stoichiometry (sensor: Cu^{2+}), naked-eye detection concentrations of sensor and Cu^{2+}, competition assay concentrations of a sensor, Cu^{2+}, and other metal ions, and solvent conditions used when determining LOD, are provided.

4.1   8 nM – 90 nM

The sensors in this category were able to achieve the lowest LOD of copper(II) to date [40,78–84]. Common structural moieties utilized for copper(II) detection include rhodamine [79,83], Schiff-base [40,79,80], and coumarin [40,83]. Interestingly, Gao et al., Sengupta et al., and Basurto et al. were the only groups to develop a sensor specific for copper(II) detection, whereas the other reported sensors simultaneously detected other cations, (Al^{3+}, Co^{2+}, Fe^{3+} and Cr^{3+}), anions (AcO$^-$, F$^-$, and S^{2-}) or cysteine.

Gao et al. [78] synthesized a heptamethine cyanine dye that detected copper(II) through the inhibition reaction of L-cysteine with sensor **36** and subsequent oxidation of L-cysteine to its disulfide derivative (Table 6 Sensor #36). **36** contains two key units, ketone-cyanine, and *p*-nitrobenzoyl, that are important in the inhibition reaction (**Fig. 9**). When there is no copper(II) in solution, 20 μM of L-cysteine is reacted at room temperature for 10 minutes with 10 μM of **36**. The thiol from L-cysteine will cleave the ester in **36** resulting in the intramolecular rearrangement of *p*-nitrobenzoyl and L-cysteine to form S-(4-nitrobenzoyl)cysteine and cyanine dye (ketone-cyanine). The release of the dye provides the red color, indicating an absence of

475   copper(II). When copper(II) is introduced in solution with L-cysteine for 12 minutes at room

476   temperature, L-cysteine will catalytically oxidize to L-cystine, thus inhibiting the cyclization and

477   release of the cyanine dye. The addition of **36** and reaction at room temperature for 10 minutes

478   consequently turns the solution green, indicating the presence of copper(II). In addition to its low

479   limit of detection of 8.6 nM, this sensor was able to detect copper(II) in practical samples such as

480   tap water, seawater, and biological samples spiked with two concentrations of copper(II), 0.5 μM

481   and 1 μM. However, the fact that this sensor is dependent on the oxidation of L-cysteine might

482   hinder the in-field application because chemicals such as $NaHSO_3$ can consume oxygen in the

483   sample and favor the inhibition reaction of L-cysteine. It was shown that introducing 0.2 M

484    $NaHSO_3$ into solution considerably decreases the absorbance peak at 770 nm, which is associated

485   with the colorimetric detection of copper(II), over the control without $NaHSO_3$. This could

486   potentially lead to a false negative.

487
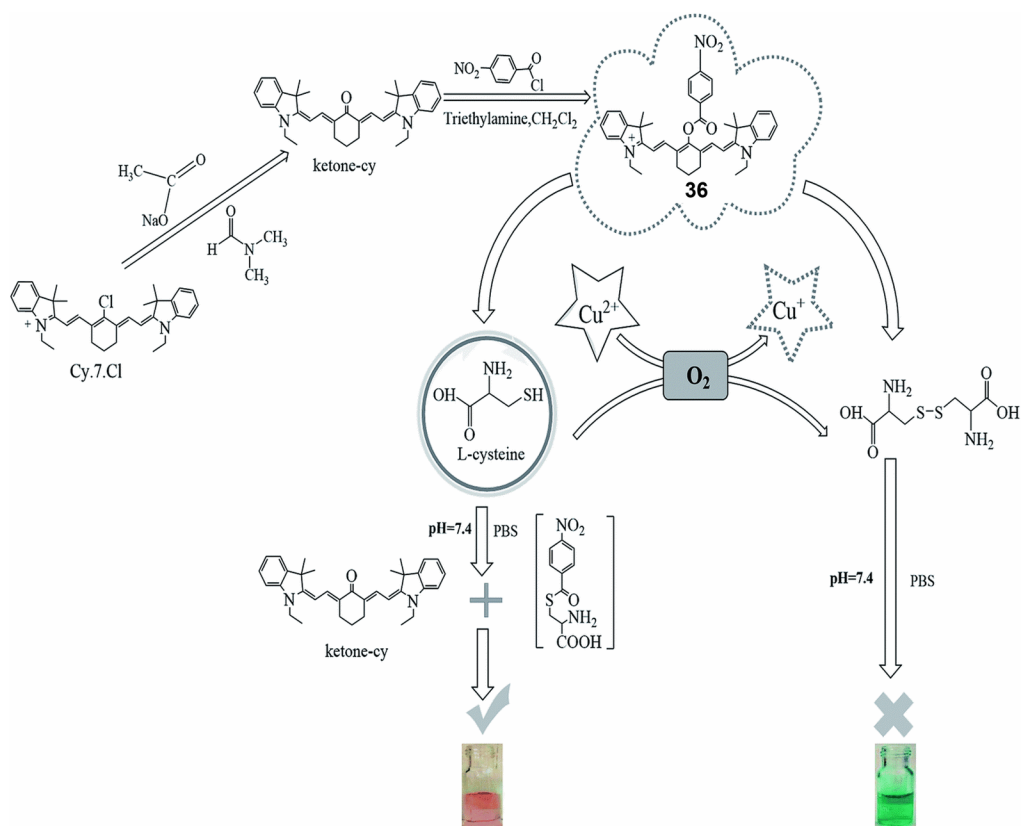
Fig. 9: *Synthesis of sensor **36** and proposed mechanism for detecting copper(II). Cy.7.Cl (0.19*

mmol) was dissolved in triethylamine (0.6 mmol) and CH_2Cl_2 and chilled to 0^oC. To this solution

*p-nitrobenzoyl was added dropwise and stirred overnight at room temperature to afford **36**, the*

*green product. When copper is absent and **36** and L-cysteine are present in solution, **36** reacts*

with L-cysteine to produce S-(4-nitrobenzoyl) cysteine and ketone-cy, thus changing the color

from green to red. When copper(II) is present in solution, L-cysteine is oxidized by copper(II) to

*produce L-cystine, therefore keeping **36** intact and the color remains green. Modified from Gao*

et al. [78].

496

497   Gupta et al. [79] developed a rhodamine-spirolactam sensor, **37**, containing a Schiff-base

498   unit, that was able to detect metal ions such as copper(II) (LOD = 9.9 nM), aluminum(III),

499   iron(III) colorimetrically and iron(III) fluorometrically (Table 6 Sensor #37). Sensor **37** is

500   initially colorless in MeOH: H_2O (1:1, v/v) solution, and upon addition of various metal ions, a

501   strong absorbance band appeared at 555 nm when copper(II), aluminum(III), or iron(III) was

502   bound. The metal binding to **37** changed the color from colorless to magenta and this color

503   change was attributed to the spirocyclic ring-opening of spirolactam. Furthermore, when **37** and

504   aluminum(III) were bound and in the magenta **37**-Al^{3+} complex, detection of anions, F^- and AcO^-

505   was possible through the release of Al^{3+} and thus retrieving the initial colorless **37** complex. To

506   utilize the sensor for paper test strips for naked-eye detection of Cu^{2+}, Fe^{3+}, Al^{3+}, **2**-Al^{3+} +

507   F^-/AcO^-, 1 mM of **37** was fixed to Whatman filter paper. When the test strips were sprayed with

508   100 μM of these ions, the color changes mentioned above were observed. Although they were

509   able to successfully fix the sensor to paper and test the strips for ions Cu^{2+}, Fe^{3+}, Al^{3+}, **2**-Al^{3+} + $F^-/$

510   AcO^-, no other metal ions were tested, and no competition studies were done to determine if the

511   test strip in fact achieved the same results when fixed to paper as it did in solution.

512   Yuan Wang (2019) et al. [83] synthesized **41**, utilizing a rhodamine-spirolactam sensor

513   and incorporating a coumarin moiety (Table 6 Sensor #41). When **41** (10 μM) was dissolved in

514   pure MeOH and exposed to 2 equivalents of metal ions, an absorbance peak arose at 523 nm

515   when subjected to copper(II). However, other metals such as Co^{2+}, Zn^{2+}, Fe^{3+}, and Mn^{2+}

516   confounded analysis at this wavelength and therefore became difficult to detect only copper(II).

517   Interestingly, when **41** (20 μM) was dissolved in pure H_2O and again exposed to 2 equivalents of

518   metal ions, only the copper(II) solution displayed a strong absorbance band at 532 nm and a

significant color change from colorless to pale pink (**Fig. 10A**). This difference in selectivity for copper(II) in MeOH and H_2O is believed to be due to the induced aggregation of **41** as the solvent polarity increases. DLS measurements support this concept as the average size of **41** increased from 36.75 nm, 89.08 nm and 122.40 nm as water content increased from 20%, 50%, and 100% respectively. Transmission electron microscopy (TEM) image of **41** in 100% H_2O is shown in **Fig. 10B** and when copper(II) is introduced to the solution of **41**, a noticeable change in size is observed in the TEM image (**Fig. 10C**). Additionally, DLS measurements substantiate this visible change in size as a decrease is seen for **41** from 122.40 nm to 48.51 nm of **7**+Cu^{2+} in 100% H_2O.
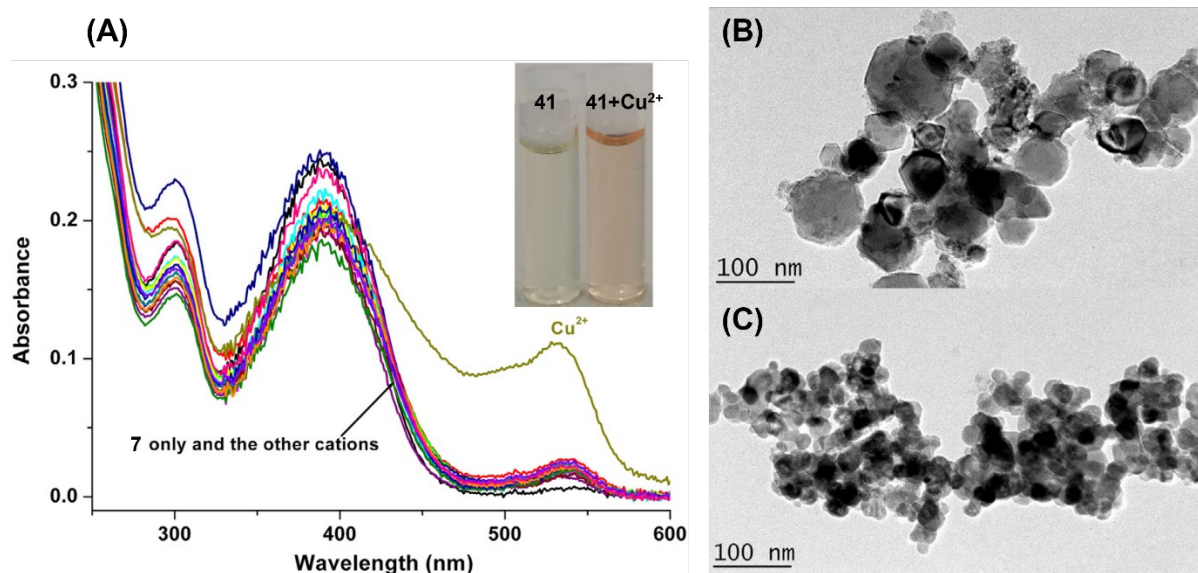
*Fig. 10: (A) UV-Vis absorbance profile of **41**, 20 μM, upon the addition of 40 μM metal ions in H_2O: Ag^+, Al^{3+}, Ca^{2+}, Cd^{2+}, Co^{2+}, Cr^{3+}, Fe^{3+}, Hg^{2+}, K^+, Mg^{2+}, Na^+, Ni^{2+}, Pb^{2+}, Zn^{2+} and Cu^{2+}. Inset: Color changes of **41** from colorless to pale pink upon the addition of 2 equivalents copper(II). Transmission electron microscopy (TEM) images of (B) **41** and (C) **41**+Cu^{2+} in H_2O. Modified from Wang(2020) et al. [83].*

534   Min Seon Kim (2017) et al. [80] synthesized a copper(II) sensor that contains a Schiff-

535   base unit that bridges the quinoline unit to the trifluoromethyl pyrimidine component, sensor **38**

536   (Table 6 Sensor #38). When copper(II) or cobalt(II) was present in 10 mM bis-tris buffer:DMF

537   (4:1, v/v, pH = 7.0) solution of **38**, an imine from the Schiff-base unit, quinoline, and pyrimidine,

538   chelated the metal ion via binding stoichiometry of 2:1 sensor to metal. A noticeable absorbance

539   band at 460 nm appeared when 18 μM of Cu^{2+} or Co^{2+} was present in a solution with 10 μM of **38**

540   and was accompanied by colorimetric detection from colorless to yellow. When copper(II) was

541   bound to **38** and S^{2-} was present in the solution, the absorbance band at 460 nm, attributed to **38-**

542   Cu^{2+}, decreased and the appearance of the original sensor **38** absorbance maximum at 340 nm re-

543   appeared. It was proposed that S^{2-} de-chelates copper(II) from the **38**-Cu^{2+} complex to form CuS

544   and sequential recovery of **38**. A pH dependence study was performed on **38** from pH 2-12 while

545   monitoring the absorbance at 460 nm. The results revealed that **38** was able to maintain its

546   sensing ability between pH 4-12, implying that this sensor can be employed under physiological

547   conditions. Further analysis of copper(II) detection was explored using UV-Vis spectral

548   measurements examining 460 nm wavelength of **38** (15 μL in DMF) dissolved in 0.84 mL of 100

549   mM bis-Tris buffer:DMF solution (4:1, v/v) and diluted to a total volume of 3 mL with drinking

550   water or tap water spiked with 2.40 μL of Cu^{2+}. Ultimately, **38** was able to recover 2.48 μL and

551   2.52 μL of the spiked copper(II) in the sample of drinking water or tap water, respectively. With

552   the aid of a portable UV-Vis, **38** has the potential to be an in-field copper(II) sensor. However,

553   the fact that it also senses cobalt(II) poses a problem if the detection of copper(II) only is the

554   intention.

555   Zhi-Gang Wang (2020) et al. [40] employed a naphthohydrazide-based sensor **4**

556   containing a coumarin moiety that is able to colorimetrically and fluorometrically detect

557   copper(II) and cobalt(II) (Table 6 Sensor #4). Sensor **4** (2.5 μM) exhibited a yellow color in

558   EtOH:10mM phosphate buffer (7:13, v/v, pH = 7.2) and upon addition of 1 equivalent of

559   copper(II) or cobalt(II), the color changed from yellow to orange-red, while the other metal ions

560   tested remained yellow. In order to ascertain only cobalt(II) binding, a solution of **4** (2.5 μM),

561   copper(II) (0.5 eq.), and cobalt(II) (0.5 eq.) were exposed to 10 equivalents of glutathione

562   (GSH), a known tripeptide containing a thiol moiety on cysteine that has a high binding affinity

563   for copper(II), $K_a \approx 10^{16}$ [85–87]. Consequently, GSH displaced copper(II), generating the Cu^{2+}-

564   GSH complex, while simultaneously recovering **4**, and a yellow color was observed, while

565   cobalt(II) remained orange-red in color. To distinguish only copper(II) binding, a solution of **4**

566   (2.5 μM), copper(II) (0.5 eq.), and cobalt(II) (0.5 eq.) were adjusted to pH 4 using 0.1 M HCl or

567   HNO_3, which displaced cobalt(II) and recovered sensor **4** (yellow color), while copper(II)

568   remained orange-red in color. The ability to discriminate between Cu^{2+} or Co^{2+} through the

569   introduction of GSH or pH adjustment to 4 makes **4** a promising colorimetric copper(II) in-field

570   sensor.

571   Tavallali et al. [81] employed a commercially available dye, 4-(2-pyridylazo) resorcinol,

572   sensor **39**, that could detect copper(II) in six-fold excess to confounding metal ions to copper(II)

573   in water (Table 6 Sensor #39). **39** (50 μM) exhibited an absorbance peak at 412 nm and was

574   yellow in color. When equimolar copper(II) concentration was introduced into the solution, a

575   large red-shift to the new absorbance max of 508 nm and accompanying color change from

576   yellow to red was observed. Furthermore, when the **39**-Cu^{2+} complex is produced, the detection

577   of cysteine is possible through the demetallation of copper(II) forming $[Cu(Cys)_n]$ and recovery

578   of **39**. Using the two distinct absorbances at 412 nm and 508 nm, an "IMPLICATION" and

579   "INHIBIT" logic gate were devised using the absence and presence of copper(II) and/or cysteine

580   described as "0" and "1". Due to the feasibility of obtaining **39**, its low limit of detection (31

581   nM) and the colorimetric response to copper(II) in water, **39** shows potential as an in-field

582   copper(II) sensor. If detecting copper(II) in biological applications is the goal, it is important to

583   be aware of the displacement of copper(II) from **39** due to cysteine and other possible bio-thiols,

584   such as GSH and homocysteine.

585   Sengupta et al. [82] utilized sinapic acid, a naturally occurring small molecule that is

586   commercially available, as a naked-eye copper(II) sensor that was able to detect copper down to

587   64.5 nM (Table 6 Sensor #40).When **40** (25 μM) was dissolved in MeCN:10 mM tris-HCl buffer

588   (9:1, v/v, pH 7.4), it exhibited two distinct absorbance peaks at 236 nm and 320 nm and is

589   colorless to the naked eye. When 50 μM of Cu^{2+} was introduced, a new absorbance peak at 512

590   nm appeared and the color changed from colorless to pink. Ultimately, **40** was applied as a paper

591   strip test by fixing the sensor to filter paper. When the strip was submerged into an aqueous

592   solution of copper(II), 50 μM, 100 μM and 150 μM independently, the color change from

593   colorless to pink was once again observed. It would have been interesting to test copper

594   concentrations at the maximum allowable contaminant level of copper(II) in drinking water at

595   20.5 μM and 31.5 μM determined by the Environmental Protection Agency and World Health
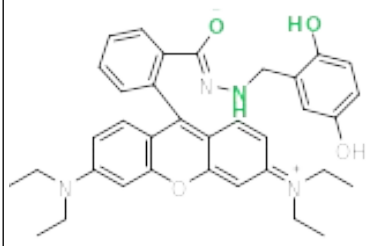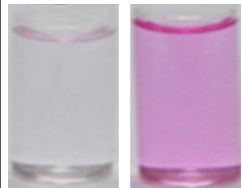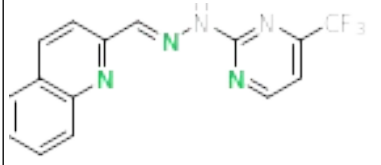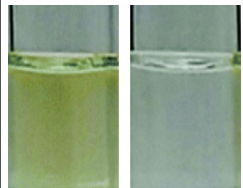
596   Organization, respectively [3,4].
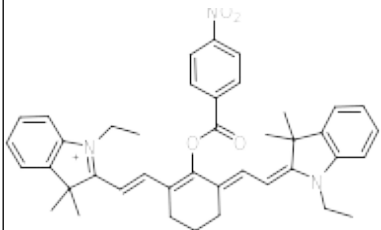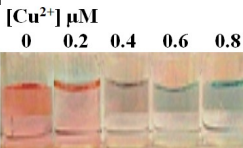
597   Basurto et al. [84] created a series of 1-dicyanomethylene-2-chloro-3-aminoindene

598   chromophores that offered cation sensing of Cu^{2+}, Fe^{3+}, Al^{3+}, Hg^{2+}, Sc^{3+}, and Sn^{2+}, and anion

599   sensing CN⁻. Of these 8 chromophores synthesized, sensor **42** bearing two allyl groups, was

600   responsive to only copper(II) (Table 6 Sensor #42). Sensor **42** possessed a deep purple color

601   when dissolved in acetonitrile and produced an absorbance band at 529 nm. As copper(II) was

602   titrated into the solution, a noticeable decrease at 539 nm was noticed. The change in color from

603   purple to colorless indicates that **42** is a "turn-off" sensor. An application has yet to be made to

604   test the sensor's ability for in-field studies but the straightforward and high yielding (97%)

605   synthesis of **42** could make it a promising option for a copper(II) sensor.

606   Of the sensors in this category with LOD from 8 nM – 90 nM, it is interesting to note that

607   three of the eight sensors employed a thiol containing molecule, such as cysteine or GSH, to

608   oxidize or displace copper from the sensor [40,78,81]. This displacement method, which

609   ultimately resulted in the recovery of the sensor, was a common method used to detect other

610   anions or to distinguish between two competing metal ions [40,79–81,84]. Lastly, two sensors, 4-

611   (2-pridylazo) resorcinol, **39**, and sinapic acid, **40**, did not require any further synthesis as they

612   were commercially bought and were able to achieve copper(II) sensing at 31 nM and 64.5 nM,
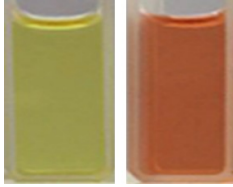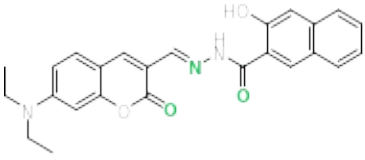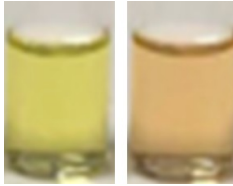
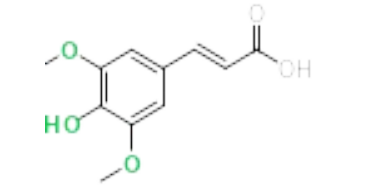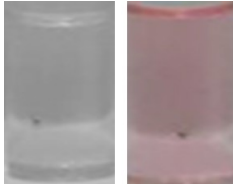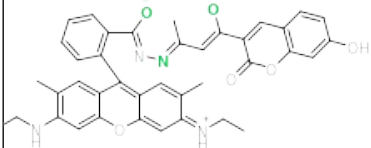613   respectively [81,82].
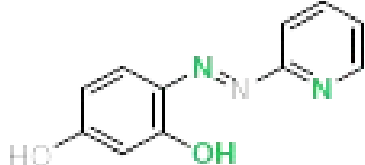
Limit of Detection Determined by UV-Vis Spectroscopy

8 nM – 90 nM

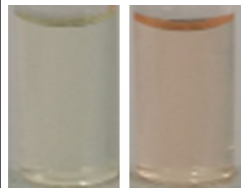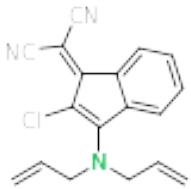| Sensor #	Cu²⁺ Sensor	Ion Sensing	Cu²⁺ LOD	K_a	Binding Stoichiometry Sensor: Cu²⁺	Naked-Eye Detection [Sensor]: [Cu²⁺]	Cu²⁺ Selectivity Assay Conditions	Solvent	Ref
36		**Cu²⁺** Colorimetric	**8.6 nM**	–	**reaction based**	[Sensor] = 0.5 µM [Cu²⁺] = 0-0.8 µM	[Sensor] = 0.5 µM [Cu²⁺] = 2.5 µM [Competing Metal Ions] = 25 µM	PBS buffer pH = 7.4	[78]
37		**Cu²⁺, Al³⁺, AcO⁻ & F⁻** Colorimetric **Fe³⁺** Fluorometric	**9.9 nM**	**$1.1 \times 10^6 \, M^{-1}$** UV-Vis	**1:1**	[Sensor] = 10 µM [Cu²⁺] = 10 µM	[Sensor] = 10 µM [Cu²⁺] = 10 µM [Competing Metal Ions] = 10 µM	MeOH: H₂O (1:1, v/v)	[79]
38		**Cu²⁺, Co²⁺, S²⁻** Colorimetric	**20 nM**	**$1.0 \times 10^{10} \, M^{-2}$** UV-Vis	**2:1**	[Sensor] = 10 µM [Cu²⁺] = 18 µM	[Sensor] = 10 µM [Cu²⁺] = 10 µM [Competing Metal Ions] = 10 µM	10 mM bis-tris buffer: DMF (4:1, v/v) pH= 7.0	[80]

50

Limit of Detection Determined by UV-Vis Spectroscopy

8 nM – 90 nM

Sensor #	Cu²⁺ Sensor	Ion Sensing	Cu²⁺ LOD	K_a	Binding Stoichiometry Sensor: Cu²⁺	Naked-Eye Detection [Sensor]: [Cu²⁺]	Cu²⁺ Selectivity Assay Conditions	Solvent	Ref
39		**Cu²⁺ & Cysteine** Colorimetric	31 nM	$2.12 \times 10^4\,M^{-1}$ UV-Vis	1:1	 [Sensor] = 50 μM [Cu²⁺] = 39 μM	[Sensor] = 50 μM [Cu²⁺] = 50 μM [Competing Metal Ions] = 300 μM	H_2O	[81]
4		**Cu²⁺ & Co²⁺** Colorimetric & Fluorometric	62.1 nM	$1.26 \times 10^6\,M^{-1}$ Fluorometer	2:1	 [Sensor] = 10 μM [Cu²⁺] = 10 μM	[Sensor] = 2.5 μM [Cu²⁺] = 2.5 μM [Competing Metal Ions] = 2.5 μM	EtOH:10 mM Phosphate buffer (7:13, v/v) pH= 7.2	[40]
40		**Cu²⁺** Colorimetric	64.5 nM	$1.7 \times 10^9\,M^{-1}$ UV-Vis	1:2	 [Sensor] = 25 μM [Cu²⁺] = 50 μM	[Sensor] = 25 μM [Cu²⁺] = 50 μM [Competing Metal Ions] = 125 μM	MeCN:10 mM tris-HCl buffer (9:1, v/v) pH= 7.4	[82]

Limit of Detection Determined by UV-Vis Spectroscopy
8 nM – 90 nM

Sensor #	Cu²⁺ Sensor	Ion Sensing	Cu²⁺ LOD	K_a	Binding Stoichiometry Sensor: Cu²⁺	Naked-Eye Detection [Sensor]: [Cu²⁺]	Cu²⁺ Selectivity Assay Conditions	Solvent	Ref
41		**Cu²⁺** Colorimetric **Al³⁺, Fe³⁺, Cr³⁺ & Co²⁺** Fluorometric	**86.8 nM**	**5.93 x 10⁵ M⁻¹** UV-Vis	**1:1**	[Sensor] = 20 µM [Cu²⁺] = 40 µM	[Sensor] = 20 µM [Cu²⁺] = 40 µM [Competing Metal Ions] = 40 µM	H_2O	[83]
42		**Cu²⁺** Colorimetric	**94.6 nM**	**8.51 x 10⁵ M⁻¹** UV-Vis	**1:1**	[Sensor] = 100 µM [Cu²⁺] = 200 µM	[Sensor] = 100 µM [Cu²⁺] = 200 µM [Competing Metal Ions] = 200 µM	MeCN	[84]

Table 6: Copper(II) sensors arranged from lowest to highest limit of detection in the range of 8 nM – 90 nM determined by UV-Vis spectroscopy. Information provided: Sensor number, chemical structure (green atoms indicate the proposed mechanism of Cu²⁺ coordination. Shaded green indicates the proposed sensing unit/s in Cu²⁺ coordination), additional cations and anions detected by the sensor, K_a = association constant, binding stoichiometry (sensor: Cu²⁺), concentration of sensor and Cu²⁺ for naked eye detection, the Cu²⁺ selectivity assay conditions including concentration of sensor, Cu²⁺ and competing metal ions tested and solvent.

4.2   0.10 µM – 0.19 µM

620   Lin et al. [88] synthesized a series of three acylthiosemicarbazides bearing a nitrophenyl

621   with no nitro-group, one nitro-group, and two nitro-groups. Sensor **43**, having two nitro groups,

622   was the only sensor that was able to detect and provide a colorimetric response to copper(II) with

623   a limit of detection of 0.10 µM (Table 7 Sensor #43). When **43** (20 µM) was incubated with

624   copper(II) (100 µM), a noticeable color change from brown to green was observed. This

625   observation was also seen when **43** and copper(II) were in the presence of various cations (100

626   µM). To take advantage of the colorimetric response of **43** to copper(II), test strips were created

627   by soaking **43** (0.1 M) dissolved in DMSO onto filter paper and air drying. Once exposed to

628   copper(II), the test strip turned green, while the test trips for other cations were yellow. Although

629   no concentration of copper was reported for the test strip experiment, this discernment between

630   copper and other cations, in conjunction with the test strip application, makes **43** a possible

631   candidate for in-field copper(II) detection.

632   In our work, Trevino et al. [73] developed a dimethylamine-functionalized spiropyran-

633   based copper(II) sensor **44**, and achieved a limit of detection of 0.11 µM (Table 7 Sensor #44). A

634   Job's plot experiment determined that the binding stoichiometry for sensor **44** to copper was 1:1.

635   DFT calculations were performed to determine that in the presence of copper(II), spiropyran **44**

636   isomerizes to its ring-open merocyanine **44** species and binds copper(II) at the phenolic oxygen

637   thus, changing the color from pale pink to green (**Fig. 11**). While spiropyrans are notorious for

638   ring-opening in the presence of UV light, a study was conducted by irradiating **44** with 302 nm

639   light for 15 minutes to demonstrate that light does not induce isomerization. Competition studies

640   were applied with **44** (100 µM), copper(II) (100 µM), and 10 equivalent of various other cations

641   (1 mM), which are the highest equivalents of competing metal ions to copper tested in this 0.10

642   μM – 0.19 μM LOD category of sensors. It was shown that 10 equivalents Pb^{2+} and 10

643   equivalents Fe^{3+} interfered with the copper(II) sensing ability, rendering a false positive or false

644   negative, respectively. Pre-treatment methods could be used to remove these two cations prior to

645   testing, therefore making this sensor a viable option.

Spiropyran **44**   Merocyanine **44**-Cu^{2+}

646
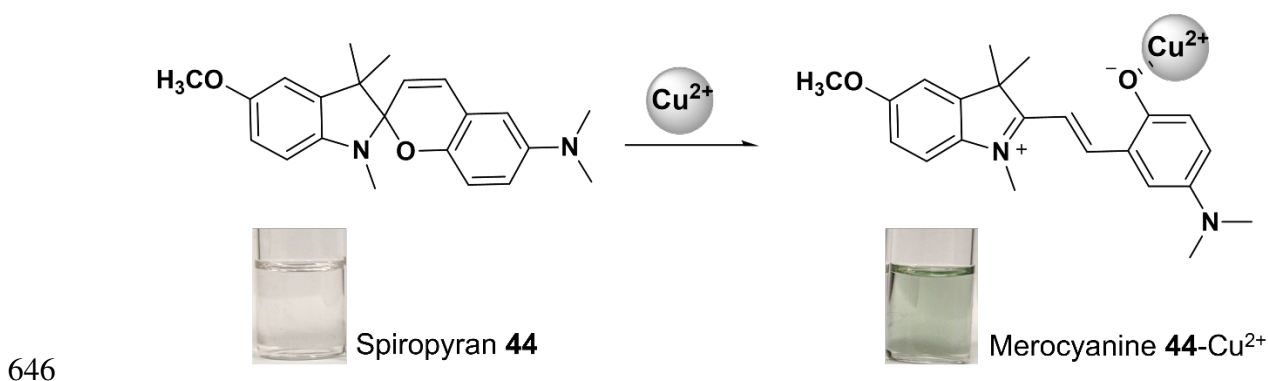
647   *Fig. 11: Isomerization and respective color change of the spiropyran **44**, pale pink, to*

648   *merocyanine **44**, green, in the presence of copper(II). Modified from Trevino et al. [73].*

649

650   Xie et al. [47] utilized rhodamine 101 dye combined with spirolactam to develop **13** with

651   ratiometric changes in absorbance intensities (583 nm/370 nm) for the detection of Cu^{2+} and Co^{2+}

652   (Table 7 Sensor #13). When **13** (20 μM) was exposed to 20 μM of Cu^{2+} or Co^{2+} there was a

653   colorimetric response from colorless to purple, due to the ring-opening of the spirolactam and

654   subsequent binding of the metal. This observation was also witnessed in the UV-Vis spectrum

655   with a decrease in absorbance at 370 nm and an appearance of a band at 583 nm when **13** was

656   subjected to Cu^{2+} or Co^{2+}. Interestingly, when **13** was bound to Cu^{2+} or Co^{2+}, only **13**-Cu^{2+} was

657   reversible upon the addition of ethylenediaminetetraacetic acid (EDTA), a common metal

658   chelator. This approach could be a potential method to discern copper(II) from cobalt(II).

659   Mohammadi and Ghasemi   [61] employed a pyrimidine-based chemosensor **23**

660   containing an aminothiazole to assist in copper(II) chelation through the sulfur and nitrogen

661   atoms (Table 7 Sensor #23). Sensor **23** (10 μM) absorbs at 439 nm when dissolved in DMSO:

662   H_2O (8:2, v/v) and is yellow in color. In the presence of 10 equivalents of 13 metal ions, 12

663   anions, or 14 amino acids, only Cu^{2+} changed to red, with the appearance of a new band at 304

664   nm. Additional colorimetric detection of CN^- (LOD = 0.320 μM) via displacement of Cu^{2+} from

665   **23**-Cu^{2+} was also seen in the presence of 30 equivalents of various anions. Lastly, test strips were

666   assembled by immersing filter paper in **23** (100 mM) dissolved in acetonitrile and oven drying.

667   When the test strips were submerged in aqueous copper(II) concentrations ranging from 0.10 μM

668   – 50 μM, there was a detectable difference between the test strip with copper(II) at 1 μM (red
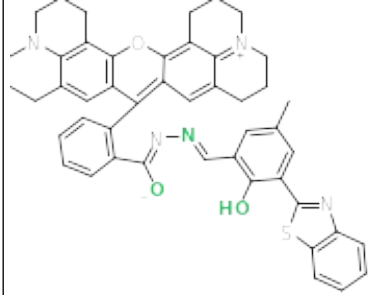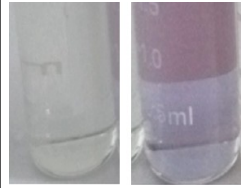
669   brown) and without (yellow).
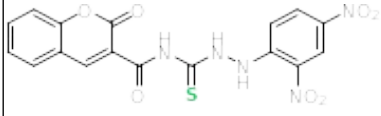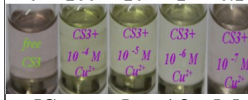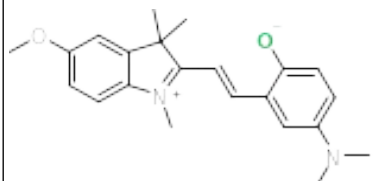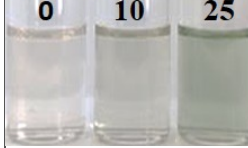
670   Lui et al. [89] synthesized N,N'bis(2-methoxy-ethyl)-2,3,3-trimethyl-3H-squarine, sensor

671   **49**, that achieved a limit of detection for copper(II) at 0.188 μM (Table 7 Sensor #49). **49**

672   (10μM) was evaluated in eight different polar solvents, and acetonitrile was the only solvent that

673   afforded selectivity for copper(II) (20 μM) by exhibiting a "turn-off" response, changing from

674   blue to colorless. When **49** was subjected to 50 μM competing metal ions followed by 50 μM

675   copper(II), it was shown that Cd^{2+} interfered with the "turn-off" capability, which could result in

676   a false reading of Cu^{2+} detection.

677   A commonality noticed in this group of sensors was the employment of sulfur, whether it

678   be in a thiosemicarbazine or thiazole, to aid in copper(II) binding or usage for its electronic

679 spectral properties [47,61,88,90]. Moreover, four sensors utilized the switching capability of a

680 spiro-carbon to achieve a colorimetric response [47,73,91,92].
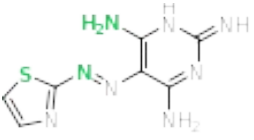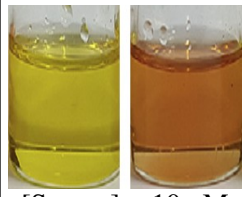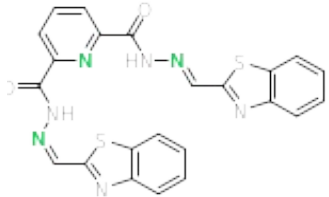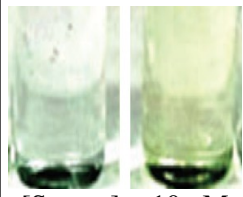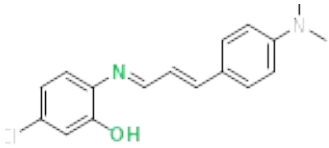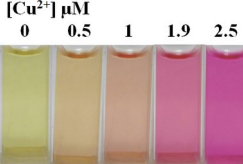
Limit of Detection Determined by UV-Vis Spectroscopy

0.10 µM – 0.19 µM

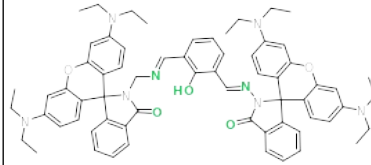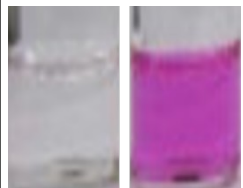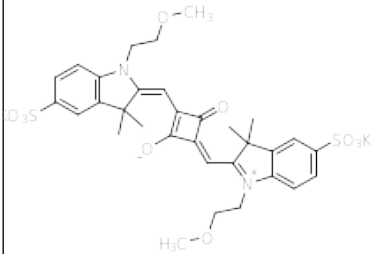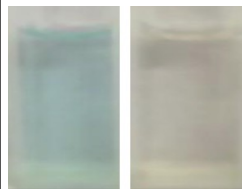| Sensor #	Cu^{2+} Sensor	Ion Sensing	Cu^{2+} LOD	K_a	Binding Stoichiometry Sensor: Cu^{2+}	Naked-Eye Detection [Sensor]: [Cu^{2+}]	Cu^{2+} Selectivity Assay Conditions	Solvent	Ref
43		Cu^{2+} Colorimetric	0.10 µM	1.5 x 10^4 M^{-1} UV-Vis	2:1	[Sensor] = 10 µM [Cu^{2+}] = 1 µM	[Sensor] = 20 µM [Cu^{2+}] = 100 µM [Competing Metal Ions] = 100 µM	DMSO: HEPES buffer (9:1, v/v) pH= 7.0	[88]
44		Cu^{2+} Colorimetric	0.11 µM	–	1:1	[Sensor] = 100 µM [Cu^{2+}] = 6 µM	[Sensor] = 100 µM [Cu^{2+}] = 100 µM [Competing Metal Ions] = 1 mM	EtOH	[73]
13		Cu^{2+}, Co^{2+} Colorimetric Cu^{2+}, Co^{2+} Ni^{2+} Fluorometric	0.11 µM	9.9 x 10^4 M^{-1} UV-Vis	1:1	[Sensor] = 20 µM [Cu^{2+}] = 20 µM	[Sensor] = 20 µM [Cu^{2+}] = 20 µM [Competing Metal Ions] = 20 µM	10 mM PBS buffer: 40% EtOH (1:1, v/v) pH= 7.4	[47]
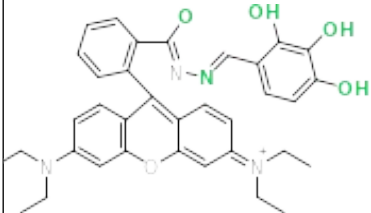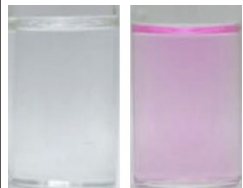
Limit of Detection Determined by UV-Vis Spectroscopy
0.10 μM – 0.19 μM

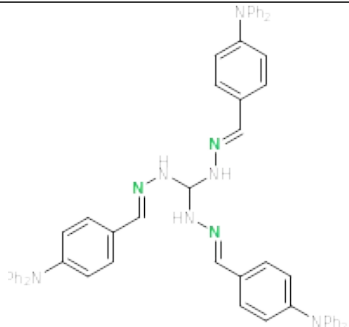| Sensor #	Cu²⁺ Sensor	Ion Sensing	Cu²⁺ LOD	K_a	Binding Stoichiometry Sensor: Cu²⁺	Naked-Eye Detection [Sensor]: [Cu²⁺]	Cu²⁺ Selectivity Assay Conditions	Solvent	Ref
23		Cu²⁺ & CN⁻ Colorimetric & Fluorometric	0.116 μM	$1.55 \times 10^5\,M^{-1}$ UV-Vis	1:1	[Sensor] = 10 μM [Cu²⁺] = 100 μM	[Sensor] = 10 μM [Cu²⁺] = 100 μM [Competing Metal Ions] = 100 μM	DMSO: H_2O (8:2, v/v)	[61]
45		Cu²⁺, AMP²⁻, F⁻, AcO⁻ Colorimetric	0.12 μM	$9.08 \times 10^4\,M^{-1}$ UV-Vis	1:1	[Sensor] = 10 μM [Cu²⁺] = 10 μM	[Sensor] = 10 μM [Cu²⁺] = 10 μM [Competing Metal Ions] = 10 μM	DMSO: H_2O (8:2, v/v)	[90]
46		Cu²⁺ Colorimetric	0.125 μM	$1.08 \times 10^6\,M^{-1}$ UV-Vis	2:1	[Sensor] = 25 μM [Cu²⁺] = 1.9 μM	[Sensor] = 25 μM [Cu²⁺] = 25 μM [Competing Metal Ions] = 50 μM	MeCN: H_2O (10:1, v/v)	[93]

Limit of Detection Determined by UV-Vis Spectroscopy

0.10 µM – 0.19 µM

Sensor #	Cu²⁺ Sensor	Ion Sensing	Cu²⁺ LOD	K_a	Binding Stoichiometry Sensor: Cu²⁺	Naked-Eye Detection [Sensor]: [Cu²⁺]	Cu²⁺ Selectivity Assay Conditions	Solvent	Ref
47		Cu²⁺ & Co²⁺ Colorimetric	0.140 µM	$1.88 \times 10^3\,M^{-1}$ UV-Vis	1:2	[Sensor] = 5 µM [Cu²⁺] = 5 µM	[Sensor] = 5 µM [Cu²⁺] = 5 µM [Competing Metal Ions] = 5 µM	DMF: HEPES (7:3, v/v) pH = 7.0	[92]
48		Cu²⁺ Colorimetric	0.15 µM	$3.5 \times 10^{10}\,M^{-2}$ UV-Vis	1:2	[Sensor] = 10 µM [Cu²⁺] = 100 µM	None	MeCN: 10 mM HEPES buffer (4:1, v/v) pH= 7.4	[91]
49		Cu²⁺ Colorimetric	0.188 µM	–	1:2	[Sensor] = 10 µM [Cu²⁺] = 20 µM	[Sensor] = 10 µM [Cu²⁺] = 50 µM [Competing Metal Ions] = 50 µM	MeCN	[89]

					Binding Stoichiometry	Naked-Eye Detection			
Limit of Detection Determined by UV-Vis Spectroscopy **0.10 μM – 0.19 μM**									
Sensor #	**Cu²⁺ Sensor**	**Ion Sensing**	**Cu²⁺ LOD**	**Kₐ**	**Binding Stoichiometry Sensor: Cu²⁺**	**Naked-Eye Detection [Sensor]: [Cu²⁺]**	**Cu²⁺ Selectivity Assay Conditions**	**Solvent**	**Ref**
50		**Cu²⁺** Colorimetric **Fe³⁺** Fluorometric	**0.188 μM**	**4.94 x 10³ M⁻¹** UV-Vis	**1:1**	[Sensor] = 5 μM [Cu²⁺] = 30 μM	[Sensor] = 5 μM [Cu²⁺] = 10 μM [Competing Metal Ions] = 10 μM	MeOH: Tris- HCl (6:4, v/v) pH = 7.2	[94]

681   **Table 7**: Copper(II) sensors arranged from lowest to highest limit of detection in the range of 0.10 μM – 0.19 μM determined by UV-Vis
682   spectroscopy. Information provided: Sensor number, chemical structure (green atoms indicate the proposed mechanism of Cu²⁺ coordination. Shaded
683   green indicates the proposed sensing unit/s in Cu²⁺ coordination), additional cations and anions detected by the sensor, Kₐ = association constant,
684   binding stoichiometry (sensor: Cu²⁺), concentration of sensor and Cu²⁺ for naked eye detection, the Cu²⁺ selectivity assay conditions including
685   concentration of sensor, Cu²⁺ and competing metal ions tested and solvent.

686

4.3   0.20 μM – 0.49 μM

688   This tier of sensors incorporated the Schiff-base motif into eight out of the nine total

689   copper(II) sensors listed. Furthermore, seven sensors utilized the Schiff-base imine to directly

690   coordinate with copper(II) [44,68,95–99]. Interestingly, all the sensors displayed a yellow color,

691   either in the "on" or "off" colorimetric response to copper(II).

692   In 2013, Zhou et al. [96] developed two diaminomaleonitrile-based derivatives with an

693   aza-crown ether linker for improved solubility in aqueous solutions (Table 8 Sensor #52). Sensor

694   **52** contained an aza-15-crown-5 ether, which showed superior selectivity and sensitivity for

695   Cu^{2+}, LOD = 0.20 μM in THF: H_2O (1:4 v/v), than its other counterpart, aza-18 crown-6 ether,

696   LOD = 1 μM in MeCN. Since **52** encompasses a smaller ring cavity size, Cu^{2+} binds at the

697   diamines only with a binding stoichiometry of 1:1 sensor: Cu^{2+}, while the aza-18 derivative can

698   coordinate Cu^{2+} at the diamines and the crown ether. In this review, this is the only instance of

699   applying a macrocycle for improved solubility in an aqueous environment. Since most sensors

700   are lacking solubility in water, this study could guide further designs incorporating this idea.

701   Manna et al. [68] created a benzohydrazide-based sensor **31** with a Schiff-base unit that

702   was able to detect Cu^{2+} and Ni^{2+}, both colorimetrically and fluorometrically (Table 8 Sensor #31).

703   Sensor **31** offered a "turn-on" response, changing from colorless to yellow, in the presence of

704   either metal ion. In the presence of EDTA, **31** exhibited reversibility with the disappearance of

705   **31**-M^{2+} absorbance max at 394 nm and recovery of **31** at 270 nm. This reversibility was seen

706   when cysteine was added to the **31**-Cu^{2+} complex and not observed for the **31**-Ni^{2+} complex. This

707   concept was used to develop an "OR" and "INHIBIT" logic gate. Utilizing cysteine's high

708 binding affinity for copper(II), $K_a \approx 10^{16}$ [85–87], as a way to distinguish between Cu^{2+} and Ni^{2+},

709 could be the basis of further development of **31** for in-field applications.

710   Dolai et al. [98] synthesized an ortho-hydroxy naphthaldimine-based probe **54** containing

711 a gluco-furanose moiety (Table 8 Sensor #54). The C-5 carbon of the sugar was modified to have

712 an -OH or -MeOH group to demonstrate the importance of the hydroxyl in Cu^{2+} metal chelation.

713 Sensor **54** (100 µM), containing -OH, changed from pale yellow to colorless in the presence of

714 Cu^{2+} (200 µM) (**Fig. 12A**). This observation was not evident with the compound having -MeOH

715 group. DFT calculations (**Fig. 12B**) and ^{1}H NMR of **54**-Cu^{2+} show metal coordination at the -OH

716 on the C-5 carbon of the sugar, Schiff-base imine, and -OH on the naphthaldimine. Furthermore,

717 a reversibility assay was done with EDTA and revealed that **54** can be recovered up to two

718 cycles before absorbance and naked-eye detection were no longer observable. This reversibility

719 is appealing as **54** is recyclable however, the discernment between pale yellow and colorless may

720 be difficult to deduce.

721
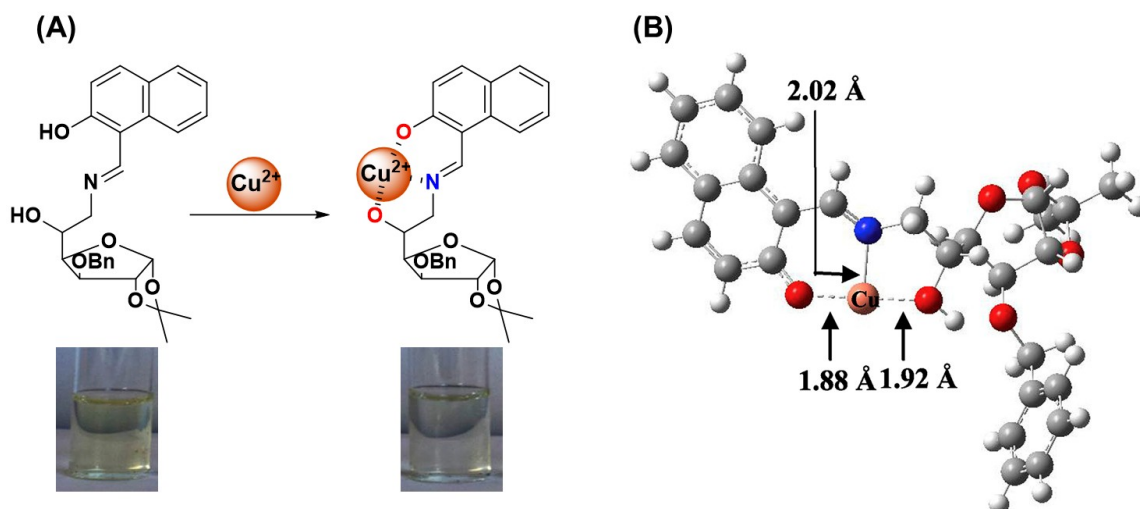
722 ***Fig. 12****: (**A**) Proposed binding of Cu²⁺ (200 μM), to sensor **54** (100 μM), with respective color*

723 *change from pale yellow to colorless in MeCN:H₂O (1:4, v/v). (**B**) DFT calculation suggesting*

724 *coordination to Cu²⁺occurs at the two oxygens (red) and one imine (blue) of **54**. Modified from*

725 *Dolai et al. [98].*

726   Mohammadi, Khalili and Haghayegh [100] made a chromone-based colorimetric sensor

727 **56** (1 μM) that demonstrated a naked-eye color change from colorless to yellow upon addition of

728 1 μM of Cu²⁺ and remained colorless for all other twelve metal ions tested individually at that

729 concentration (Table 8 Sensor #56). Furthermore, **56** exhibited a fast response time for

730 complexation with Cu²⁺ and reached its absorbance max at 306 nm within 10 seconds. This **56**-

731 Cu²⁺ complex remained stable over several weeks. Test strips were prepared by coating filter

732 paper with **56** (10 mM) in acetonitrile and air drying. When the test strips were dipped into

733 varying aqueous Cu²⁺ concentrations (10^{-3} M – 10^{-7} M) separately, a detectable pale-yellow color

734 was observed at 10^{-6} M (**Fig. 13A**). This detection is far below the maximum allowable

735 contaminant level of copper(II) in drinking water at 20 μM and 31.5 μM determined by the

736 Environmental Protection Agency and World Health Organization, respectively [3,4].

737   Chen et al. [58] synthesized sensor **20** through the coupling of the aldehyde of 4-

738 (bis(pyridin-2-ylmethyl)amino)benzaldehyde to an electron acceptor, 2-(3-cyano-4,5,5-

739 trimethylfuran-2(5H)-ylidene)malononitrile, to develop a colorimetric and fluorometric sensor

740 for copper(II) (Table 8 Sensor #20). They also created test strips for the detection of Cu²⁺ by

741 immersing filter paper in an acetone solution containing **20** (1 mM) and air drying. After

742 exposing the test strip separately to varying aqueous concentrations of Cu²⁺ (10^{-3} M – 10^{-6} M), an

743 obvious color change from purple to yellow was noticed at 10^{-3} M concentration (**Fig. 13B**).

744 However the minimal color change from purple to faint purple at concentrations 10^{-4} M- 10^{-5} M

745 poses a problem in providing definitive detection of copper(II) at this concentration range.
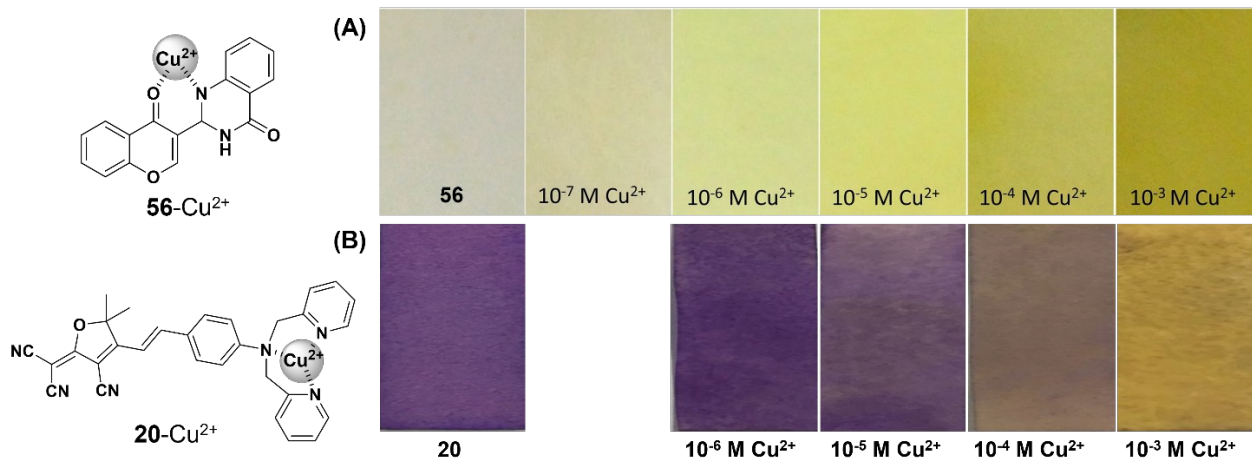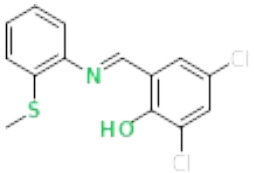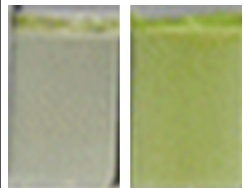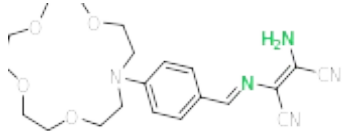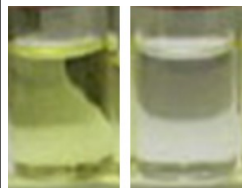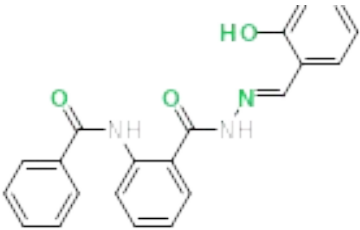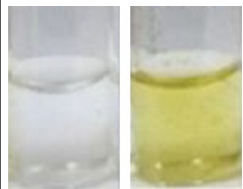

747 **Fig. 13**: *Test strips of (A) 56 and (B) 20 prepared by immersing filter paper in 10mM and 1 mM,*

748 *respectively and air drying. Naked-eye analysis after exposing strips to varying concentrations*

749 *of Cu^{2+}. Modified from Mohammadi et al. [100] and Chen et al. [58].*
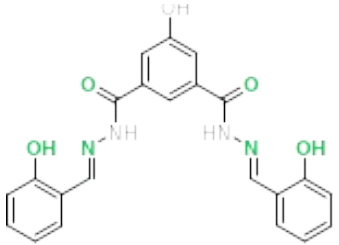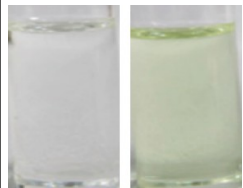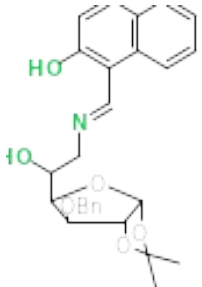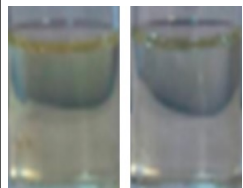
Limit of Detection Determined by UV-Vis Spectroscopy
0.20 µM – 0.49 µM

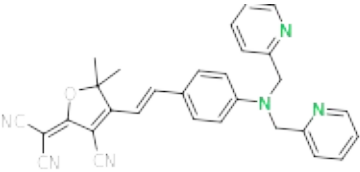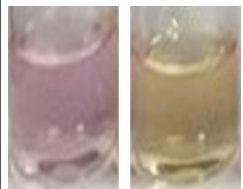| Sensor #	Cu²⁺ Sensor	Ion Sensing	Cu²⁺ LOD	K_a	Binding Stoichiometry Sensor: Cu²⁺	Naked-Eye Detection [Sensor]: [Cu²⁺]	Cu²⁺ Selectivity Assay Conditions	Solvent	Ref
51		**Cu²⁺ & Zn²⁺** Colorimetric & Fluorometric	0.20 µM	**5.9 x 10⁴ M⁻¹** UV-Vis	1:1	[Sensor]= 30µM [Cu²⁺] = 39µM	[Sensor]=30 µM [Cu²⁺] =39 µM [Competing Metal Ions] =39 µM	DMSO: 10 mM bis-tris buffer (3:2, v/v) pH= 7.0	[95]
52		**Cu²⁺** Colorimetric	0.20 µM	**4.97 x 10⁶ M⁻¹** UV-Vis	1:1	[Sensor] = 10 µM [Cu²⁺] = 10 µM	[Sensor] = 10 µM [Cu²⁺] = 10 µM [Competing Metal Ions] = 50 µM	THF: H₂O (1:4, v/v)	[96]
31		**Cu²⁺, Ni²⁺** Colorimetric & Fluorometric	0.204 µM	**1.13 x 10⁶ M⁻¹** UV-Vis	1:1	[Sensor] = 10 µM [Cu²⁺] = 50 µM	[Sensor]= 10 µM [Cu²⁺] = 30 µM [Competing Metal Ions] = 30 µM	MeOH: H₂O (1:1, v/v)	[68]
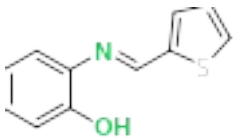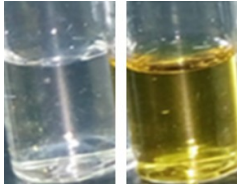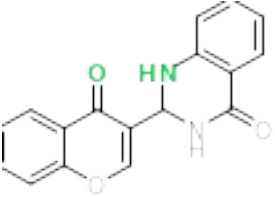
Limit of Detection Determined by UV-Vis Spectroscopy

0.20 μM – 0.49 μM

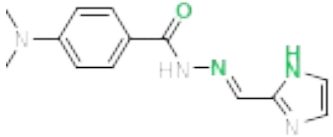| Sensor #	Cu²⁺ Sensor	Ion Sensing	Cu²⁺ LOD	K_a	Binding Stoichiometry Sensor: Cu²⁺	Naked-Eye Detection [Sensor]: [Cu²⁺]	Cu²⁺ Selectivity Assay Conditions	Solvent	Ref
53		**Cu²⁺** Colorimetric & Fluorometric	0.22 μM	3.51×10^4 M⁻¹ Fluorometer	1:2	[Sensor] = 20 μM [Cu²⁺] = 100 μM	[Sensor] = 20 μM [Cu²⁺] = 100 μM [Competing Metal Ions] = 100 μM	DMSO	[97]
54		**Cu²⁺** Colorimetric	0.23 μM	9.7×10^5 M⁻¹ UV-Vis	1:1	[Sensor] = 100 μM [Cu²⁺] = 200 μM	[Sensor] = 30 μM [Cu²⁺] = 60 μM [Competing Metal Ions] = 60 μM	MeCN: H₂O (1:4, v/v)	[98]
20		**Cu²⁺** Colorimetric & Fluorometric	0.24 μM	3.6×10^4 M⁻¹ Fluorometer	1:1	[Sensor] = 10 μM [Cu²⁺] = 50 μM	[Sensor] = 10 μM [Cu²⁺] = 50 μM [Competing Metal Ions] = 50 μM	EtOH: HEPES (1:4, v/v) pH= 7.2	[58]

Limit of Detection Determined by UV-Vis Spectroscopy
0.20 μM – 0.49 μM

Sensor #	Cu^{2+} Sensor	Ion Sensing	Cu^{2+} LOD	K$_a$	Binding Stoichiometry Sensor: Cu^{2+}	Naked-Eye Detection [Sensor]: [Cu^{2+}]	Cu^{2+} Selectivity Assay Conditions	Solvent	Ref
55		Cu^{2+}, Hg^{2+} Colorimetric Cu^{2+} Fluorometric	0.29 μM	3.67 x 10^4 M^{-1} UV-Vis	2:1	[Sensor] = 50 μM [Cu^{2+}] = 100 μM	None	MeCN	[99]
7		Cu^{2+} & S^{2-} Colorimetric & Fluorometric	0.46 μM	4.3 x 10^7 M^{-1} UV-Vis 5.4 x 10^7 M^{-1} Fluorimeter	1:1	[Sensor] = 10 μM [Cu^{2+}] = 500 μM	[Sensor] = 10 μM [Cu^{2+}] = 500 μM [Competing Metal Ions] = 500 μM	MeCN: Tris-HCl (3:2, v/v) pH= 7.4	[44]
56		Cu^{2+} Colorimetric	0.46 μM	3.27 x 10^4 M^{-1} UV-Vis	1:1	[Sensor] = 1 μM [Cu^{2+}] = 1 μM	[Sensor] = 62.5 μM [Cu^{2+}] = 625 μM [Competing Metal Ions] = 625 μM	MeCN: H$_2$O (9:1, v/v)	[100]

750 **Table 8**: Copper(II) sensors arranged from lowest to highest limit of detection in the range of 0.20 μM – 0.49 μM determined by UV-Vis
751 spectroscopy. Information provided: Sensor number, chemical structure (green atoms indicate the proposed mechanism of Cu^{2+} coordination. Shaded
752 green indicates the proposed sensing unit/s in Cu^{2+} coordination), additional cations and anions detected by the sensor, K$_a$ = association constant,

753 binding stoichiometry (sensor: Cu^{2+}), concentration of sensor and Cu^{2+} for naked eye detection, the Cu^{2+} selectivity assay conditions including
754 concentration of sensor, Cu^{2+} and competing metal ions tested and solvent.

4.4   0.50 μM – 0.99 μM

756   Sensors in this category contained the most sensors that were reported to solely detect

757   copper(II) colorimetrically [101–107]. Other ions detected were I$^-$ [108] or CN$^-$ [109]

758   colorimetrically and Zn^{2+} [106] fluorometrically by the remaining sensors. In addition, three

759   groups were able to synthesize and test their sensors in 100% fully aqueous buffer solutions with

760   pH 4.75 and 7.0 [101,103,109].

761   Patil et al. [108] assembled sensor **57** composed of a pyrimidine unit and a *p*-toluidine

762   unit that was able to achieve the lowest limit of detection (LOD = 0.54 μM) for Cu^{2+} in this tier

763   of sensors (Table 9 Sensor #57). **57** (30 μM) was able to detect Cu^{2+} (150 μM) colorimetrically

764   through a color change (colorless to red) in MeCN:H$_2$O (40:60, v/v). Additional detection of I$^-$

765   was possible through UV-Vis with an absorbance peak at 232 nm but did not offer a color

766   change. Sensor **57** (10 mM) was treated to filter paper to make test strips and silica gel to create a

767   solid support system for aqueous detection of Cu^{2+} (10^{-3} M – 10^{-6} M). Metal ions Ca^{2+}, Hg^{2+}, Li$^+$,

768   and Pb^{2+} had a noticeable interference in the 1:1 Cu^{2+}: M^{n+} competition assay in solution, so

769   examining these metals using the solid support system under the same conditions would

770   demonstrate **57** practicality for sensing copper(II).

771   Ciarrocchi et al. [101] used phenothiazinium, commonly known as methylene blue (MB)

772   dye, for its UV-Vis absorption properties, and cyclam, a common macrocyclic metal chelator, as

773   the receptor for copper(II). Utilizing these two components, two derivatives were synthesized.

774   Both possessed MB but differed in the number of cyclams affixed; one sensor bearing a single

775   cyclam and the other bearing two cyclams. Unfortunately, the sensor with two cyclams was not

776   suitable for accurate detection of Cu^{2+} due to the interference with other metal ions, such as Cr^{3+},

777   Fe^{3+}, Ru^{3+}, and Hg^{2+}. Therefore, sensor **58**, bearing one cyclam, was examined further (Table 9

778   Sensor #58). The UV-Vis absorption properties were investigated in 0.1 M acetate buffer with

779   pH = 4.75 and MB exhibited its typical absorption maxima at 665 nm with a shoulder at 615 nm.

780   Sensor **58** displayed a similar absorbance profile as to MB, with a slight blue-shift having an

781   absorbance max of 653 nm with a shoulder at 610 nm. **Fig. 14** shows the time-dependent

782   interaction of sensor **58** (10 μM) with Cu^{2+} (20 μM). Initially, there is an absorbance decrease ≈

783   0.4 a.u. at λ_{max}= 653 nm at time point < 1 min, where the absorbance profile is still fairly

784   maintained with a peak and a shoulder. Full complexation is not achieved until roughly 5

785   minutes with the appearance of a broad peak centered at 573 nm and accompanied by a color

786   change from blue to purple (**Fig. 14 inset**). This color and absorbance change was observed in

787   the metal ion studies when the same concentration of **58** was exposed to excess amounts of metal

788   ions (200 μM), except for Hg^{2+}. When Hg^{2+} was introduced to **58**, the absorbance profile

789   resembled the absorbance profile of time point < 1 min from **Fig. 14**, possibly leading to a false

790   positive. It is interesting to note that sensor **58** was the first encountered sensor that employed a

791   macrocyclic chelator as the receptor for copper(II). Since cyclam can chelate other metal ions, it

792   is surprising other metal ions did not cause additional interference. This could be due to the fact

793   that cyclam contains high stability constant for copper(II), log K = 27.2, whereas Hg^{2+} is the

794   second closest metal with a stability constant of log K = 23.0 [110,111].

795
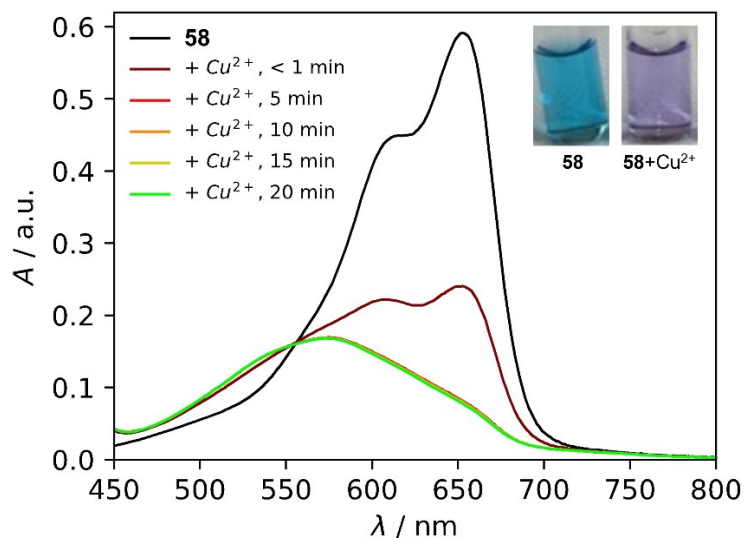
*Fig. 14: UV-Vis spectra of monitored time-dependent complexation between 58 (10 μM) and Cu²⁺(20 μM) from 0 min (black), <1 min (brown), 5 min (red), 10 min (orange), 15 min (yellow), and 20 min (green), in 0.1 M acetate buffer, pH = 4.75. **Inset:** respective color change of 58 (10 μM) from blue to purple after full complexation with Cu²⁺(20 μM) in 0.1 M acetate buffer, pH = 4.75. Modified from Ciarrocchi et al. [101].*

796
797
798
799
800

801

802   Arvind and Satish Kumar [104] utilized a spiropyran-based Cu²⁺ sensor **61**, comprising a
803   thiazole moiety on the indole side and a methoxy group on the *ortho*-position to the phenolic
804   oxygen (Table 9 Sensor #61). It was found that **61** in MeCN:1 mM HEPES (1:1, v/v, pH = 7.6)
805   did not show any switching response when exposed to UV or visible light. It is only when Cu²⁺ is
806   present in solution causing isomerization of the spiropyran to merocyanine, creating the **61-**Cu²⁺
807   complex, that can be reversed with 532 nm light. Five cycles of reversibility consisting of
808   irradiation and placement in the dark were conducted with minimal to no degradation.

71

809   Combining this reversibility with the selectivity for copper(II) in the 1:1 Cu^{2+}:M^{n+} competition

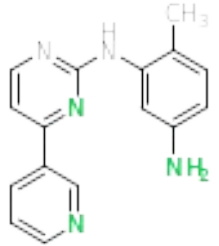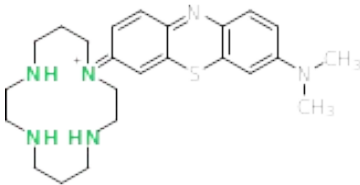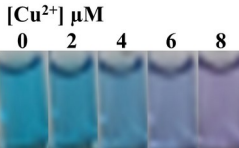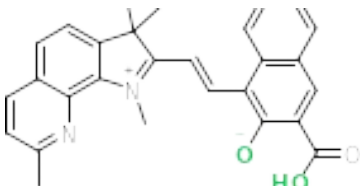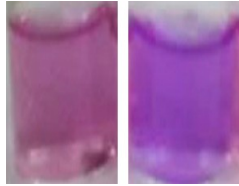810   studies makes this an attractive recyclable sensor for Cu^{2+}.

811   You et al. [109] coupled a thiadiazole and julolidine units to produce sensor **63**, where

812   Cu^{2+} binding occurs in a 2:1 sensor:Cu^{2+} fashion at the hydroxy position on the julolidine and

813   Schiff-base C=N that bridges the two moieties together (Table 9 Sensor #63). Analyzing the

814   absorbance spectrum of **63** (10 μM) with individual metal ions (5 μM) in 10 mM bis-tris buffer

815   pH =7 revealed that Cd^{2+} severely interfered with Cu^{2+} detection at 450 nm and 525 nm. This

816   interference was not seen in the naked-eye studies suggesting **63** could be potentially applied as a

817   naked-eye sensor for qualitative purposes. Since most sensors lack solubility in completely

818   aqueous conditions, it is commendable that Ciarrocchi and You were able to achieve this in

819   100% buffer solution.

820   Kim (2019) et al. [106] developed probe **64** to act as a dual sensor for Zn^{2+} via

821   fluorescence spectroscopy and Cu^{2+} via UV-Vis spectroscopy (Table 9 Sensor #64). **64** offers a

822   "turn-on" response as **64** (10 μM) is colorless in MeCN:10 mM bis-tris buffer (95:5, v/v, pH =

823   7.0) with an absorbance max at 290 nm. When 16 μM of Cu^{2+} is added to the solution, the color

824   changes from colorless to pink with a new peak at 503 nm. After examining the absorbance

825   spectrum from the competition studies of **64** (10 μM) with M^{n+} (16 μM) and Cu^{2+}, it was found

826   that Hg^{2+}, Ag^+, and Fe^{2+}, obstructed Cu^{2+} absorbance by 30%, 50%, and 90% respectively. After

827   examining the naked-eye analysis, under the same conditions, a colorless solution was observed

828   when **64** was incubated with Fe^{2+} and Cu^{2+}, resulting in a false negative, as the expected color of

829   copper(II) incubation was anticipated to be pink. Therefore, **64** would be best suited for Zn^{2+}

830   detection as the sensor was ultimately applied to fluorescence imaging of Zn^{2+} in HeLa, cervical

831   cancer cells.
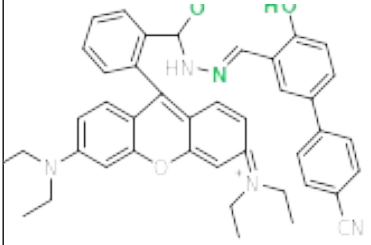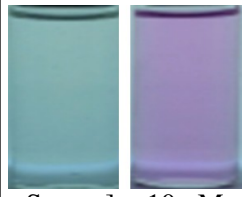
Limit of Detection Determined by UV-Vis Spectroscopy
0.50 µM – 0.99 µM

Sensor #	Cu²⁺ Sensor	Ion Sensing	Cu²⁺ LOD	K_a	Binding Stoichiometry Sensor: Cu²⁺	Naked-Eye Detection [Sensor]: [Cu²⁺]	Cu²⁺ Selectivity Assay Conditions	Solvent	Ref
57		Cu²⁺, I⁻ Colorimetric	0.54 µM	5.17×10^3 M⁻¹ UV-Vis	1:1	[Sensor] = 30 µM [Cu²⁺] = 150 µM	[Sensor] = 30 µM [Cu²⁺] = 150 µM [Competing Metal Ions] = 150 µM	MeCN: H₂O (40:60, v/v)	[108]
58		Cu²⁺ Colorimetric	0.6 µM	–	1:1	[Sensor] = 10 µM [Cu²⁺] = 8 µM	[Sensor] = 10 µM [Cu²⁺] = 10 µM [Competing Metal Ions] = 200 µM	0.1 M acetate buffer, pH = 4.75	[101]
59		Cu²⁺ Colorimetric	0.63 µM	1.9×10^5 M⁻¹ UV-Vis	1:1	[Sensor] = 20 µM [Cu²⁺] = 20 µM	[Sensor] = 20 µM [Cu²⁺] = 200 µM [Competing Metal Ions] = 200 µM	MeOH: H₂O (9:1, v/v)	[102]

Limit of Detection Determined by UV-Vis Spectroscopy

0.50 μM – 0.99 μM

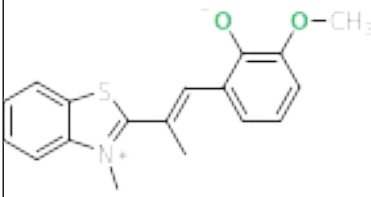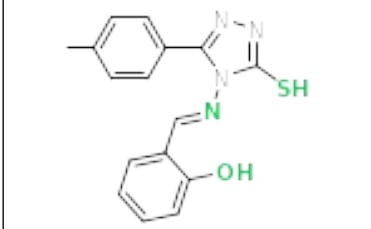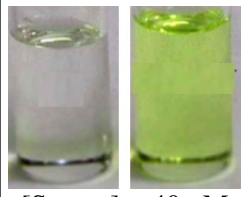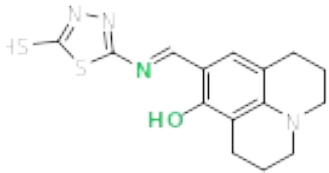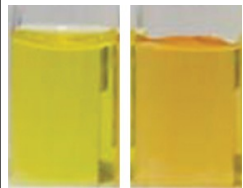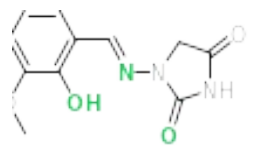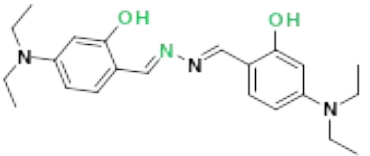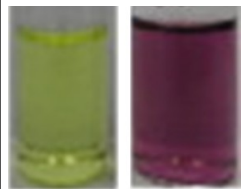| Sensor #	Cu²⁺ Sensor	Ion Sensing	Cu²⁺ LOD	K_a	Binding Stoichiometry Sensor: Cu²⁺	Naked-Eye Detection [Sensor]: [Cu²⁺]	Cu²⁺ Selectivity Assay Conditions	Solvent	Ref
60		Cu²⁺ Colorimetric	0.69 μM	5.56×10^4 M⁻¹ UV-Vis	1:1	Sensor] = 10 μM [Cu²⁺] = 10 μM	[Sensor] = 10 μM [Cu²⁺] = 100 μM [Competing Metal Ions] = 100 μM	HEPES buffer pH = 7.0	[103]
61		Cu²⁺ Colorimetric	0.75 μM	–	1:1	[Sensor] = 20 μM [Cu²⁺] = 20 μM	[Sensor] = 20 μM [Cu²⁺] = 20 μM [Competing Metal Ions] = 20 μM	MeCN: 1 mM HEPES (1:1, v/v) pH= 7.6	[104]
62		Cu²⁺ Colorimetric	0.80 μM	4.3×10^5 M⁻¹ UV-Vis	1:1	[Sensor] = 40 μM [Cu²⁺] = 40 μM	[Sensor] = 40 μM [Cu²⁺] = 40 μM [Competing Metal Ions] = 40 μM	DMSO: H₂O (9:1, v/v)	[105]

Limit of Detection Determined by UV-Vis Spectroscopy
0.50 μM – 0.99 μM

Sensor #	Cu²⁺ Sensor	Ion Sensing	Cu²⁺ LOD	K_a	Binding Stoichiometry Sensor: Cu²⁺	Naked-Eye Detection [Sensor]: [Cu²⁺]	Cu²⁺ Selectivity Assay Conditions	Solvent	Ref
63		Cu²⁺ & CN⁻ Colorimetric	0.9 μM	1.0×10^{10} M⁻² UV-Vis	2:1	 [Sensor] = 30 μM [Cu²⁺] = 15 μM	[Sensor] = 10 μM [Cu²⁺] = 5 μM [Competing Metal Ions] = 5 μM	10 mM bis-tris buffer pH = 7.0	[109]
64		Cu²⁺ Colorimetric Zn²⁺ Fluorometric	0.91 μM	3.3×10^{2} M⁻¹ UV-Vis	1:1	 [Sensor] = 10 μM [Cu²⁺] = 16 μM	[Sensor] = 10 μM [Cu²⁺] = 16 μM [Competing Metal Ions] = 16 μM	MeCN: 10 mM bis-tris (95:5, v/v) pH= 7.0	[106]
65		Cu²⁺ Colorimetric	0.98 μM	4.16×10^{6} M⁻¹ UV-Vis	1:1	 [Sensor] = 5 μM [Cu²⁺] = 30 μM	[Sensor] = 5 μM [Cu²⁺] = 10 μM [Competing Metal Ions] = 50 μM	MeCN	[107]

832   **Table 9**: Copper(II) sensors arranged from lowest to highest limit of detection in the range of 0.50 μM – 0.99 μM determined by UV-Vis

833   spectroscopy. Information provided: Sensor number, chemical structure (green atoms indicate the proposed mechanism of Cu²⁺ coordination. Shaded

834   green indicates the proposed sensing unit/s in Cu²⁺ coordination), additional cations and anions detected by the sensor, K_a = association constant,

835   binding stoichiometry (sensor: Cu^{2+}), concentration of sensor and Cu^{2+} for naked eye detection, the Cu^{2+} selectivity assay conditions including

836   concentration of sensor, Cu^{2+} and competing metal ions tested and solvent.

4.5   ***1.0 μM – 4.90 μM***

838   While most of the sensors in this category detected copper(II) in their respective

839   solutions, others in this group were able to employ their sensors as test strips [112,113], as a pH

840   probe when bound to Cu^{2+} [114], in tap water spiked with Cu^{2+} [115–117], in simulated wastewater

841   using a smartphone application [118], and for fluorescence bioimaging [119,120].

842   Rezaeian, Khanmohammadi, and Arab [112] synthesized an azo-azomethine derivative to

843   perform as a Cu^{2+} sensor **66** in THF:Tris-HCl buffer (9:1, v/v, pH = 7.0) that offered a color

844   change from yellow to brown (Table 10 Sensor #66). Upon addition of 60 μM of Cu^{2+} to 20 μM

845   of **66**, the UV-Vis absorbance spectrum demonstrated a decrease in absorbance at 355 nm,

846   associated with free sensor **66**, and an increase in absorbance at 482 nm, related to **66**-Cu^{2+}

847   complex. A clear isosbestic point at 430 nm is also present, representing the free sensor **66** to **66**-

848   Cu^{2+} formation. Test strips were designed for Cu^{2+} detection in water, but the only concentration

849   of copper(II) tested was 1 mM. **66** performed well in the pH 6-12, so physiological and in-field

850   testing may be possible in this range if lower concentrations of Cu^{2+} were tested in the presence

851   of competing metal ions.

852   In 2017 Chang et al. [118] selected 3-hydroxynaphthalimide to act at the signaling unit,

853   and coupled it to diaminomaleonitrile to create sensor **69** (Table 10 Sensor #69). Copper(II) was

854   able to coordinate to **69** through the hydroxyl on the naphthalimide, an amine on the

855   diaminomaleonitrile, and the Schiff-base imine in a 1:1 binding stoichiometry (**Fig. 15A**). Sensor

856   **69** was able to detect Cu^{2+} in various organic solvents such as DMSO, THF, and EtOH, offering a

857   color change from yellow to pink. Since practical applications for Cu^{2+} sensors require detection

858   in aqueous conditions, a 1:1 liquid-liquid extraction was performed, with **69** (10 μM) in ethyl

859   acetate and Cu^{2+} (1 mM) with competing metal ions (1 mM) in 10 mM acetate buffer (pH = 4.8).

860   After vigorously shaking, followed by phase separation, the ethyl acetate organic extractant was

861   collected, and a pink color was observed. The UV-Vis absorption spectrum was analyzed and

862   exhibited Cu^{2+} detection over the various metal ions tested. This method was applied using

863   simulated wastewater [121,122] and varying the Cu^{2+} concentration. After extraction and

864   collection, the ethyl acetate layer was analyzed via a smartphone app, RBG Grabber,

865   Shumamicode (**Fig. 15B**). The ratio of the two channels, Green/Red and Blue/Red, were plotted

866   against the varying copper(II) concentration to generate a calibration curve for Cu^{2+} (**Fig. 15C**),

867   and the limit of detection for the smartphone-based app was found to be 48 μM. This liquid-

868   liquid extraction method for Cu^{2+} detection in aqueous samples combined with the smartphone

869   application was the only technique encountered in this review that could offer a workaround for

870   sensors that lack solubility in water.

871
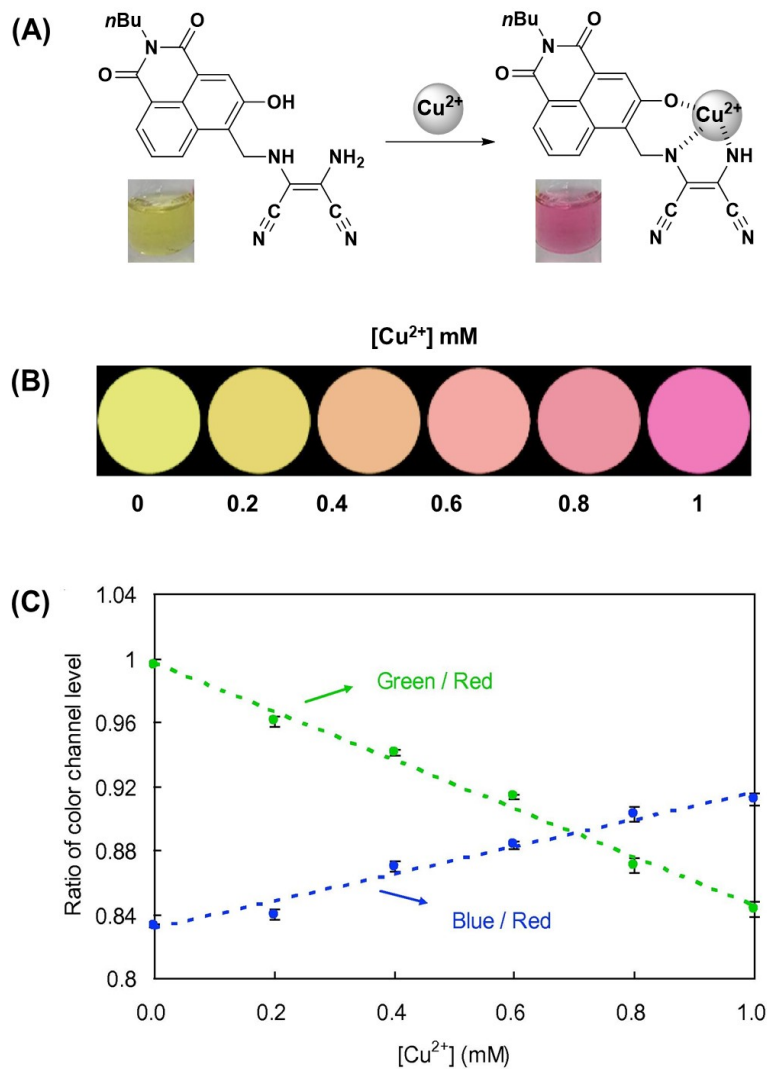
Fig. 15: **(A)** *Proposed binding and naked eye color change of sensor* **69**, *in the presence of* Cu^{2+}.

(B) *RBG Grabber Shumamicode images of* **69** *(50 μM) extractant of ethyl acetate and the*

resulting **(C)** *ratio of color channel level after exposure to varying concentrations of* Cu^{2+} *(0-1*
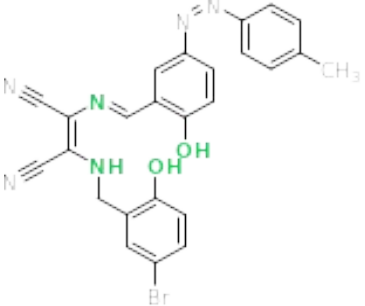
mM). Modified from Chang(2017) et al. [118].
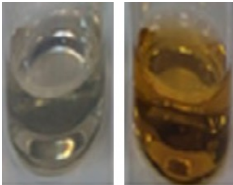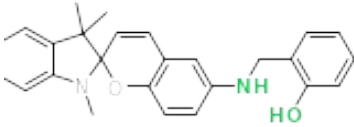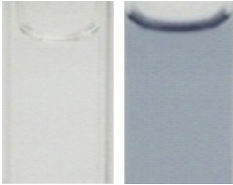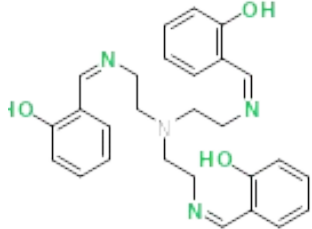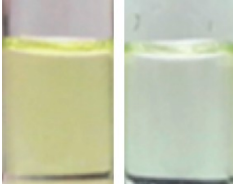
Noh et al. [114] employed triaminoguanidinium as the backbone for sensor **74** and is one

of nine sensors that are in a completely aqueous solvent, 10 mM bis-tris buffer: DI H_2O (999:1,

879   v/v, pH = 7.0) (Table 10 Sensor #74). When **74** (30 μM) was in the presence of Cu^{2+} (180 μM),

880   an emergence of two absorbance peaks at 275 nm and 425 nm was noticed. However, Fe^{2+} and

881   Fe^{3+} confounded copper(II) detection at 275 nm, so analyzing at 425 nm wavelength is necessary

882   for quantitative purposes. Additionally, sensor **74**-Cu^{2+} was used as a pH indicator to discern the

883   pH at 5.4. When the pH was less than 5.4, the solution was colorless and as the pH was gradually

884   increased to a pH of 5.4, the observed color change was pale yellow. Reversibility of the color

885   was seen through the addition of HCl or NaOH. Three samples, DI water, tap water, and soda,

886   were assessed with the sensor **74**-Cu^{2+} complex and a pH meter for measurement. For DI water,

887   tap water, and soda, the pH was found to be 6.18, 7.09, and 3.15 via pH meter and the

888   corresponding color was yellow, yellow, and colorless by means of **74**-Cu^{2+} sensor,

889   correspondingly. Although this is an interesting discovery, **74** will be more applicable for the

890   recognition of Cu^{2+} in aqueous media through analysis at 425 nm than as a pH ± 5.4 indicator.
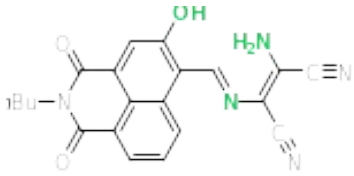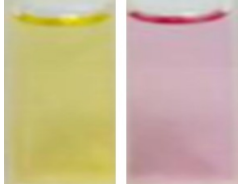
Limit of Detection Determined by UV-Vis Spectroscopy

1.0 μM – 4.9 μM

Sensor #	Cu²⁺ Sensor	Ion Sensing	Cu²⁺ LOD	K_a	Binding Stoichiometry Sensor: Cu²⁺	Naked-Eye Detection [Sensor]: [Cu²⁺]	Cu²⁺ Selectivity Assay Conditions	Solvent	Ref
66		**Cu²⁺** Colorimetric	1.07 μM	**5.46 x 10⁴ M⁻¹** UV-Vis	**1:1**	[Sensor] = 20 μM [Cu²⁺] = 60 μM	[Sensor] = 20 μM [Cu²⁺] = 60 μM [Competing Metal Ions] = 60 μM	THF: Tris-HCl (9:1, v/v) pH= 7.0	[112]
67		**Cu²⁺** Colorimetric	1.2 μM	–	**2:1**	[Sensor] = 20 μM [Cu²⁺] = 40 μM	[Sensor] = 20 μM [Cu²⁺] = 40 μM [Competing Metal Ions] = 20 μM	100 mM HEPES: MeCN (1:1, v/v) pH= 7.0	[123]
68		**Cu²⁺, Fe²⁺ & Zn²⁺** Colorimetric **Zn²⁺** Fluorometric	1.5 μM	**5.01 x 10⁴ M⁻¹** UV-Vis	**1:1**	[Sensor] = 50 μM [Cu²⁺] = 100 μM	[Sensor] = 20 μM [Cu²⁺] = 40 μM [Competing Metal Ions] = 40 μM	10 mM HEPES: MeOH (99:1, v/v)	[119]
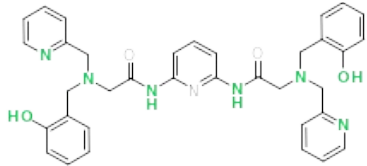
Limit of Detection Determined by UV-Vis Spectroscopy

1.0 µM – 4.9 µM

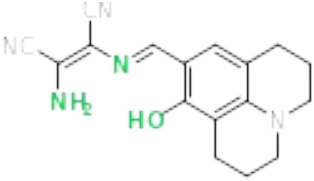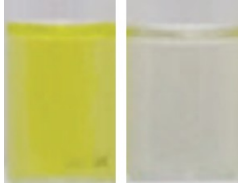| Sensor #	Cu^{2+} Sensor	Ion Sensing	Cu^{2+} LOD	K_a	Binding Stoichiometry Sensor: Cu^{2+}	Naked-Eye Detection [Sensor]: [Cu^{2+}]	Cu^{2+} Selectivity Assay Conditions	Solvent	Ref
69		**Cu^{2+}** Colorimetric	**1.6 µM**	**5.9 x 10^4 M^{-1}** UV-Vis	**1:1**	 [Sensor] = 10 µM [Cu^{2+}] = 500 µM	[Sensor] = 10 µM [Cu^{2+}] = 500 µM [Competing Metal Ions] = 500 µM	DMSO	[118]
70		**Cu^{2+} & F$^-$** Colorimetric	**2.1 µM**	**2.3 x 10^4 M^{-1}** UV-Vis	**1:1**	 [Sensor] = 10 µM [Cu^{2+}] = 30 µM	[Sensor] = 10 µM [Cu^{2+}] = 30 µM [Competing Metal Ions] = 30 µM	MeCN: bis-tris buffer (6:4, v/v)	[115]
71		**Cu^{2+}** Colorimetric **Fe^{3+}** Fluorometric	**2.17 µM**	–	**1:1**	 [Sensor] = 50 µM [Cu^{2+}] = 200 µM	[Sensor] = 50 µM [Cu^{2+}] = 200 µM [Competing Metal Ions] = 200 µM	DMSO: HEPES (8:2, v/v) pH= 7.4	[120]
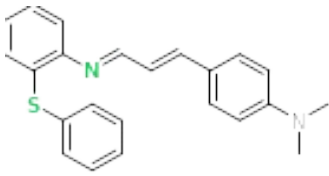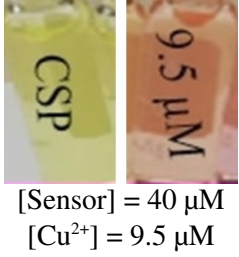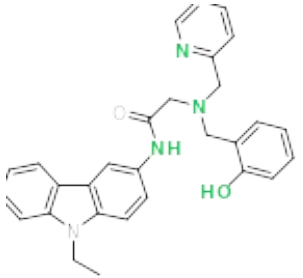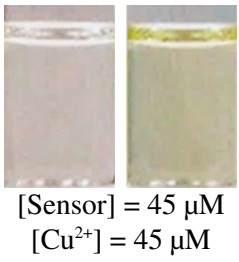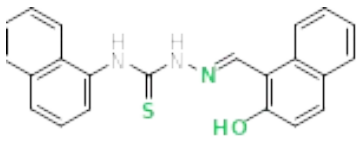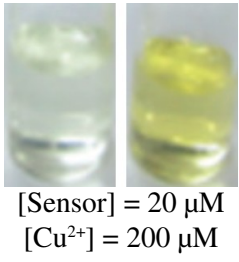
Limit of Detection Determined by UV-Vis Spectroscopy
1.0 µM – 4.9 µM

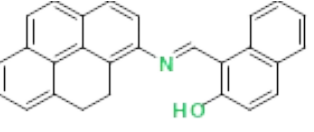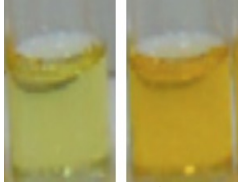| Sensor #	Cu²⁺ Sensor	Ion Sensing	Cu²⁺ LOD	K_a	Binding Stoichiometry Sensor: Cu²⁺	Naked-Eye Detection [Sensor]: [Cu²⁺]	Cu²⁺ Selectivity Assay Conditions	Solvent	Ref
72		Cu²⁺ & Fe²⁺ Colorimetric	2.29 µM	1.66×10^9 M⁻¹ UV-Vis	1:2	[Sensor] = 20 µM [Cu²⁺] = 60 µM	[Sensor] = 20 µM [Cu²⁺] = 60 µM [Competing Metal Ions] = 60 µM	Bis-tris: DMF (8:2, v/v) pH=7.0	[113]
73		Cu²⁺ Colorimetric	2.51 µM	–	2:1	[Sensor] = 200 µM [Cu²⁺] = 1 mM	[Sensor] = 200 µM [Cu²⁺] = 1 mM [Competing Metal Ions] = 1 mM	MeCN	[116]
74		Cu²⁺ Colorimetric	2.7 µM	1.1×10^5 M⁻¹ UV-Vis	1:1	[Sensor] = 30 µM [Cu²⁺] = 180 µM	[Sensor] = 30 µM [Cu²⁺] = 180 µM [Competing Metal Ions] = 180 µM	10 mM bis-tris: distilled H₂O (999:1, v/v) pH=7.0	[114]

Limit of Detection Determined by UV-Vis Spectroscopy
1.0 μM – 4.9 μM

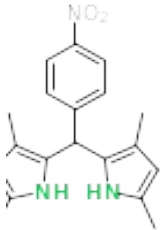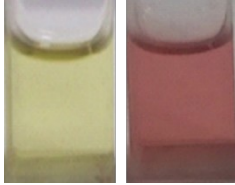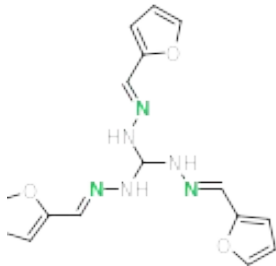| Sensor #	Cu²⁺ Sensor	Ion Sensing	Cu²⁺ LOD	K_a	Binding Stoichiometry Sensor: Cu²⁺	Naked-Eye Detection [Sensor]: [Cu²⁺]	Cu²⁺ Selectivity Assay Conditions	Solvent	Ref
75		**Cu²⁺** Colorimetric	**2.85 μM**	**2.4 x 10¹⁰ M⁻²** UV-Vis	**2:1**	[Sensor] = 40 μM [Cu²⁺] = 9.5 μM	[Sensor] = 40 μM [Cu²⁺] = 40 μM [Competing Metal Ions] = 40 μM	MeCN: H₂O (2:1, v/v)	[117]
76		**Cu²⁺, Fe²⁺, Fe³⁺ & CN⁻** Colorimetric **CN⁻** Fluorometric	**2.9 μM**	**4.2 x 10³ M⁻¹** UV-Vis	**1:1**	[Sensor] = 45 μM [Cu²⁺] = 45 μM	[Sensor] = 45 μM [Cu²⁺] = 45 μM [Competing Metal Ions] = 45 μM	DMF: 10 mM bis-tris (1:1, v/v) pH= 7	[124]
77		**Cu²⁺ & F⁻** Colorimetric **Zn²⁺ & Al³⁺** Fluorometric	**4.64 μM**	**3.33 x 10⁴ M⁻¹** UV-Vis	**1:1**	[Sensor] = 20 μM [Cu²⁺] = 200 μM	None	MeOH: 5 mM HEPES (9:1, v/v) pH= 7.3	[125]

891 **Table 10**: Copper(II) sensors arranged from lowest to highest limit of detection in the range of 1.0 μM – 4.9 μM determined by UV-Vis
892 spectroscopy. Information provided: Sensor number, chemical structure (green atoms indicate the proposed mechanism of Cu²⁺ coordination. Shaded
893 green indicates the proposed sensing unit/s in Cu²⁺ coordination), additional cations and anions detected by the sensor, K_a = association constant,

894   binding stoichiometry (sensor: Cu^{2+}), concentration of sensor and Cu^{2+} for naked eye detection, the Cu^{2+} selectivity assay conditions including
895   concentration of sensor, Cu^{2+} and competing metal ions tested and solvent

4.6   5.0 μM – 15 μM

897   Sharma and Singh [126] created **78**, containing perylene-diimide, for its optical and

898   fluorescent properties, and *tert*-butyl acetate linked by 1,4-diaminobutane, for chelating

899   copper(II) (Table 11 Sensor #78). **78** was able to detect Cu^{2+} colorimetrically (LOD = 5.22 μM)

900   and fluorometrically (LOD = 4.8 μM) in HEPES:MeCN (4:6, v/v, pH = 7.2). It is only when

901   copper(II) was bound to the sensor, forming the **78**-Cu^{2+} complex, that detection of anions such

902   as CN^-, through replacement of a solvent molecule coordinated to **78**-Cu^{2+}, and S^{2-}, through the

903   displacement of copper from **78**-Cu^{2+}, was possible by means of colorimetric and fluorometric

904   detection. Naked-eye detection of sensor **78** (50 μM) offered a "turn-off" response changing from

905   blue to colorless in the presence of Cu^{2+} (750 μM) only. When competing metal ions (1mM) were

906   tested against copper(II), a decolorization of the solution was observed for all metal ions except

907   Pd^{2+}, Fe^{2+}, and Cd^{2+}, which appeared as faint blue and may hinder analysis.

908   Huo et al. [127] synthesized sensor **80** through nucleophilic addition of salicylaldehyde,

909   converting hydrazine to hydrazone in an 89% yield (Table 11 Sensor #80). Ratiometric detection

910   of **80** (10 μM) at wavelengths A_{442}/A_{360} was used to detect Cu^{2+} (20 μM) over competing metal

911   ions (20 μM) in DMSO:HEPES (4:1, v/v, pH = 7.0), changing from colorless to yellow. A "real-

912   life" multi-component system that contained several metals and anions was reproduced [128] and

913   spiked with 40 μM Cu^{2+}. When 25 μM of sensor **80** was added to the solution, the concentration

914   of copper(II) was measured from an A_{442}/A_{360} vs. $[Cu^{2+}]$ absorption calibration curve to

915   quantitatively calculate the amount of Cu^{2+} in the system. This demonstrates the ability of **80** to

916   quantitatively and qualitatively detect Cu^{2+}. Since the chosen media was in DMSO:HEPES (4:1,

917   v/v, pH = 7.0), it would be beneficial and interesting if this could be adapted to a 100% aqueous

918   solvent system.

919   Tang et al. [129] employed a rhodamine-based Cu^{2+} sensor, **81**, that can detect S^{2-}

920   through the displacement of copper(II) from **81**-Cu^{2+} complex (Table 11 Sensor #81). This

921   displacement and recovery of **81** was tested through five cycles and showed little to no

922   degradation, confirming **81**'s reversibility. Due to this reversibility, an "INHIBIT" logic gate was

923   developed, analyzing at wavelength 556 nm. When **81** is alone in solution, the output will read 0

924   owing to the low absorbance at 556 nm. When there is a high absorbance at 556 nm (**81**-Cu^{2+}, no

925   S^{2-}), the output will read 1. When S^{2-} is added to **81** or **81**-Cu^{2+}, the output will read 0 due to the

926   low absorbance at 556 nm (**81**).

927   Kuar, Sareen, and Singh [130] created sensor **85** (10 μM) with an observable color

928   change from yellow to purple upon the addition of 30 μM of Cu^{2+} in MeCN (Table 11 Sensor

929   #85). Furthermore, **85** showed selectivity for copper(II) in the ratio of 1:10 Cu^{2+}:M^{n+} competition

930   studies,   an   achievement   that   only   7   sensors   in   this   review   were   able   to   attain

931   [52,55,73,78,101,130,131]. A solid support system was created by fixing sensor **85** (30 μM) to

932   silica, 60-120 and 100-200 mesh. When 300 μM Cu^{2+} in water was added to the silica, a color

933   change from yellow to purple was observed (**Fig. 16A & B**). Naked-eye detection of Cu^{2+} was

934   recognized at 10 μM in solution (**Fig. 16C**).

935
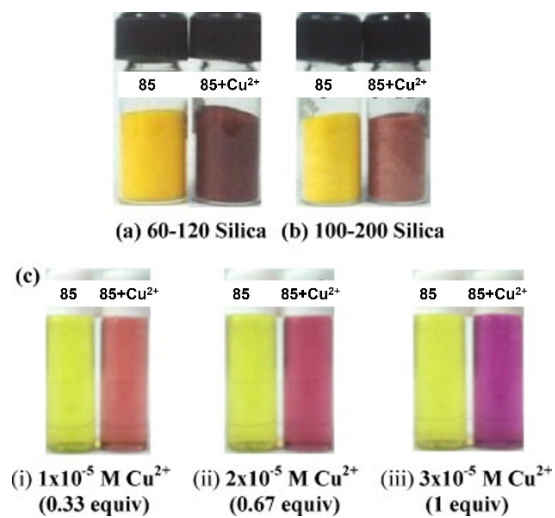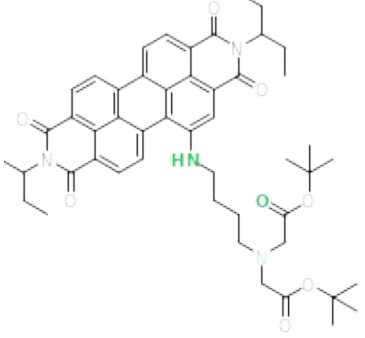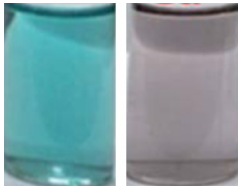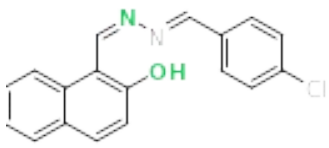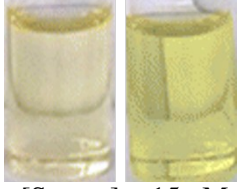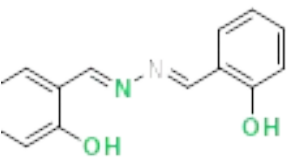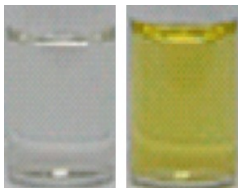
Fig. 16: *Solid silica support of sensor **85** (30 μM) fixed to **(A)** 60-120 mesh **(B)** 100-200 mesh before and after exposure to Cu^{2+} (300 μM). **(C)** Naked-eye detection of **85** (30 μM) in MeCN after addition of aqueous amounts of Cu^{2+} (i) $1x10^{-5}$ M, (ii))$2x10^{-5}$ M, and (iii) $3x10^{-5}$M. Modified from Kaur et al. [130].*
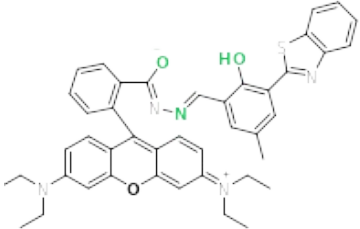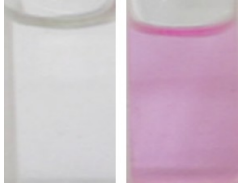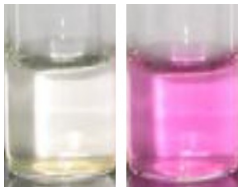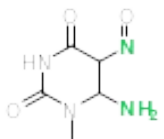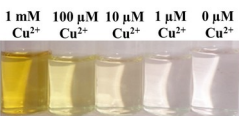
Limit of Detection Determined by UV-Vis Spectroscopy
5.0 µM – 15 µM

Sensor #	Cu²⁺ Sensor	Ion Sensing	Cu²⁺ LOD	K_a	Binding Stoichiometry Sensor: Cu²⁺	Naked-Eye Detection [Sensor]: [Cu²⁺]	Cu²⁺ Selectivity Assay Conditions	Solvent	Ref
78		**Cu²⁺ & CN⁻** Colorimetric **Cu²⁺, CN⁻ & S²⁻** Fluorometric	5.22 µM	–	1:1	[Sensor] = 10 µM [Cu²⁺] = 150 µM	[Sensor] = 10 µM [Cu²⁺] = 200 µM [Competing Metal Ions] = 200 µM	HEPES: MeCN (4:6, v/v) pH= 7.2	[126]
79		**Cu²⁺ & F⁻** Colorimetric	5.8 µM	1.2×10^4 M⁻¹ UV-Vis	2:1	[Sensor] = 15 µM [Cu²⁺] = 15 µM	[Sensor] = 15 µM [Cu²⁺] = 15 µM [Competing Metal Ions] = 15 µM	DMSO	[132]
80		**Cu²⁺** Colorimetric	6.5 µM	1.3×10^6 M⁻¹ UV-Vis	1:1	[Sensor] = 10 µM [Cu²⁺] = 20 µM	[Sensor] = 10 µM [Cu²⁺] = 20 µM [Competing Metal Ions] = 20 µM	DMSO: 10 mM HEPES (4:1, v/v) pH=7.0	[127]
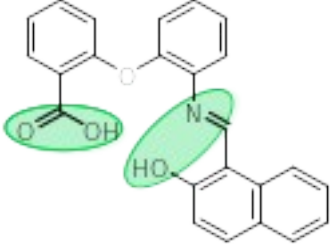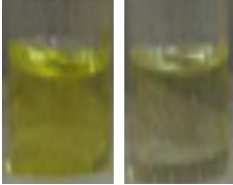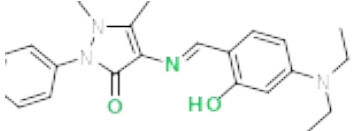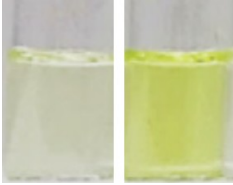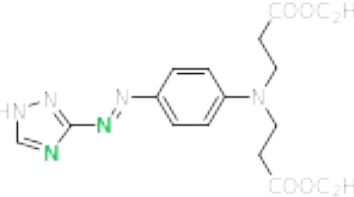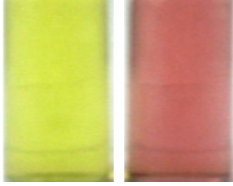
Limit of Detection Determined by UV-Vis Spectroscopy

5.0 μM – 15 μM

Sensor #	Cu²⁺ Sensor	Ion Sensing	Cu²⁺ LOD	K_a	Binding Stoichiometry Sensor: Cu²⁺	Naked-Eye Detection [Sensor]: [Cu²⁺]	Cu²⁺ Selectivity Assay Conditions	Solvent	Ref
81		Cu²⁺ & S²⁻ Colorimetric	6.89 μM	1.01×10^6 M⁻¹ UV-Vis	1:1	[Sensor] = 10 μM [Cu²⁺] = 70 μM	[Sensor] = 10 μM [Cu²⁺] = 70 μM [Competing Metal Ions] = 70 μM	MeCN: 10 mM HEPES (1:1, v/v) pH=7.0	[129]
3		Cu²⁺ Colorimetric & Fluorometric	8.147 μM	4.65×10^7 M⁻¹ Fluorometer	2:1	[Sensor] = 50 μM [Cu²⁺] = 100 μM	[Sensor] = 50 μM [Cu²⁺] = 100 μM [Competing Metal Ions] = 200 μM	MeCN: HEPES (1:1, v/v) pH=7.1	[43]
82		Cu²⁺ Colorimetric	10 μM	2.8×10^4 M⁻¹ UV-Vis	1:1	[Sensor] = 100 μM [Cu²⁺] = 10 μM	[Sensor] = 50 μM [Cu²⁺] = 250 μM [Competing Metal Ions] = 250 μM	MeOH: H₂O (10:90, v/v)	[133]
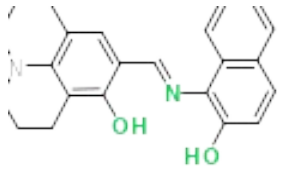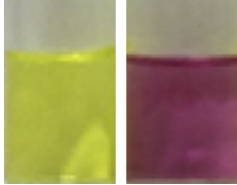
Limit of Detection Determined by UV-Vis Spectroscopy
5.0 μM – 15 μM

Sensor #	Cu²⁺ Sensor	Ion Sensing	Cu²⁺ LOD	K_a	Binding Stoichiometry Sensor: Cu²⁺	Naked-Eye Detection [Sensor]: [Cu²⁺]	Cu²⁺ Selectivity Assay Conditions	Solvent	Ref
83		**Cu²⁺** Colorimetric **Zn²⁺** Fluorometric	10 μM	2.57×10^5 M⁻¹ UV-Vis	1:1	[Sensor] = 1 mM [Cu²⁺] = 1 mM	[Sensor] = 1 μM [Cu²⁺] = 1 μM [Competing Metal Ions] = 1 mM	MeCN	[131]
84		**Cu²⁺ & F⁻** Colorimetric **F⁻** Fluorometric	12 μM	5.3×10^3 M⁻¹ UV-Vis	1:1	[Sensor] = 10 μM [Cu²⁺] = 170 μM	[Sensor] = 10 μM [Cu²⁺] = 170 μM [Competing Metal Ions] = 170 μM	DMSO: bis-tris (1:1, v/v)	[134]
85		**Cu²⁺** Colorimetric	13.6 μM	1.8×10^6 M⁻¹ UV-Vis	1:1	[Sensor] = 30 μM [Cu²⁺] = 10 μM	[Sensor] = 30 μM [Cu²⁺] = 30 μM [Competing Metal Ions] = 300 μM	MeCN	[130]

Limit of Detection Determined by UV-Vis Spectroscopy
5.0 µM – 15 µM

Sensor #	Cu²⁺ Sensor	Ion Sensing	Cu²⁺ LOD	K_a	Binding Stoichiometry Sensor: Cu²⁺	Naked-Eye Detection [Sensor]: [Cu²⁺]	Cu²⁺ Selectivity Assay Conditions	Solvent	Ref
86		**Cu²⁺** Colorimetric **CN⁻** Fluorometric	**14 µM**	**3.3 x 10³ M⁻¹** UV-Vis	**1:1**	[Sensor] = 30 µM [Cu²⁺] = 300 µM	[Sensor] = 30 µM [Cu²⁺] = 300 µM [Competing Metal Ions] = 300 µM	MeOH	[135]

Table 11: Copper(II) sensors arranged from lowest to highest limit of detection in the range of 5.0 µM – 15 µM determined by UV-Vis spectroscopy. Information provided: Sensor number, chemical structure (green atoms indicate the proposed mechanism of Cu²⁺ coordination. Shaded green indicates the proposed sensing unit/s in Cu²⁺ coordination), additional ca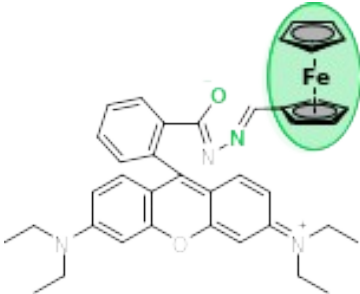tions and anions detected by the sensor, K_a = association constant, binding stoichiometry (sensor: Cu²⁺), concentration of sensor and Cu²⁺ for naked eye detection, the Cu²⁺ selectivity assay conditions including concentration of sensor, Cu²⁺ and competing metal ions tested and solvent.

5. Limit of detection not reported

       The sensors in this section did not report a respective LOD for Cu^{2+} detection (Table 12) and were mostly employed as purely solvent-based sensors [136–145]. Nonetheless, some sensors were fixed to a test strip for Cu^{2+} detection [146,147], used for fluorescence bioimaging of Cu^{2+} in cells [148,149], demonstrated reversibility when exposed to EDTA [150,151] and achieved solubility in a fully aqueous solution [145,148].

       Maity et al. [149] synthesized several novel Schiff-base ligands for the detection of Cu^{2+}. Julolidine–thiocarbonohydrazone sensor **96** (10 μM) obtained the best optical response by providing a stepwise color change upon addition of 1, 2, 5, and 10 equivalents of Cu^{2+} in 50 mM HEPES:MeCN (6:4, v/v, pH= 7.2) (Table 12 Sensor #96). Sensor **96** (10 μM) displayed a strong absorbance peak at 400 nm with an optical color of greenish-yellow. With the addition of 10 μM Cu^{2+}, the appearance of two absorbance bands at 570 nm and 980 nm and changed from greenish-yellow to light purple was observed. The addition of 20 μM Cu^{2+} caused the color to change to violet, 50 μM Cu^{2+} to light blue, and the final color was greenish aqua at 100 μM Cu^{2+}. At 100 μM Cu^{2+} to **96**, a blue shift of the 980 nm peak to 820 nm was seen. No further color change was observed for concentrations greater than 100 μM. Competition studies were completed to observe the selectivity of sensor **96** (10 μM) using 5 equivalents of Cu^{2+} and 10 equivalents of other competing metals. A greenish-blue color persisted once Cu^{2+} was added and therefore confirmed no interference from these competing metals, even in excess. **96** was also utilized as a "turn-off" fluorescent sensor that was able to track Cu^{2+} in HEK293T human kidney cells using fluorescence microscopy. Cells incubated with 10 μM of **96** displayed green fluorescence and showed cell permeability. The fluorescence was quenched once 10 μM of Cu^{2+}

968   was added, and the fluorescence intensity was regained when 10 μM of EDTA was introduced

969   thereafter. The experiments conducted demonstrate that sensor **96** is a selective colorimetric and

970   fluorometric reversible sensor for Cu^{2+} that could be applied for in-field and/or living cells.

971   Milindanuth and Pisitsak [147] applied a rhodamine-based sensor **98** that offered naked

972   eye detection at 4 μM in EtOH:H_2O (1:1, v/v) (Table 12 Sensor #98). Instead of fixing the sensor

973   to filter paper, i.e., traditional cellulosic paper, which was commonly found in this review, **98**

974   was fixed to bacterial cellulose due to its smaller nanofibrils and high surface area of 27.2 m^2/g

975   [152], compared to 1.09 m^2/g [153] found in the traditional cellulosic paper. Indeed, **Fig. 17**

976   shows the **98** treated bacterial cellulose had a higher color strength, determined by CIELab color

977   space, over increasing copper(II) concentration than the **98** treated traditional cellulosic paper.

978   This finding might encourage experimentation with immobilizing sensors to bacterial cellulose

979   paper instead of the commonly used cellulosic paper.
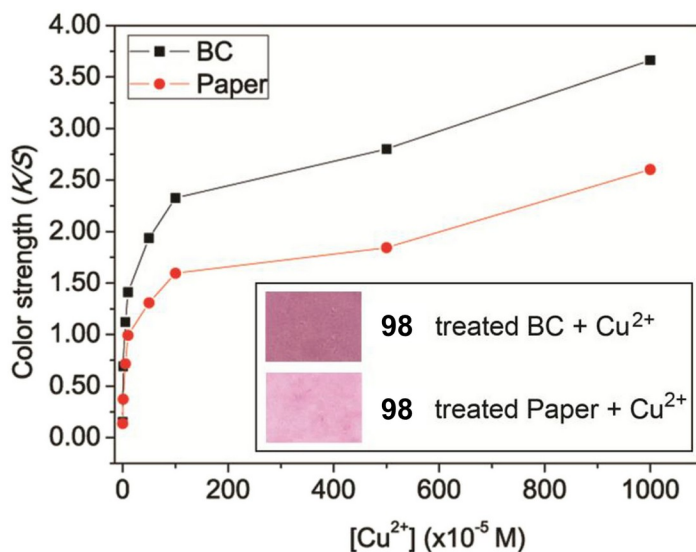
980

981   *Fig. 17: Color strength (K/S) values, determined by CIELab color space, of bacterial cellulose*

982   *paper (BC) and traditional cellulosic paper plotted against varying Cu^{2+} concentrations. **Inset:***

983 *Observed color of BC and traditional cellulosic paper treated with **98** and subjected to 100 μM*

984 *Cu^{2+}. Reproduced from Milindanuth et al. [147].*
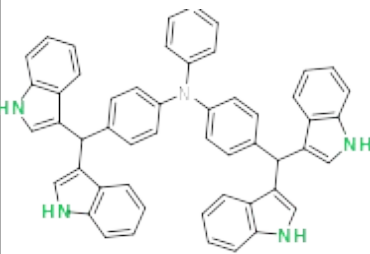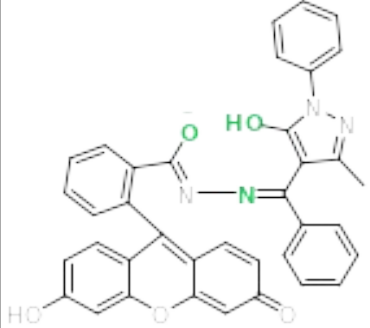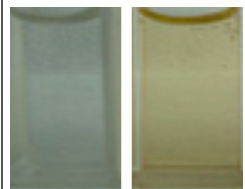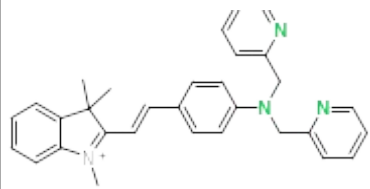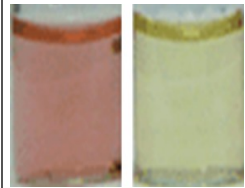
985   Inwon Kim (2015) et al. [143] utilized a spiropyran-based sensor, **100**, with a 1-benzyl-

986 1,2,3-triazole linker stemming from the amine on the indoline (Table 12 Sensor #100). Since

987 some spiropyrans inherently isomerize under UV light, **100** was irradiated with 365 nm light for

988 0-90 seconds, which isomerized spiropyran **100**, colorless, to merocyanine **100**, violet, and the

989 accompanied UV-Vis absorbance max was found to be 571 nm (**Fig. 18 route 1**). Visible light

990 was shown to reverse merocyanine **100** back to spiropyran **100**. When spiropyran **100** is in the

991 presence of Cu^{2+}, a visible color change from colorless to pink was observed (**Fig. 18 route 2**).

992 Interestingly, the binding stoichiometry of sensor **100**: Cu^{2+} was found to be 2:3 and was verified

993 through Job's plot analysis, MALDI-TOF mass spectrometry, and ^{1}H NMR. This unique binding

994 stoichiometry was the only one of its kind found in this review. Moreover, Cu^{2+} binding induces

995 a λ_{max} at 520 nm, which is blue-shifted 51 nm from the merocyanine **100** produced through UV

996 light.

997
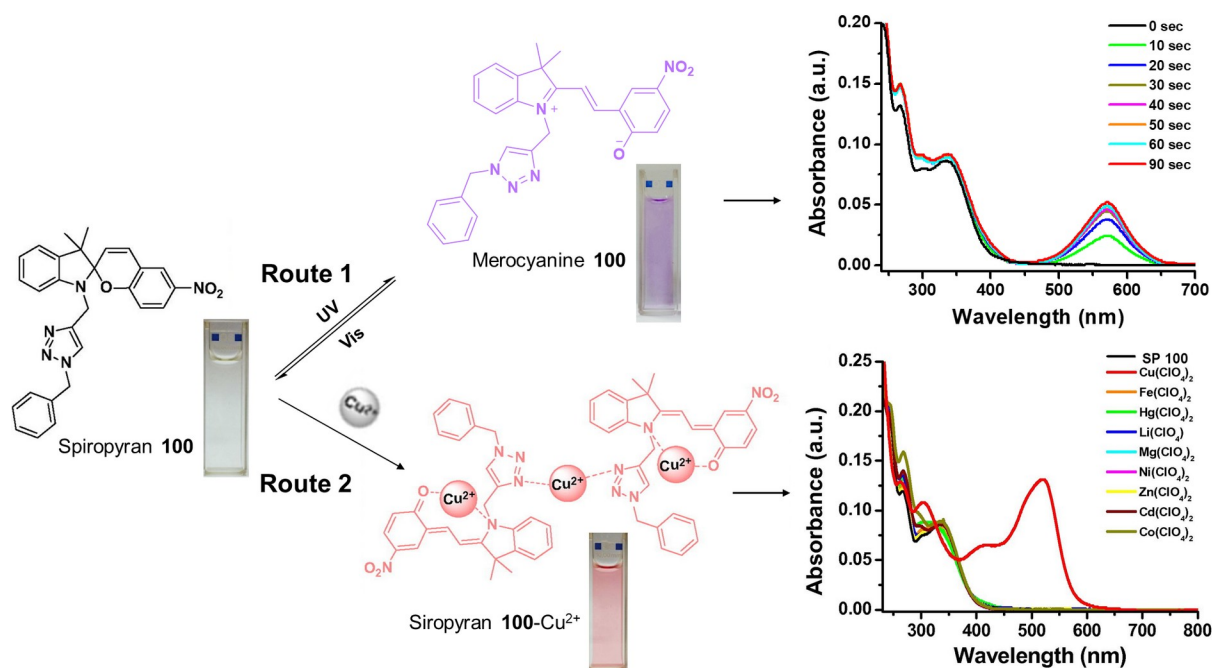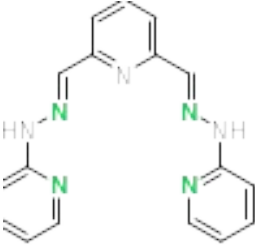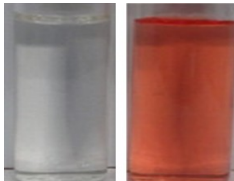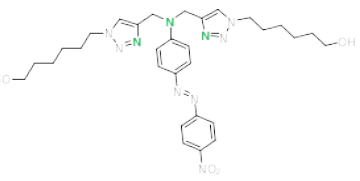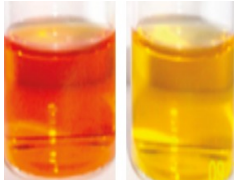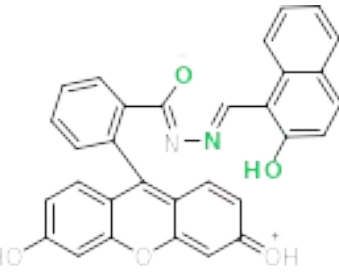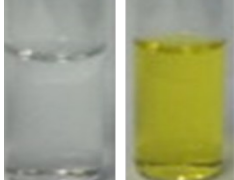
Fig. 18: *Route 1: Irradiation of 365 nm light for 0-90 seconds isomerizes spiropyran **100**, colorless, to merocyanine **100**, violet. This is accompanied by a UV-Vis absorbance spectrum with λ_{max} = 571 nm and can be reversed with visible light. Route 2:* Spiropyran **100** *is in the presence of Cu^{2+} consists of a 2:3 binding stoichiometry sensor:Cu^{2+} and a visible color change from colorless to pink. This is accompanied by a UV-Vis absorbance spectrum with λ_{max} = 520 nm. Modified from Kim(2015) et al. [143].*
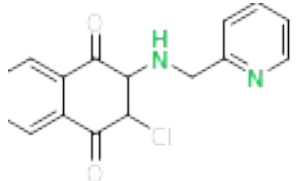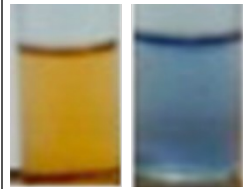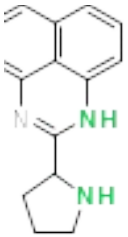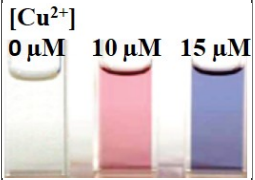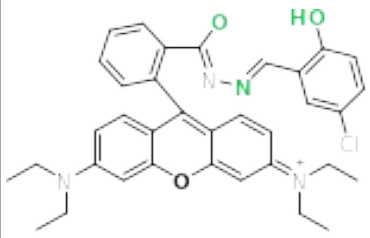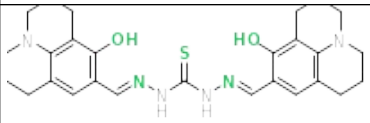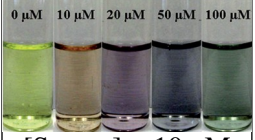
Limit of Detection Not Reported

Sensor #	Cu²⁺ Sensor	Ion Sensing	K_a	Binding Stoichiometry Sensor: Cu²⁺	Naked-Eye Detection [Sensor]: [Cu²⁺]	Cu²⁺ Selectivity Assay Conditions	Solvent	Ref
87		**Cu²⁺** Colorimetric & Fluorometric	**3.35 x 10⁴ M⁻¹** UV-Vis **3.59 x 10⁵ M⁻¹** Fluorometer	**1:2**	[Sensor] = 10 μM [Cu²⁺] = 10 μM	None	MeCN: H₂O (70:30, v/v)	[136]
88		**Cu²⁺** Colorimetric & Fluorometric	**3.3 x 10⁴ M⁻¹** UV-Vis	**1:1**	[Sensor] = 10 μM [Cu²⁺] = 10 μM	[Sensor] = 10 μM [Cu²⁺] = 20 μM [Competing Metal Ions] = 20 μM	DMSO: H₂O (4:6, v/v)	[137]
89		**Cu²⁺** Colorimetric & Fluorometric	**1.5 x 10⁴ M⁻¹** UV-Vis	**1:1**	[Sensor] = 12.5 μM [Cu²⁺] = 12.5 μM	[Sensor] = 12.5 μM [Cu²⁺] = 12.5 μM [Competing Metal Ions] = 12.5 μM	25 mM HEPES, 0.1 M NaClO₄ pH = 7.4	[148]
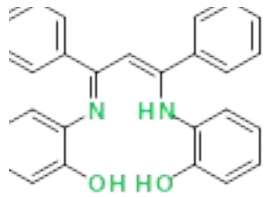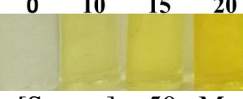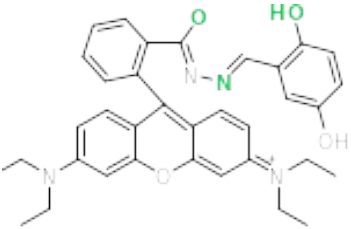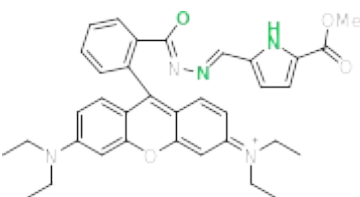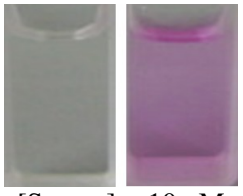
Limit of Detection Not Reported

Sensor #	Cu²⁺ Sensor	Ion Sensing	K_a	Binding Stoichiometry Sensor: Cu²⁺	Naked-Eye Detection [Sensor]: [Cu²⁺]	Cu²⁺ Selectivity Assay Conditions	Solvent	Ref
90		Cu²⁺ Colorimetric	1.98×10^8 M⁻¹ UV-Vis	1:1	 [Sensor] = 45 μM [Cu²⁺] = 45 μM	None	DMSO: H₂O (1:9, v/v)	[150]
91		Cu²⁺ Colorimetric	0.7×10^4 M⁻¹ UV-Vis	1:1	 [Sensor] = 20 μM [Cu²⁺] = 60 μM	None	MeCN: H₂O (80:20, v/v)	[138]
92		Cu²⁺ Colorimetric & Fluorometric	3.7×10^4 M⁻¹ UV-Vis	1:1	 [Sensor] = 10 μM [Cu²⁺] = 20 μM	[Sensor] = 10 μM [Cu²⁺] = 20 μM [Competing Metal Ions] = 20 μM	2% DMSO in 10 mM Tris-HCl pH = 7.0	[151]

Limit of Detection Not Reported

Sensor #	Cu^{2+} Sensor	Ion Sensing	K$_a$	Binding Stoichiometry Sensor: Cu^{2+}	Naked-Eye Detection [Sensor]: [Cu^{2+}]	Cu^{2+} Selectivity Assay Conditions	Solvent	Ref
93		Cu^{2+} Colorimetric & Fluorometric	1.6 x 10^4 M^{-1} UV-Vis 1.4 x 10^4 M^{-1} Fluorometer	1:1	 [Sensor] = 100 μM [Cu^{2+}] = 200 μM	[Sensor] = 100 μM [Cu^{2+}] = 100 μM [Competing Metal Ions] = 100 μM	H$_2$O: EtOH (90:10, v/v)	[139]
94		Cu^{2+} Colorimetric & Fluorometric	2.58 x 10^4 M^{-1} UV-Vis 3.25 x 10^4 M^{-1} Fluorometer	1:1	 [Cu^{2+}] 0 μM 10 μM 15 μM [Sensor] = 10 μM [Cu^{2+}] = 0-15 μM	None	MeCN: H$_2$O (8:2, v/v) buffered with 50 mM HEPES pH = 7.2	[140]
95		Cu^{2+} Colorimetric V^{2+} Fluorometric	–	1:1	 [Sensor] = 20 μM [Cu^{2+}] = 20 μM	None	MeOH: 10 mM HEPES (1:1, v/v) pH = 7.0	[141]
96		Cu^{2+} Colorimetric & Fluorometric	2.3 x 10^{14} M^{-1} UV-Vis	1:2	 0 μM 10 μM 20 μM 50 μM 100 μM [Sensor] = 10 μM	[Sensor] = 10 μM [Cu^{2+}] = 50 μM [Competing Metal Ions] = 100 μM	50 mM HEPES: MeCN (6:4, v/v) pH = 7.2	[149]

Limit of Detection Not Reported

Sensor #	Cu²⁺ Sensor	Ion Sensing	K_a	Binding Stoichiometry Sensor: Cu²⁺	Naked-Eye Detection [Sensor]: [Cu²⁺]	Cu²⁺ Selectivity Assay Conditions	Solvent	Ref
					$[Cu^{2+}]$ = 0-100 μM			
97		**Cu²⁺** Colorimetric	**1.0 x 10⁶ M⁻¹** UV-Vis	**1:1**	$[Cu^{2+}]$ μM 0 10 15 20 [Sensor] = 50 μM $[Cu^{2+}]$ = 0-20 μM	[Sensor] = 50 μM $[Cu^{2+}]$ = 50 μM [Competing Metal Ions] = 50 μM	MeOH	[146]
98		**Cu²⁺** Colorimetric	–	**1:1**	$[Cu^{2+}]$ μM 4 8 16 [Sensor] = 100 μM $[Cu^{2+}]$ = 4-16 μM	None	EtOH: H₂O (1:1, v/v)	[147]
99		**Cu²⁺** Colorimetric **Hg²⁺** Fluorometric	**2.44 x 10⁵ M⁻¹** UV-Vis	**1:1**	[Sensor] = 10 μM $[Cu^{2+}]$ = 10 μM	[Sensor] = 10 μM $[Cu^{2+}]$ = 20 μM [Competing Metal Ions] = 20 μM	MeOH: 10 mM HEPES (3:1, v/v) pH = 7.4	[142]

Limit of Detection Not Reported

Sensor #	Cu²⁺ Sensor	Ion Sensing	K_a	Binding Stoichiometry Sensor: Cu²⁺	Naked-Eye Detection [Sensor]: [Cu²⁺]	Cu²⁺ Selectivity Assay Conditions	Solvent	Ref
100		Cu²⁺ Colorimetric	6.8×10^5 M⁻¹ UV-Vis	2:3	[Cu²⁺] μM 0 30 40 50 [Sensor] = 50 μM [Cu²⁺] = 0-50 μM	None	MeCN	[143]
101		Cu²⁺ Colorimetric	–	1:1	[Sensor] = 100 μM [Cu²⁺] = 1 mM	[Sensor] = 100 μM [Cu²⁺] = 1 mM [Competing Metal Ions] = 1 mM	DMF: H2O (9:1, v/v)	[144]
102		Cu²⁺ Colorimetric	1.0×10^{10} M⁻² UV-Vis	2:1	[Cu²⁺] μM 0 0.5 1 5 10 [Sensor] = 10 μM [Cu²⁺] = 1 μM	[Sensor] = 10 μM [Cu²⁺] = 10 μM [Competing Metal Ions] = 50 μM	PBS buffer pH = 9.18	[145]

1004 **Table 12**: Copper(II) sensors that did not report a limit of detection but provided naked eye detection. Information provided: Sensor number,
1005 chemical structure (green atoms indicate the proposed mechanism of Cu²⁺ coordination. Shaded green indicates the proposed sensing unit/s in Cu²⁺
1006 coordination), additional cations and anions detected by the sensor, K_a = association constant, binding stoichiometry (sensor: Cu²⁺), concentration of

1007   sensor and Cu^{2+} for naked eye detection, the Cu^{2+} selectivity assay conditions including concentration of sensor, Cu^{2+} and competing metal ions tested
1008   and solvent.

1009

6. Conclusions and Outlook

1010

1011   Upon evaluation of the copper(II) sensors in Table 1-12, metals such as Fe^{3+}, Fe^{2+}, Pb^{2+},

1012 Hg^{2+}, and Co^{2+} were commonly found to offer dual detection. According to the hard-soft acid-

1013   base (HSAB) theory, metals are classified as either hard acids (small ionic radii with a high

1014   positive charge) or soft acids (large ionic radii with a low positive charge). Utilizing Pearson's

1015   absolute hardness values ranging from 3.4-45.8, where the lower the value reflects the softer

1016   metal, hardness values for these metal ions were 7.3 (Fe^{2+}), 7.7 (Hg^{2+}), 8.3 (Cu^{2+}), 8.5 (Pb^{2+}), and

1017   13.1 (Fe^{3+}) [154]. Co^{2+} was not listed but is considered borderline, displaying intermediate

1018   characteristics [155]. Since Cu^{2+} is considered a borderline soft acid, it is reasonable to suggest

1019   interference from Fe^{2+}, Pb^{2+}, Hg^{2+}, and Co^{2+} are due to HSAB theory. Although Fe^{3+} is regarded

1020   as a hard acid, it is plausible that HSAB does not apply in this case. Recognition of Fe^{3+} was

1021   primarily in the form of fluorescence "turn-on" detection. Interestingly, all sensors utilized a

1022   Schiff-base unit in the sensing mechanism. It is well known that various metal ions preferentially

1023   bind a Schiff-base imine due to the non-bonded electrons on nitrogen in the C=N unit [156–158].

1024   Depending on several factors such as pH, coordinating ability of the counter anions, the amine or

1025   aldehyde fragment regenerated, etc. [159–162], two possible mechanisms could explain this

1026   phenomenon. (1) Coordination of Fe^{3+} in the binding pocket containing a Schiff-base unit induces

1027   hydrolytic cleavage of the C=N and formation of an amine and carbonyl. This results in partial

1028   decomposition of the sensor and generation of a fluorophore enabling fluorescent enhancement.

1029   (2) The second possible sensing mechanism involves the coordination of Fe^{3+} in the binding

1030   pocket containing a Schiff-base unit but instead of undergoing hydrolysis, the Fe^{3+}-sensor

1031   complex is stabilized by the donation of the electrons from nitrogen on C=N imine. Upon

1032 emission of this complex, PET is inhibited due to the Fe^{3+}-sensor stabilization, allowing for full

1033 relaxation of the electrons back to the ground state, resulting in fluorescence. As for Cu^{2+}, it has

1034 been often used as a fluorescent "turn-off" sensor due to its paramagnetism [60,62,64–

1035 66,148,149,163–165]. Upon emission of a Cu^{2+}-fluorophore complex, PET is possible when an

1036 excited electron relaxes to the dx^2-y^2 orbital, resulting in fluorescence quenching [19,20,25].

1037   Common anions that interfered with copper sensing, and offered dual detection, were S^{2-},

1038 CN^-, and F^-. Further expanding on HSAB theory, hard acids preferentially react with hard bases

1039 and analogously, soft acids preferentially react with soft bases. Therefore, the HSAB theory

1040 could account for interference by sulfur and cyanide acting as soft bases. The high affinity of

1041 copper(II) for these ligands can displace the metal from the sensor to form CuS or $Cu(CN)_2$.

1042 Since fluoride is considered a hard base, the possible mechanism for detection of F^- could be due

1043 to its electronegativity and high propensity to intermolecular hydrogen bond. Of the sensors that

1044 detected F^-, this is particularly seen with hydrogens covalently bound to either an amine or

1045 phenol. The lone pair electrons on nitrogen and oxygen induce a dipole creating a partial positive

1046 charge on hydrogen, making it susceptible to intermolecular hydrogen bonding with fluoride.

1047   Overall, the ideal copper(II) sensor used for in-field analysis would be able to detect

1048 copper only, even in the presence of competing metal ions, and be able to do so in a 100%

1049 aqueous medium, whether it be free in solution or fixed to a test strip. Even though there are 102

1050 sensors reported in this review paper, only 60 sensors detect solely copper(II). From these 60

1051 sensors, 51 of the reports performed competition studies to rule out interference from other metal

1052 ions. 39 sensors were able to selectively detect copper(II) exclusively, over other competing

1053 metal ions. After inspecting the number of sensors that were selective for copper(II) detection

1054   with no interference, it is clear that there is a necessity to analyze beyond 1:1 Cu^{2+}: M^{n+} for

1055   competition studies. Only 11 sensors analyzed selectivity at higher ratios of competing metals;

1056   yet this is a very important aspect of developing an in-field sensor. Assessing the selectivity of

1057 Cu^{2+} with excess metal ions can reveal if the sensor renders a false positive or false negative. If

1058   so, pretreatment methods will need to be administered.

1059   Another important feature in developing an in-field sensor for detecting Cu^{2+}

1060   contamination in soil and water is the ability of the sensor to be applied to aqueous solutions. In

1061   this review, 9 sensors achieved solubility in 100% aqueous medium

1062   [78,81,83,101,103,109,114,145,148]. A common workaround to adapt a sensor that was soluble

1063   in an organic or mixed-organic solvent, was to fix them to paper and make test strips. This is a

1064   practical option as long as competition studies are performed to confirm that Cu^{2+} selectivity

1065   remains. However, this was not fulfilled in the papers discussing paper-based copper sensors that

1066   are reviewed here. Interference studies, especially with excess competing metal ions and

1067   solubility in water, should be a priority that is addressed for future advancement of sensors being

1068   developed for copper(II) detection.

1069

7. Future scope

1070

1071   Naked eye detection of copper would be of greatest utility for in-the-field measurements

1072   where quick assays are desired. Clearly the selectivity of copper sensors is improving but for

1073   optimal sensitivity, even greater selection against interfering metal ions will be required from

1074   some of the sensors reported. As aqueous solubility improves, a wider range of applications will

1075 become available and should be a priority that is addressed for future advancement of sensors

1076 being developed for copper(II) detection. Greater uniformity in testing and reporting of sensors

1077 would aid the community. For example, interference studies should be included and examined

1078 for up to at least 10x excess competing metal ions. As illustrated by the efforts summarized here,

1079 there is great interest in copper sensors, particularly for rapid, naked-eye detection of copper. We

1080 hope this review will be a handy reference tool for researchers interested in the development and

1081 use of small molecule copper sensors

1082

1083 **Corresponding Author**

1084 * E-mail: aylouie@ucdavis.edu, joel.garcia@dlsu.edu.ph

1085 Kimberly M. Trevino: kmtrevino@ucdavis.edu

1086 Caitlyn R. Wagner: crwagner@ucdavis.edu

1087 Eric K. Tamura: ektamura@ucdavis.edu

1088

1091

1092 **References**

1093 [1] Tapiero H, Townsend DM, Tew KD. Trace elements in human physiology and pathology.
1094   Copper. Biomed Pharmacother 2003;57:386–98. https://doi.org/10.1016/S0753-
1095   3322(03)00012-X.
1096 [2] Elkhatat AM, Soliman M, Ismail R, Ahmed S, Abounahia N, Mubashir S, et al. Recent
1097   trends of copper detection in water samples. Bull Natl Res Cent 2021;45:218. https://doi.org/
1098   10.1186/s42269-021-00677-w.
1099 [3] Guidelines for drinking-water quality: fourth edition incorporating the first addendum.
1100   Geneva: World Health Organization; 2017. License: CC BY-NC-SA 3.0 IGO. n.d.
1101 [4] United States Environmental Protection Agency. Office of the Federal Register. National
1102   Archives and Records Administration. National Primary Drinking Water Regulations.

1103 govinfo. (July 1, 2020). https://www.govinfo.gov/app/details/CFR-2020-title40-vol25/CFR-
1104 2020-title40-vol25-part141 n.d.
1105 [5] Xie D-H, Wang X-J, Sun C, Han J. Calix[4]arene based 1,3,4-oxadiazole as a fluorescent
1106 chemosensor for copper(II) ion detection. Tetrahedron Lett 2016;57:5834–6.
1107 https://doi.org/10.1016/j.tetlet.2016.11.051.
1108 [6] Hsieh Y-C, Chir J-L, Yang S-T, Chen S-J, Hu C-H, Wu A-T. A sugar-aza-crown ether-based
1109 fluorescent sensor for Cu2+ and Hg2+ ions. Carbohydr Res 2011;346:978–81.
1110 https://doi.org/10.1016/j.carres.2011.03.010.
1111 [7] Ho F-C, Huang Y-J, Weng C-C, Wu C-H, Li Y-K, Wu JI, et al. Efficient FRET Approaches
1112 toward Copper(II) and Cyanide Detections via Host–Guest Interactions of Photo-Switchable
1113 [2]Pseudo-Rotaxane Polymers Containing Naphthalimide and Merocyanine Moieties. ACS
1114 Appl Mater Interfaces 2020;12:53257–73. https://doi.org/10.1021/acsami.0c15049.
1115 [8] Bhatt KD, Gupte HS, Makwana BA, Vyas DJ, Maity D, Jain VK. Calix Receptor Edifice;
1116 Scrupulous Turn Off Fluorescent Sensor for Fe(III), Co(II) and Cu(II). J Fluoresc
1117 2012;22:1493–500. https://doi.org/10.1007/s10895-012-1086-5.
1118 [9] Costa AI, Barata PD, Fialho CB, Prata JV. Highly Sensitive and Selective Fluorescent
1119 Probes for Cu(II) Detection Based on Calix[4]arene-Oxacyclophane Architectures.
1120 Molecules 2020;25:2456. https://doi.org/10.3390/molecules25102456.
1121 [10] Ding H, Liang C, Sun K, Wang H, Hiltunen JK, Chen Z, et al. Dithiothreitol-capped
1122 fluorescent gold nanoclusters: An efficient probe for detection of copper(II) ions in aqueous
1123 solution. Biosens Bioelectron 2014;59:216–20. https://doi.org/10.1016/j.bios.2014.03.045.
1124 [11] Ding L, Zhao Z, Li D, Wang X, Chen J. An "off-on" fluorescent sensor for copper ion using
1125 graphene quantum dots based on oxidation of l-cysteine. Spectrochim Acta A 2019;214:320–
1126 5. https://doi.org/10.1016/j.saa.2019.02.048.
1127 [12] Shi Y, Liu Q, Yuan W, Xue M, Feng W, Li F. Dye-Assembled Upconversion
1128 Nanocomposite for Luminescence Ratiometric in Vivo Bioimaging of Copper Ions. ACS
1129 Appl Mater Interfaces 2019;11:430–6. https://doi.org/10.1021/acsami.8b19961.
1130 [13] Ngamdee K, Chaiendoo K, Saiyasombat C, Busayaporn W, Ittisanronnachai S, Promarak V,
1131 et al. Highly selective circular dichroism sensor based on
1132 d-penicillamine/cysteamine-cadmium sulfide quantum dots for copper (II) ion detection.
1133 Spectrochim Acta A 2019;211:313–21. https://doi.org/10.1016/j.saa.2018.12.027.
1134 [14] Wang Q, Yu X, Zhan G, Li C. Fluorescent sensor for selective determination of copper ion
1135 based on N-acetyl-l-cysteine capped CdHgSe quantum dots. Biosens Bioelectron
1136 2014;54:311–6. https://doi.org/10.1016/j.bios.2013.11.008.
1137 [15] Liu H, Jia L, Wang Y, Wang M, Gao Z, Ren X. Ratiometric fluorescent sensor for visual
1138 determination of copper ions and alkaline phosphatase based on carbon quantum dots and
1139 gold nanoclusters. Anal Bioanal Chem 2019;411:2531–43. https://doi.org/10.1007/s00216-
1140 019-01693-6.
1141 [16] Wang Y, Zhang C, Chen X, Yang B, Yang L, Jiang C, et al. Ratiometric fluorescent paper
1142 sensor utilizing hybrid carbon dots–quantum dots for the visual determination of copper ions.
1143 Nanoscale 2016;8:5977–84. https://doi.org/10.1039/C6NR00430J.
1144 [17] Sivaraman G, Iniya M, Anand T, Kotla NG, Sunnapu O, Singaravadivel S, et al. Chemically
1145 diverse small molecule fluorescent chemosensors for copper ion. Coord Chem Rev
1146 2018;357:50–104. https://doi.org/10.1016/j.ccr.2017.11.020.

1147 [18] Chowdhury S, Rooj B, Dutta A, Mandal U. Review on Recent Advances in Metal Ions
1148   Sensing Using Different Fluorescent Probes. J Fluoresc 2018;28:999–1021.
1149   https://doi.org/10.1007/s10895-018-2263-y.
1150 [19] Liu S, Wang Y-M, Han J. Fluorescent chemosensors for copper(II) ion: Structure,
1151   mechanism and application. Journal of Photochemistry and Photobiology C: Photochemistry
1152   Reviews 2017;32:78–103. https://doi.org/10.1016/j.jphotochemrev.2017.06.002.
1153 [20] Kumar N, Bhalla V, Kumar M. Resonance energy transfer-based fluorescent probes for
1154   Hg2+, Cu2+ and Fe2+/Fe3+ ions. Analyst 2013;139:543–58.
1155   https://doi.org/10.1039/C3AN01896B.
1156 [21] Saleem M, Rafiq M, Hanif M, Shaheen MA, Seo S-Y. A Brief Review on Fluorescent
1157   Copper Sensor Based on Conjugated Organic Dyes. J Fluoresc 2018;28:97–165.
1158   https://doi.org/10.1007/s10895-017-2178-z.
1159 [22] Sharma S, Ghosh KS. Recent advances (2017–20) inthe detection of copper ion by using
1160   fluorescence sensors working through transfer of photo-induced electron (PET), excited-state
1161   intramolecular proton (ESIPT) and Förster resonance energy (FRET). Spectrochim Acta A
1162   2021;254:119610. https://doi.org/10.1016/j.saa.2021.119610.
1163 [23] Hazarika SI, Atta AK. Carbohydrate-based fluorometric and colorimetric sensors for Cu2+
1164   ion recognition. C R Chim 2019;22:599–613. https://doi.org/10.1016/j.crci.2019.07.003.
1165 [24] Kowser Z, Rayhan U, Akther T, Redshaw C, Yamato T. A brief review on novel pyrene
1166   based fluorometric and colorimetric chemosensors for the detection of Cu2+. Mater Chem
1167   Front 2021;5:2173–200. https://doi.org/10.1039/D0QM01008A.
1168 [25] Udhayakumari D, Naha S, Velmathi S. Colorimetric and fluorescent chemosensors for
1169   Cu2+. A comprehensive review from the years 2013–15. Anal Methods 2017;9:552–78.
1170   https://doi.org/10.1039/C6AY02416E.
1171 [26] Chopra T, Sasan S, Devi L, Parkesh R, Kapoor KK. A comprehensive review on recent
1172   advances in copper sensors. Coord Chem Rev 2022;470:214704.
1173   https://doi.org/10.1016/j.ccr.2022.214704.
1174 [27] Liu B, Zhuang J, Wei G. Recent advances in the design of colorimetric sensors for
1175   environmental monitoring. Environ Sci: Nano 2020;7:2195–213.
1176   https://doi.org/10.1039/D0EN00449A.
1177 [28] Gerdan Z, Saylan Y, Denizli A. Recent Advances of Optical Sensors for Copper Ion
1178   Detection. Micromachines 2022;13:1298. https://doi.org/10.3390/mi13081298.
1179 [29] Upadhyay S, Singh A, Sinha R, Omer S, Negi K. Colorimetric chemosensors for d-metal
1180   ions: A review in the past, present and future prospect. J Mol Struct 2019;1193:89–102.
1181   https://doi.org/10.1016/j.molstruc.2019.05.007.
1182 [30] Kaur B, Kaur N, Kumar S. Colorimetric metal ion sensors – A comprehensive review of the
1183   years 2011–2016. Coord Chem Rev 2018;358:13–69.
1184   https://doi.org/10.1016/j.ccr.2017.12.002.
1185 [31] Rasheed T, Li C, Bilal M, Yu C, Iqbal HMN. Potentially toxic elements and
1186   environmentally-related pollutants recognition using colorimetric and ratiometric fluorescent
1187   probes. Sci Total Environ 2018;640–641:174–93.
1188   https://doi.org/10.1016/j.scitotenv.2018.05.232.
1189 [32] Choudhury N, De P. Recent progress in pendant rhodamine-based polymeric sensors for the
1190   detection of copper, mercury and iron ions. J Macromol Sci A 2021;58:835–48.
1191   https://doi.org/10.1080/10601325.2021.1960172.

1192 [33] Armbruster DA, Pry T. Limit of Blank, Limit of Detection and Limit of Quantitation. Clin
1193   Biochem Rev 2008;29:S49–52.
1194 [34] Loock H-P, Wentzell PD. Detection limits of chemical sensors: Applications and
1195   misapplications. Sens Actuators B Chem 2012;173:157–63.
1196   https://doi.org/10.1016/j.snb.2012.06.071.
1197 [35] Belter M, Sajnóg A, Barałkiewicz D. Over a century of detection and quantification
1198   capabilities in analytical chemistry – Historical overview and trends. Talanta 2014;129:606–
1199   16. https://doi.org/10.1016/j.talanta.2014.05.018.
1200 [36] Pum J. Chapter Six - A practical guide to validation and verification of analytical methods
1201   in the clinical laboratory. In: Makowski GS, editor. Advances in Clinical Chemistry, vol. 90,
1202   Elsevier; 2019, p. 215–81. https://doi.org/10.1016/bs.acc.2019.01.006.
1203 [37] Shrivastava A, Gupta VB. Methods for the determination of limit of detection and limit of
1204   quantitation of the analytical methods. Chronicles of Young Scientists 2011;2:21–5.
1205   https://doi.org/10.4103/2229-5186.79345.
1206 [38] MacDougall Daniel, Crummett WB, et al. . Guidelines for data acquisition and data quality
1207   evaluation in environmental chemistry. Anal Chem 1980;52:2242–9. https://doi.org/10.1021/
1208   ac50064a004.
1209 [39] Paul A, Anbu S, Sharma G, Kuznetsov ML, Guedes da Silva MFC, Koch B, et al.
1210   Intracellular detection of Cu2+ and S2- ions through a quinazoline functionalized
1211   benzimidazole-based new fluorogenic differential chemosensor. Dalton Trans
1212   2015;44:16953–64. https://doi.org/10.1039/C5DT02662H.
1213 [40] Wang Z-G, Wang Y, Ding X-J, Sun Y-X, Liu H-B, Xie C-Z, et al. A highly selective
1214   colorimetric and fluorescent probe for quantitative detection of Cu2+/Co2+: The unique ON-
1215   OFF-ON fluorimetric detection strategy and applications in living cells/zebrafish.
1216   Spectrochim Acta A 2020;228:117763. https://doi.org/10.1016/j.saa.2019.117763.
1217 [41] Liu Y-L, Yang L, Li P, Li S-J, Li L, Pang X-X, et al. A novel colorimetric and "turn-off"
1218   fluorescent probe based on catalyzed hydrolysis reaction for detection of Cu2+ in real water
1219   and in living cells. Spectrochim Acta A 2020;227:117540.
1220   https://doi.org/10.1016/j.saa.2019.117540.
1221 [42] Liu Y, Sun Y, Du J, Lv X, Zhao Y, Chen M, et al. Highly sensitive and selective turn-on
1222   fluorescent and chromogenic probe for Cu2+ and ClO− based on a N-picolinyl rhodamine B-
1223   hydrazide derivative. Org Biomol Chem 2011;9:432–7.
1224   https://doi.org/10.1039/C0OB00411A.
1225 [43] Mi Y-S, Cao Z, Chen Y-T, Xie Q-F, Xu Y-Y, Luo Y-F, et al. Determination of trace amount
1226   of Cu2+ with a multi-responsive colorimetric and reversible chemosensor. Analyst
1227   2013;138:5274. https://doi.org/10.1039/c3an00741c.
1228 [44] Fang H, Huang P-C, Wu F-Y. A novel jointly colorimetric and fluorescent sensor for Cu2+
1229   recognition and its complex for sensing S2− by a Cu2+ displacement approach in aqueous
1230   media. Spectrochim Acta A 2018;204:568–75. https://doi.org/10.1016/j.saa.2018.06.068.
1231 [45] Kaur M, Ahn Y-H, Choi K, Cho MJ, Choi DH. A bifunctional colorimetric fluorescent
1232   probe for Hg2+ and Cu2+ based on a carbazole–pyrimidine conjugate: chromogenic and
1233   fluorogenic recognition on TLC, silica-gel and filter paper. Org Biomol Chem
1234   2015;13:7149–53. https://doi.org/10.1039/C5OB00907C.

1235 [46] Gu B, Huang L, Xu Z, Tan Z, Meng H, Yang Z, et al. A reaction-based, colorimetric and
1236   near-infrared fluorescent probe for Cu2+ and its applications. Sens Actuators B Chem
1237   2018;273:118–25. https://doi.org/10.1016/j.snb.2018.06.032.
1238 [47] Xie P, Zhu Y, Huang X, Gao G, Wei F, Guo F, et al. A novel probe based on rhodamine 101
1239   spirolactam and 2-(2′-hydroxy-5′-methylphenyl)benzothiazole moieties for three-in-one
1240   detection of paramagnetic Cu2+, Co2+ and Ni2+. Spectrochim Acta A 2019;222:117171.
1241   https://doi.org/10.1016/j.saa.2019.117171.
1242 [48] Guo Z, Niu Q, Li T, Sun T, Chi H. A fast, highly selective and sensitive colorimetric and
1243   fluorescent sensor for Cu2+ and its application in real water and food samples. Spectrochim
1244   Acta A 2019;213:97–103. https://doi.org/10.1016/j.saa.2019.01.044.
1245 [49] Su J-X, Wang X-T, Chang J, Wu G-Y, Wang H-M, Yao H, et al. Colorimetric and
1246   fluorescent chemosensor for highly selective and sensitive relay detection of Cu2+ and
1247   H2PO4− in aqueous media. Spectrochim Acta A 2017;182:67–72.
1248   https://doi.org/10.1016/j.saa.2017.03.071.
1249 [50] Liu A, Yang L, Zhang Z, Zhang Z, Xu D. A novel rhodamine-based colorimetric and
1250   fluorescent sensor for the dual-channel detection of Cu2+ and Fe3+ in aqueous solutions.
1251   Dyes Pigm 2013;99:472–9. https://doi.org/10.1016/j.dyepig.2013.06.007.
1252 [51] Zhang X, Shen L-Y, Zhang Q-L, Yang X-J, Huang Y-L, Redshaw C, et al. A Simple Turn-
1253   off Schiff Base Fluorescent Sensor for Copper (II) Ion and Its Application in Water Analysis.
1254   Molecules 2021;26:1233. https://doi.org/10.3390/molecules26051233.
1255 [52] Zhang J, Zhao B, Li C, Zhu X, Qiao R. A BODIPY-based "turn-on" fluorescent and
1256   colorimetric sensor for selective detection of Cu2+ in aqueous media and its application in
1257   cell imaging. Sens Actuators B Chem 2014;196:117–22.
1258   https://doi.org/10.1016/j.snb.2014.01.116.
1259 [53] Zhou Z, Chen S, Huang Y, Gu B, Li J, Wu C, et al. Simultaneous visualization and
1260   quantification of copper (II) ions in Alzheimer's disease by a near-infrared fluorescence
1261   probe. Biosens Bioelectron 2022;198:113858. https://doi.org/10.1016/j.bios.2021.113858.
1262 [54] Mani KS, Rajamanikandan R, Murugesapandian B, Shankar R, Sivaraman G, Ilanchelian
1263   M, et al. Coumarin based hydrazone as an ICT-based fluorescence chemosensor for the
1264   detection of Cu2+ ions and the application in HeLa cells. Spectrochim Acta A
1265   2019;214:170–6. https://doi.org/10.1016/j.saa.2019.02.020.
1266 [55] Hanmeng O, Chailek N, Charoenpanich A, Phuekvilai P, Yookongkaew N, Sanmanee N, et
1267   al. Cu2+-selective NIR fluorescence sensor based on heptamethine cyanine in aqueous media
1268   and its application. Spectrochim Acta A 2020;240:118606.
1269   https://doi.org/10.1016/j.saa.2020.118606.
1270 [56] Nair RR, Raju M, Patel NP, Raval IH, Suresh E, Haldar S, et al. Naked eye instant
1271   reversible sensing of Cu2+ and its in situ imaging in live brine shrimp Artemia. Analyst
1272   2015;140:5464–8. https://doi.org/10.1039/C5AN00957J.
1273 [57] Deepa A, Srinivasadesikan V, Lee S-L, Padmini V. Highly Selective and Sensitive
1274   Colorimetric and Fluorimetric Sensor for Cu2+. J Fluoresc 2020;30:3–10.
1275   https://doi.org/10.1007/s10895-019-02450-9.
1276 [58] Chen D, Chen P, Zong L, Sun Y, Liu G, Yu X, et al. Colorimetric and fluorescent probes for
1277   real-time naked eye sensing of copper ion in solution and on paper substrate. R Soc Open Sci
1278   2017;4:171161. https://doi.org/10.1098/rsos.171161.

1279   [59] Na S, Jin JY, Wang H, Zhang Y, Yang RH, Chan WH. Tunable Photochromism of
1280   Spirobenzopyran via Selective Metal Ion Coordination: An Efficient Visual and Ratioing
1281   Fluorescent Probe for Divalent Copper Ion. Anal Chem 2008;80:3466–75.
1282   https://doi.org/10.1021/ac800072y.
1283   [60] An R, Zhang D, Chen Y, Cui Y. A "turn-on" fluorescent and colorimetric sensor for
1284   selective detection of Cu2+ in aqueous media and living cells. Sens Actuators B Chem
1285   2016;222:48–54. https://doi.org/10.1016/j.snb.2015.08.035.
1286   [61] Mohammadi A, Ghasemi Z. A simple pyrimidine based colorimetric and fluorescent
1287   chemosensor for sequential detection of copper (II) and cyanide ions and its application in
1288   real samples. Spectrochim Acta A 2020;228:117730.
1289   https://doi.org/10.1016/j.saa.2019.117730.
1290   [62] Fu Y, Fan C, Liu G, Pu S. A colorimetric and fluorescent sensor for Cu2+ and F− based on
1291   a diarylethene with a 1,8-naphthalimide Schiff base unit. Sens Actuators B Chem
1292   2017;239:295–303. https://doi.org/10.1016/j.snb.2016.08.020.
1293   [63] Gu Z, Cheng H, Shen X, He T, Jiang K, Qiu H, et al. A BODIPY derivative for colorimetric
1294   fluorescence sensing of Hg2+, Pb2+ and Cu2+ ions and its application in logic gates.
1295   Spectrochim Acta A 2018;203:315–23. https://doi.org/10.1016/j.saa.2018.05.094.
1296   [64] Yeh J-T, Chen W-C, Liu S-R, Wu S-P. A coumarin-based sensitive and selective fluorescent
1297   sensor for copper(II) ions. NJC 2014;38:4434–9. https://doi.org/10.1039/C4NJ00695J.
1298   [65] Long C, Hu J-H, Fu Q-Q, Ni P-W. A new colorimetric and fluorescent probe based on
1299   Rhodamine B hydrazone derivatives for cyanide and Cu2+ in aqueous media and its
1300   application in real life. Spectrochim Acta A 2019;219:297–306.
1301   https://doi.org/10.1016/j.saa.2019.04.052.
1302   [66] Hu Y, Chen A, Kong Z, Sun D. A Reversible Colorimetric and Fluorescence "Turn-Off"
1303   Chemosensor for Detection of Cu2+ and Its Application in Living Cell Imaging. Molecules
1304   2019;24:4283. https://doi.org/10.3390/molecules24234283.
1305   [67] He T, Lin C, Gu Z, Xu L, Yang A, Liu Y, et al. Sensing behavior and logic operation of a
1306   colorimetric fluorescence sensor for Hg2+ /Cu2+ ions. Spectrochim Acta A 2016;167:66–71.
1307   https://doi.org/10.1016/j.saa.2016.05.032.
1308   [68] Manna AK, Mondal J, Rout K, Patra GK. A benzohydrazide based two-in-one Ni2+/Cu2+
1309   fluorescent colorimetric chemosensor and its applications in real sample analysis and
1310   molecular logic gate. Sens Actuators B Chem 2018;275:350–8.
1311   https://doi.org/10.1016/j.snb.2018.08.060.
1312   [69] Wang Y, Xu Z, Dai X, Li H, Yu S, Meng W. A New Spiropyran-Based Sensor for
1313   Colorimetric and Fluorescent Detection of Divalent Cu2+ and Hg2+ Ions and Trivalent
1314   Ce3+, Cr3+ and Al3+ Ions. J Fluoresc 2019;29:569–75. https://doi.org/10.1007/s10895-019-
1315   02372-6.
1316   [70] Shen B, Gao M, Franco FC, Kapre R, Zhou J, Li X, et al. Effect of Structure and
1317   Intramolecular Distances on Photoswitchable Magnetic Resonance Imaging Contrast Agents.
1318   J Org Chem 2020;85:7333–41. https://doi.org/10.1021/acs.joc.0c00706.
1319   [71] Tautges B, Or V, Garcia J, Shaw JT, Louie AY. Preparation of a conjugation-ready thiol
1320   responsive molecular switch. Tetrahedron Lett 2015;56:6569–73.
1321   https://doi.org/10.1016/j.tetlet.2015.10.019.

1322 [72] Garcia J, Addison JB, Liu SZ, Lu S, Faulkner AL, Hodur BM, et al. Antioxidant Sensing by
1323   Spiropyrans: Substituent Effects and NMR Spectroscopic Studies. J Phys Chem B
1324   2019;123:6799–809. https://doi.org/10.1021/acs.jpcb.9b03424.
1325 [73] Trevino KM, Tautges BK, Kapre R, Franco Jr FC, Or VW, Balmond EI, et al. Highly
1326   Sensitive and Selective Spiropyran-Based Sensor for Copper(II) Quantification. ACS Omega
1327   2021;6:10776–89. https://doi.org/10.1021/acsomega.1c00392.
1328 [74] Bayindir S, Toprak M. A novel pyrene-based selective colorimetric and ratiometric turn-on
1329   sensing for copper. Spectrochim Acta A 2019;213:6–11.
1330   https://doi.org/10.1016/j.saa.2019.01.053.
1331 [75] Lin W-C, Wu C-Y, Liu Z-H, Lin C-Y, Yen Y-P. A new selective colorimetric and
1332   fluorescent sensor for Hg2+ and Cu2+ based on a thiourea featuring a pyrene unit. Talanta
1333   2010;81:1209–15. https://doi.org/10.1016/j.talanta.2010.02.012.
1334 [76] Jung JY, Kang M, Chun J, Lee J, Kim J, Kim J, et al. A thiazolothiazole based Cu2+
1335   selective colorimetric and fluorescent sensor via unique radical formation. Chem Commun
1336   2013;49:176–8. https://doi.org/10.1039/C2CC36626F.
1337 [77] Kumar J, Bhattacharyya PK, Das DK. New duel fluorescent "on–off" and colorimetric
1338   sensor for Copper(II): Copper(II) binds through N coordination and pi cation interaction to
1339   sensor. Spectrochim Acta A 2015;138:99–104. https://doi.org/10.1016/j.saa.2014.11.030.
1340 [78] Gao Q, Ji L, Wang Q, Yin K, Li J, Chen L. Colorimetric sensor for highly sensitive and
1341   selective detection of copper ion. Anal Methods 2017;9:5094–100.
1342   https://doi.org/10.1039/C7AY01335C.
1343 [79] Gupta VK, Mergu N, Kumawat LK. A new multifunctional rhodamine-derived probe for
1344   colorimetric sensing of Cu(II) and Al(III) and fluorometric sensing of Fe(III) in aqueous
1345   media. Sens Actuators B Chem 2016;223:101–13. https://doi.org/10.1016/j.snb.2015.09.060.
1346 [80] Kim MS, Lee SY, Jung JM, Kim C. A new Schiff-base chemosensor for selective detection
1347   of Cu2+ and Co2+ and its copper complex for colorimetric sensing of S2- in aqueous
1348   solution. Photochem Photobiol Sci 2017;16:1677–89. https://doi.org/10.1039/C7PP00229G.
1349 [81] Tavallali H, Deilamy-Rad G, Karimi MA, Rahimy E. A novel dye-based colorimetric
1350   chemosensors for sequential detection of Cu2+ and cysteine in aqueous solution. Anal
1351   Biochem 2019;583:113376. https://doi.org/10.1016/j.ab.2019.113376.
1352 [82] Sengupta P, Ganguly A, Bose A. A phenolic acid based colourimetric 'naked-eye'
1353   chemosensor for the rapid detection of Cu(II) ions. Spectrochim Acta A 2018;198:204–11.
1354   https://doi.org/10.1016/j.saa.2018.03.005.
1355 [83] Wang Y, Wu H, Wu W-N, Mao X-J, Zhao X-L, Xu Z-Q, et al. Novel rhodamine-based
1356   colorimetric and fluorescent sensor for the dual-channel detection of Cu2+ and
1357   Co2+/trivalent metal ions and its AIRE activities. Spectrochim Acta A 2019;212:1–9. https://
1358   doi.org/10.1016/j.saa.2018.12.017.
1359 [84] Basurto S, Miguel D, Moreno D, Neo AG, Quesada R, Torroba T. Simple 1-
1360   dicyanomethylene-2-chloro-3-aminoindene push–pull chromophores: applications in cation
1361   and anion sensing. Org Biomol Chem 2010;8:552–8. https://doi.org/10.1039/B916700E.
1362 [85] Berthon G. Critical evaluation of the stability constants of metal complexes of amino acids
1363   with polar side chains (Technical Report). Pure Appl Chem 1995;67:1117–240.
1364   https://doi.org/10.1351/pac199567071117.
1365 [86] Ngamchuea K, Batchelor-McAuley C, Compton RG. The Copper(II)-Catalyzed Oxidation
1366   of Glutathione. Chem Eur J 2016;22:15937–44. https://doi.org/10.1002/chem.201603366.

1367 [87] Shtyrlin VG, Zyavkina YI, Ilakin VS, Garipov RR, Zakharov AV. Structure, stability, and
1368 ligand exchange of copper(II) complexes with oxidized glutathione. J Inorg Biochem
1369 2005;99:1335–46. https://doi.org/10.1016/j.jinorgbio.2005.03.008.
1370 [88] Lin Q, Chen P, Liu J, Fu Y-P, Zhang Y-M, Wei T-B. Colorimetric chemosensor and test kit
1371 for detection copper(II) cations in aqueous solution with specific selectivity and high
1372 sensitivity. Dyes Pigm 2013;98:100–5. https://doi.org/10.1016/j.dyepig.2013.01.024.
1373 [89] Liu Y, Wang L, Guo C, Hou Y. A colorimetric squaraine-based probe and test paper for
1374 rapid naked eyes detection of copper ion (II). Tetrahedron Lett 2018;59:3930–3.
1375 https://doi.org/10.1016/j.tetlet.2018.09.042.
1376 [90] Kumar R, Jain H, Gahlyan P, Joshi A, Ramachandran CN. A highly sensitive pyridine-
1377 dicarbohydrazide based chemosensor for colorimetric recognition of Cu2+ , AMP2−, F− and
1378 AcO− ions. NJC 2018;42:8567–76. https://doi.org/10.1039/C8NJ00918J.
1379 [91] Lee HY, Swamy KMK, Jung JY, Kim G, Yoon J. Rhodamine hydrazone derivatives based
1380 selective fluorescent and colorimetric chemodosimeters for Hg2+ and selective colorimetric
1381 chemosensor for Cu2+. Sens Actuators B Chem 2013;182:530–7.
1382 https://doi.org/10.1016/j.snb.2013.03.050.
1383 [92] Chan WC, Saad HM, Sim KS, Lee VS, Ang CW, Yeong KY, et al. A rhodamine based
1384 chemosensor for solvent dependent chromogenic sensing of cobalt (II) and copper (II) ions
1385 with good selectivity and sensitivity: Synthesis, filter paper test strip, DFT calculations and
1386 cytotoxicity. Spectrochim Acta A 2021;262:120099.
1387 https://doi.org/10.1016/j.saa.2021.120099.
1388 [93] Peralta-Domínguez D, Rodriguez M, Ramos-Ortiz G, Maldonado JL, Luna-Moreno D,
1389 Ortiz-Gutierrez M, et al. A Schiff base derivative used as sensor of copper through
1390 colorimetric and surface plasmon resonance techniques. Sens Actuators B Chem
1391 2016;225:221–7. https://doi.org/10.1016/j.snb.2015.11.013.
1392 [94] Mathivanan M, Tharmalingam B, Mani KS, Thiagarajan V, Murugesapandian B. Simple
1393 C3-symmetric triaminoguanidine-triphenylamine conjugate as an efficient colorimetric
1394 sensor for Cu(II) and fluorescent sensor for Fe(III) ions. Spectrochim Acta A
1395 2020;234:118235. https://doi.org/10.1016/j.saa.2020.118235.
1396 [95] Kim MS, Jo TG, Ahn HM, Kim C. A Colorimetric and Fluorescent Chemosensor for the
1397 Selective Detection of Cu2+ and Zn2+ Ions. J Fluoresc 2017;27:357–67.
1398 https://doi.org/10.1007/s10895-016-1964-3.
1399 [96] Zhou H, Wang J, Chen Y, Xi W, Zheng Z, Xu D, et al. New diaminomaleonitrile derivatives
1400 containing aza-crown ether: Selective, sensitive and colorimetric chemosensors for Cu(II).
1401 Dyes Pigm 2013;98:1–10. https://doi.org/10.1016/j.dyepig.2013.01.018.
1402 [97] Li J, Guo Y, Yao H, Lin Q, Xie Y, Wei T, et al. A Highly Selective Colorimetric Sensor for
1403 Cu2+ Based on Phenolic Group Biscarbonyl Hydrazone. Chin J Chem 2013;31:271–6.
1404 https://doi.org/10.1002/cjoc.201200741.
1405 [98] Dolai B, Bhaumik A, Pramanik N, Ghosh KS, Atta AK. Naphthaldimine-based simple
1406 glucose derivative as a highly selective sensor for colorimetric detection of Cu2+ ion in
1407 aqueous media. J Mol Struct 2018;1164:370–7.
1408 https://doi.org/10.1016/j.molstruc.2018.03.066.
1409 [99] Udhayakumari D, Suganya S, Velmathi S, MubarakAli D. Naked eye sensing of toxic metal
1410 ions in aqueous medium using thiophene-based ligands and its application in living cells. J
1411 Mol Recognit 2014;27:151–9. https://doi.org/10.1002/jmr.2343.

1412 [100] Mohammadi A, Khalili B, Haghayegh AS. A novel chromone based colorimetric sensor
1413   for highly selective detection of copper ions: Synthesis, optical properties and DFT
1414   calculations. Spectrochimica Acta Part A: Molecular and Biomolecular Spectroscopy
1415   2019;222:117193. https://doi.org/10.1016/j.saa.2019.117193.
1416 [101] Ciarrocchi C, Tumino A, Sacchi D, Orbelli Biroli A, Licchelli M. Detection of Copper(II)
1417   in Water by Methylene Blue Derivatives. Chem Phys Chem 2020;21:2432–40.
1418   https://doi.org/10.1002/cphc.202000676.
1419 [102] Kumbhar HS, Gadilohar BL, Shankarling GS. A highly selective quinaldine–indole based
1420   spiropyran with intramolecular H-bonding for visual detection of Cu(II) ions. Sens Actuators
1421   B Chem 2016;222:35–42. https://doi.org/10.1016/j.snb.2015.08.025.
1422 [103] Tang X, Zhu Z, Wang Y, Han J, Ni L, Wang L, et al. A dual site controlled probe for
1423   fluorescent monitoring of intracellular pH and colorimetric monitoring of Cu2+. Sens
1424   Actuators B Chem 2018;270:35–44. https://doi.org/10.1016/j.snb.2018.04.173.
1425 [104] Kumar A, Kumar S. A benzothiazolinic spiropyran for highly selective, sensitive and
1426   visible light controlled detection of copper ions in aqueous solution. J Photochem Photobiol
1427   2020;390:112265. https://doi.org/10.1016/j.jphotochem.2019.112265.
1428 [105] Liu M-X, Wei T-B, Lin Q, Zhang Y-M. A novel 5-mercapto triazole Schiff base as a
1429   selective chromogenic chemosensor for Cu2+. Spectrochim Acta A 2011;79:1837–42.
1430   https://doi.org/10.1016/j.saa.2011.05.068.
1431 [106] Kim MS, Jo TG, Yang M, Han J, Lim MH, Kim C. A fluorescent and colorimetric Schiff
1432   base chemosensor for the detection of Zn2+ and Cu2+: Application in live cell imaging and
1433   colorimetric test kit. Spectrochim Acta A 2019;211:34–43.
1434   https://doi.org/10.1016/j.saa.2018.11.058.
1435 [107] Narayanaswamy N, Govindaraju T. Aldazine-based colorimetric sensors for Cu2+ and
1436   Fe3+. Sens Actuators B Chem 2012;161:304–10. https://doi.org/10.1016/j.snb.2011.10.036.
1437 [108] Patil SR, Nandre JP, Jadhav D, Bothra S, Sahoo SK, Devi M, et al. Imatinib intermediate
1438   as a two in one dual channel sensor for the recognition of Cu2+ and I− ions in aqueous media
1439   and its practical applications. Dalton Trans 2014;43:13299–306.
1440   https://doi.org/10.1039/C4DT01516A.
1441 [109] You GR, Park GJ, Lee JJ, Kim C. A colorimetric sensor for the sequential detection of
1442   Cu2+ and CN- in fully aqueous media: practical performance of Cu2+. Dalton Trans
1443   2015;44:9120–9. https://doi.org/10.1039/C5DT00772K.
1444 [110] Liang X, Sadler PJ. Cyclam complexes and their applications in medicine. Chem Soc Rev
1445   2004;33:246–66. https://doi.org/10.1039/B313659K.
1446 [111] Havlíčková J, Medová H, Vitha T, Kotek J, Císařová I, Hermann P. Coordination
1447   properties of cyclam (1,4,8,11-tetraazacyclotetradecane) endowed with two
1448   methylphosphonic acid pendant arms in the 1,4-positions. Dalton Trans 2008:5378–86.
1449   https://doi.org/10.1039/B803235A.
1450 [112] Rezaeian K, Khanmohammadi H, Arab V. Rational design of a novel azoimine appended
1451   maleonitrile-based Salen chemosensor for rapid naked-eye detection of copper(II) ion in
1452   aqueous media. Spectrochim Acta A 2015;151:848–53.
1453   https://doi.org/10.1016/j.saa.2015.06.127.
1454 [113] Kim H, Na YJ, Song EJ, Kim KB, Bae JM, Kim C. A single colorimetric sensor for
1455   multiple target ions: the simultaneous detection of Fe2+ and Cu2+ in aqueous media. RSC
1456   Adv 2014;4:22463–9. https://doi.org/10.1039/C4RA02776K.

1457 [114] Noh JY, Park GJ, Na YJ, Jo HY, Lee SA, Kim C. A colorimetric "naked-eye" Cu(II)
1458   chemosensor and pH indicator in 100% aqueous solution. Dalton Trans 2014;43:5652–6.
1459   https://doi.org/10.1039/C3DT53637H.
1460 [115] Jo TG, Na YJ, Lee JJ, Lee MM, Lee SY, Kim C. A diaminomaleonitrile based selective
1461   colorimetric chemosensor for copper(II) and fluoride ions. NJC 2015;39:2580–7.
1462   https://doi.org/10.1039/C5NJ00125K.
1463 [116] Rajaswathi K, Jayanthi M, Rajmohan R, Anbazhagan V, Vairaprakash P. Simple
1464   admixture of 4-nitrobenzaldehyde and 2,4-dimethylpyrrole for efficient colorimetric sensing
1465   of copper(II) ions. Spectrochim Acta A 2019;212:308–14.
1466   https://doi.org/10.1016/j.saa.2019.01.014.
1467 [117] Aydin Z, Keles M. Colorimetric Detection of Copper(II) Ions Using Schiff-Base
1468   Derivatives. ChemistrySelect 2020;5:7375–81. https://doi.org/10.1002/slct.202001041.
1469 [118] Chang IJ, Choi MG, Jeong YA, Lee SH, Chang S-K. Colorimetric determination of Cu2+
1470   in simulated wastewater using naphthalimide-based Schiff base. Tetrahedron Lett
1471   2017;58:474–7. https://doi.org/10.1016/j.tetlet.2016.12.066.
1472 [119] Kim KB, Kim H, Song EJ, Kim S, Noh I, Kim C. A cap-type Schiff base acting as a
1473   fluorescence sensor for zinc(II) and a colorimetric sensor for iron(II), copper(II), and zinc(II)
1474   in aqueous media. Dalton Trans 2013;42:16569. https://doi.org/10.1039/c3dt51916c.
1475 [120] Bhorge YR, Tsai H-T, Huang K-F, Pape AJ, Janaki SN, Yen Y-P. A new pyrene-based
1476   Schiff-base: A selective colorimetric and fluorescent chemosensor for detection of Cu(II) and
1477   Fe(III). Spectrochim Acta A 2014;130:7–12. https://doi.org/10.1016/j.saa.2014.03.110.
1478 [121] Y.C.Wong, Moganaragi V, Atiqah NA. Physico-chemical Investigation of Semiconductor
1479   Industrial Wastewater. Orient J Chem 2014;29:1421–8.
1480 [122] Onundi YB, Mamun AA, Khatib MFA, Saadi MAA, Suleyman AM. Heavy metals
1481   removal from synthetic wastewater by a novel nano-size composite adsorbent. Int J Environ
1482   Sci Technol 2011;8:799–806. https://doi.org/10.1007/BF03326263.
1483 [123] Shiraishi Y, Tanaka K, Hirai T. Colorimetric Sensing of Cu(II) in Aqueous Media with a
1484   Spiropyran Derivative via a Oxidative Dehydrogenation Mechanism. ACS Appl Mater
1485   Interfaces 2013;5:3456–63. https://doi.org/10.1021/am4005804.
1486 [124] Park GJ, You GR, Choi YW, Kim C. A naked-eye chemosensor for simultaneous detection
1487   of iron and copper ions and its copper complex for colorimetric/fluorescent sensing of
1488   cyanide. Sens Actuators B Chem 2016;229:257–71.
1489   https://doi.org/10.1016/j.snb.2016.01.133.
1490 [125] Samanta S, Manna U, Ray T, Das G. An aggregation-induced emission (AIE) active probe
1491   for multiple targets: a fluorescent sensor for Zn2+ and Al3+ & a colorimetric sensor for
1492   Cu2+ and F-. Dalton Trans 2015;44:18902–10. https://doi.org/10.1039/C5DT03186A.
1493 [126] Sharma P, Singh P. A perylene diimide-based near-IR ratiometric sensor for detection of
1494   Cu2+ ions: ensemble for discrimination of CN− and S2− ions. Anal Methods 2020;12:758–
1495   67. https://doi.org/10.1039/C9AY02726B.
1496 [127] Huo J, Liu K, Zhao X, Zhang X, Wang Y. Simple and sensitive colorimetric sensors for
1497   the selective detection of Cu2+ in aqueous buffer. Spectrochim Acta A 2014;117:789–92.
1498   https://doi.org/10.1016/j.saa.2013.09.104.
1499 [128] El-Safty SA, Ismail AA, Shahat A. Optical supermicrosensor responses for simple
1500   recognition and sensitive removal of Cu(II) Ion target. Talanta 2011;83:1341–51.
1501   https://doi.org/10.1016/j.talanta.2010.11.008.

1502 [129] Tang L, Dai X, Wen X, Wu D, Zhang Q. A rhodamine–benzothiazole conjugated sensor
1503   for colorimetric, ratiometric and sequential recognition of copper(II) and sulfide in aqueous
1504   media. Spectrochim Acta A 2015;139:329–34. https://doi.org/10.1016/j.saa.2014.12.055.
1505 [130] Kaur P, Sareen D, Singh K. Selective colorimetric sensing of Cu2+ using triazolyl
1506   monoazo derivative. Talanta 2011;83:1695–700.
1507   https://doi.org/10.1016/j.talanta.2010.11.072.
1508 [131] Kundu A, Hariharan PS, Prabakaran K, Anthony SP. Synthesis of new colori/fluorimetric
1509   chemosensor for selective sensing of biologically important Fe3+, Cu2+ and Zn2+ metal
1510   ions. Spectrochim Acta A 2015;151:426–31. https://doi.org/10.1016/j.saa.2015.06.107.
1511 [132] Anbu Durai W, Ramu A. Hydrazone Based Dual – Responsive Colorimetric and
1512   Ratiometric Chemosensor for the Detection of Cu2+/ F- Ions: DNA Tracking, Practical
1513   Performance in Environmental Samples and Tooth Paste. J Fluoresc 2020;30:275–89. https://
1514   doi.org/10.1007/s10895-020-02488-0.
1515 [133] Patil SR, Nandre JP, Patil PA, Sahoo SK, Devi M, Pradeep CP, et al. A uracil nitroso
1516   amine based colorimetric sensor for the detection of Cu2+ ions from aqueous environment
1517   and its practical applications. RSC Adv 2015;5:21464–70.
1518   https://doi.org/10.1039/C4RA10419F.
1519 [134] Na YJ, Choi YW, Yun JY, Park K-M, Chang P-S, Kim C. Dual-channel detection of Cu2+
1520   and F− with a simple Schiff-based colorimetric and fluorescent sensor. Spectrochim Acta A
1521   2015;136:1649–57. https://doi.org/10.1016/j.saa.2014.10.060.
1522 [135] Park GJ, Hwang IH, Song EJ, Kim H, Kim C. A colorimetric and fluorescent sensor for
1523   sequential detection of copper ion and cyanide. Tetrahedron 2014;70:2822–8. https://doi.org/
1524   10.1016/j.tet.2014.02.055.
1525 [136] Mahapatra AK, Hazra G, Das NK, Goswami S. A highly selective triphenylamine-based
1526   indolylmethane derivatives as colorimetric and turn-off fluorimetric sensor toward Cu2+
1527   detection by deprotonation of secondary amines. Sens Actuators B Chem 2011;156:456–62.
1528   https://doi.org/10.1016/j.snb.2011.04.009.
1529 [137] Li T, Yang Z, Li Y, Liu Z, Qi G, Wang B. A novel fluorescein derivative as a colorimetric
1530   chemosensor for detecting copper(II) ion. Dyes Pigm 2011;88:103–8.
1531   https://doi.org/10.1016/j.dyepig.2010.05.008.
1532 [138] Hrishikesan E, Saravanan C, Kannan P. Bis-Triazole-Appended Azobenzene Chromophore
1533   for Selective Sensing of Copper(II) Ion. Ind Eng Chem Res 2011;50:8225–9. https://doi.org/
1534   10.1021/ie200548j.
1535 [139] Madhupriya S, Elango KP. Highly selective colorimetric sensing of Cu(II) ions in aqueous
1536   solution via modulation of intramolecular charge transfer transition of aminonaphthoquinone
1537   chemosensor. Spectrochim Acta A 2012;97:100–4.
1538   https://doi.org/10.1016/j.saa.2012.05.044.
1539 [140] Goswami S, Sen D, Das NK. A New Highly Selective, Ratiometric and Colorimetric
1540   Fluorescence Sensor for Cu2+ with a Remarkable Red Shift in Absorption and Emission
1541   Spectra Based on Internal Charge Transfer. Org Lett 2010;12:856–9. https://doi.org/10.1021/
1542   ol9029066.
1543 [141] Huo F-J, Su J, Sun Y-Q, Yin C-X, Tong H-B, Nie Z-X. A rhodamine-based dual
1544   chemosensor for the visual detection of copper and the ratiometric fluorescent detection of
1545   vanadium. Dyes Pigm 2010;86:50–5. https://doi.org/10.1016/j.dyepig.2009.11.007.

[142] Tang L, Li F, Liu M, Nandhakumar R. Single sensor for two metal ions: Colorimetric recognition of Cu2+ and fluorescent recognition of Hg2+. Spectrochim Acta A 2011;78:1168–72. https://doi.org/10.1016/j.saa.2010.12.072.

[143] Kim I, Jeong D-C, Lee M, Khaleel ZH, Satheeshkumar C, Song C. Triazole-conjugated spiropyran: synthesis, selectivity toward Cu(II), and binding study. Tetrahedron Lett 2015;56:6080–4. https://doi.org/10.1016/j.tetlet.2015.09.055.

[144] Xue Y, Gong P, Tian J. Specific recognition of Cu2+ by simple spiropyran via forming a ternary complex of spiropyran-Cu2+-DMF. Colloids Surf, A Physicochem Eng Asp 2018;541:165–74. https://doi.org/10.1016/j.colsurfa.2018.01.017.

[145] Guo Z-Q, Chen W-Q, Duan X-M. Highly Selective Visual Detection of Cu(II) Utilizing Intramolecular Hydrogen Bond-Stabilized Merocyanine in Aqueous Buffer Solution. Org Lett 2010;12:2202–5. https://doi.org/10.1021/ol100381g.

[146] Mergu N, Gupta VK. A novel colorimetric detection probe for copper(II) ions based on a Schiff base. Sens Actuators B Chem 2015;210:408–17. https://doi.org/10.1016/j.snb.2014.12.130.

[147] Milindanuth P, Pisitsak P. A novel colorimetric sensor based on rhodamine-B derivative and bacterial cellulose for the detection of Cu(II) ions in water. Mater Chem Phys 2018;216:325–31. https://doi.org/10.1016/j.matchemphys.2018.06.003.

[148] Wang H-H, Xue L, Fang Z-J, Li G-P, Jiang H. A colorimetric and fluorescent chemosensor for copper ions in aqueous media and its application in living cells. NJC 2010;34:1239. https://doi.org/10.1039/c0nj00168f.

[149] Maity D, Manna AK, Karthigeyan D, Kundu TK, Pati SK, Govindaraju T. Visible-Near-Infrared and Fluorescent Copper Sensors Based on Julolidine Conjugates: Selective Detection and Fluorescence Imaging in Living Cells. Chem Eur J 2011;17:11152–61. https://doi.org/10.1002/chem.201101906.

[150] Liu Y-W, Chir J-L, Wang S-T, Wu A-T. A selective colorimetric sensor for Cu2+ in aqueous solution. Inorg Chem Comm 2014;45:112–5. https://doi.org/10.1016/j.inoche.2014.04.017.

[151] Abebe FA, Sinn E. Fluorescein-based fluorescent and colorimetric chemosensors for copper in aqueous media. Tetrahedron Lett 2011;52:5234–7. https://doi.org/10.1016/j.tetlet.2011.07.127.

[152] Lee K-Y, Blaker JJ, Bismarck A. Surface functionalisation of bacterial cellulose as the route to produce green polylactide nanocomposites with improved properties. Compos Sci Technol 2009;69:2724–33. https://doi.org/10.1016/j.compscitech.2009.08.016.

[153] Dorris GM, Gray DG. Adsorption of hydrocarbons on water-swollen cellulose. J Chem Soc, Faraday Trans 1 1981;77:725–40. https://doi.org/10.1039/F19817700725.

[154] Parr RG, Pearson RG. Absolute hardness: companion parameter to absolute electronegativity. J Am Chem Soc 1983;105:7512–6. https://doi.org/10.1021/ja00364a005.

[155] Hancock RD, Martell AE. Lewis Acid–Base Behavior in Aqueous Solution: Some Implications for Metal Ions in Biology. In: Sykes AG, editor. Advances in Inorganic Chemistry, vol. 42, Academic Press; 1995, p. 89–146. https://doi.org/10.1016/S0898-8838(08)60052-5.

[156] Sinn E, Harris CM. Schiff base metal complexes as ligands. Coord Chem Rev 1969;4:391–422. https://doi.org/10.1016/S0010-8545(00)80080-6.

1590 [157] Yamada S. Advancement in stereochemical aspects of Schiff base metal complexes. Coord
1591   Chem Rev 1999;190–192:537–55. https://doi.org/10.1016/S0010-8545(99)00099-5.
1592 [158] Cozzi PG, Dolci LS, Garelli A, Montalti M, Prodi L, Zaccheroni N. Photophysical
1593   poperties of Schiff-base metal complexes. NJC 2003;27:692–7.
1594   https://doi.org/10.1039/B209396K.
1595 [159] Hameed A, al-Rashida M, Uroos M, Abid Ali S, Khan KM. Schiff bases in medicinal
1596   chemistry: a patent review (2010-2015). Expert Opin Ther Pat 2017;27:63–79.
1597   https://doi.org/10.1080/13543776.2017.1252752.
1598 [160] Dash AC, Dash B, Praharaj S. Hydrolysis of imines: kinetics and mechanism of
1599   spontaneous acid-, base-, and metal ion-induced hydrolysis of N-salicylidene-2-
1600   aminothiazole. J Chem Soc, Dalton Trans 1981:2063–9.
1601   https://doi.org/10.1039/DT9810002063.
1602 [161] Chattopadhyay S, Chakraborty P, Drew MGB, Ghosh A. Nickel(II) complexes of
1603   terdentate or symmetrical tetradentate Schiff bases: Evidence of the influence of the counter
1604   anions in the hydrolysis of the imine bond in Schiff base complexes. Inorg Chim Acta
1605   2009;362:502–8. https://doi.org/10.1016/j.ica.2008.05.004.
1606 [162] Cano J, Benito A, Martínez-Máñez R, Soto J, Payá J, Lloret F, et al. Ferrocene containing
1607   chelating ligands 3. Synthesis, spectroscopic characterization, electrochemical behaviour and
1608   interaction with metal ions of new ligands obtained by condensation of
1609   ferrocenecarboxaldehyde with 2-amino-benzoic acid derivatives. Crystal structures of 2-
1610   ferrocenylmethylamino-5-methyl-benzoic acid and 2-bis(ferrocenylmethyl)ammonium-5-
1611   methyl-benzoic acid perchlorate. Inorg Chim Acta 1995;231:45–56.
1612   https://doi.org/10.1016/0020-1693(94)04318-P.
1613 [163] Gouanvé F, Schuster T, Allard E, Méallet-Renault R, Larpent C. Fluorescence Quenching
1614   upon Binding of Copper Ions in Dye-Doped and Ligand-Capped Polymer Nanoparticles: A
1615   Simple Way to Probe the Dye Accessibility in Nano-Sized Templates. Adv Funct Mater
1616   2007;17:2746–56. https://doi.org/10.1002/adfm.200601056.
1617 [164] Herten D-P, Haderspeck A, Braun F, Wadepohl H. Copper(II)-induced Fluorescence
1618   Quenching of a BODIPY Fluorophore. Journal of Inorganic and General Chemistry
1619   2018;644:735–9. https://doi.org/10.1002/zaac.201800154.
1620 [165] Teixeira Alves Duarte LG, Coelho FL, Germino JC, Gamino da Costa G, Berbigier JF,
1621   Rodembusch FS, et al. A selective proton transfer optical sensor for copper II based on
1622   chelation enhancement quenching effect (CHEQ). Dyes Pigm 2020;181:108566.
1623   https://doi.org/10.1016/j.dyepig.2020.108566.